

From the Clinic for Gastroenterology, Hepatology and Infectious Diseases at
Heinrich Heine University Düsseldorf
Director: Univ.-Prof. Dr. Tom Lüdde

Impact of USP18 and ISG15 on sensing of HIV-1 infection

Dissertation

to obtain the academic title of Doctor of Philosophy (PhD) in Medical Sciences
from the Faculty of Medicine at Heinrich Heine University Düsseldorf

submitted by

Chaohui Lin

2023

As an inaugural dissertation printed by permission of the Faculty of
Medicine at Heinrich Heine University Düsseldorf

signed:

Dean:

First examiner:

Univ.-Prof. Dr. Carsten Münk

Clinic for Gastroenterology, Hepatology and Infectiology

Faculty of Medicine, Heinrich Heine University Düsseldorf

Second examiner:

Univ.-Prof. Dr. Philipp Lang

Institute of Molecular Medicine II

Faculty of Medicine, Heinrich Heine University Düsseldorf

Zusammenfassung

Die Erkennung deroch nicht integrierten viralen DNA des humanen Immundefizienzvirus Typ 1 (HIV-1) wird durch den zyklischen GMP-AMP-Synthase-Stimulator von Interferon-Genen (cGAS-STING) vermittelt. Der aktivierte cGAS-STING-Stoffwechselweg induziert Interferone (IFN), die über IFN-Rezeptoren die Expression von hunderten von interferonstimulierten Genen auslösen, darunter das interferonstimulierte Gen 15 (ISG15), die ubiquitinspezifische Peptidase 18 (USP18) und der Tumorsuppressor p53 (TP53). Die Expression von USP18 oder die Deletion von ISG15 unterstützt die HIV-1-Infektion durch Akkumulation von fehlgefaltetem p53 in myeloischen Zellen. Sowohl Wildtyp-p53 als auch fehlgefaltetes p53 modulieren den cGAS-STING-Sensing-Weg. Darüber hinaus wirkt p53 als Transkriptionsfaktor, der die STING-Expression reguliert. Die Mechanismen, die hinter der Regulierung der HIV-1-Infektion durch fehlgefaltetes p53 stehen, sind daher noch nicht vollständig erforscht. Darüber hinaus zeigt ISG15 antivirale Aktivität durch Konjugation mit viralen und zellulären Faktoren wie cGAS und dem Nukleoprotein des Influenza-B-Virus. USP18 ist nicht nur eine ISG15-spezifische Isopeptidase, sondern reguliert auch die Signalwege von Interferon und des nuklearen Faktors kappa B (NF- κ B) negativ. Die Auswirkungen von USP18 und ISG15 auf die HIV-1-Infektion, -Erkennung und -Sensibilisierung in angeborenen Zielzellen sind noch nicht erforscht worden.

Hier zeigen wir, dass die ektopische Expression von USP18 und der Mangel an ISG15 die STING-Expression und die STING-vermittelte Induktion von angeborenen Immunreaktionen hemmen. Mechanistisch gesehen beeinträchtigt die Anhäufung von fehlgefaltetem p53 die STING-Expression und -Aktivierung in Gegenwart von USP18 oder Knockout von ISG15.

Die Aktivität von STING wird maßgeblich durch posttranslationale Modifikationen reguliert. Hier zeigen wir, dass STING als Reaktion auf zytoplasmatische DNA-Probleme und virale Infektionen durch ISG15 modifiziert wird. Mechanistisch gesehen verringert die Hemmung der ISGylierung von STING an K289 die STING-vermittelte β -IFN-Induktion durch Verringerung seiner Oligomerisierung. Darüber

hinaus ist die Eliminierung der ISGylierung von STING ausreichend, um die IFN-Produktion in Zellen mit STING-abhängigen Interferonopathien zu unterdrücken. Unsere Ergebnisse zeigen somit eine wichtige Rolle von p53 bei der Regulierung der angeborenen Immunantwort auf STING-Ebene. Darüber hinaus zeigen wir nicht nur eine wichtige Rolle der ISGylierung bei der STING-abhängigen angeborenen Immunabwehr und bei Autoimmunerkrankungen auf, sondern liefern auch wichtige Erkenntnisse darüber, wie die Induktion von IFN mechanistisch reguliert wird.

Summary

Sensing of human immunodeficiency virus type 1 (HIV-1) reverse transcript DNA is mediated by the cyclic GMP-AMP synthase-stimulator of interferon genes (cGAS-STING) pathway. The activated cGAS-STING pathway induces interferons (IFNs), which initiates the expression of hundreds of interferon-stimulated genes through IFN receptors, including interferon-stimulated gene 15 (ISG15), ubiquitin-specific peptidase 18 (USP18), and tumor suppressor p53 (TP53).

USP18 expression or ISG15 deletion supports HIV-1 infection by accumulating of misfolded p53 in myeloid cells. Both wild-type p53 and misfolded p53 modulate the cGAS-STING sensing pathway. In addition, p53 acts as a transcription factor that regulates STING expression. Therefore, the mechanisms behind the regulation of HIV-1 infection by misfolded p53 have not been fully explored. Additionally, ISG15 exhibits antiviral activity by conjugating with viral and cellular factors such as cGAS and influenza B virus nucleoprotein. USP18 is not only an ISG15-specific isopeptidase but also negatively regulates interferon signaling and nuclear factor kappa B (NF- κ B) signaling. The effects of USP18 and ISG15 on HIV-1 infection, recognition, and sensing in innate target cells have not been explored.

Here, we show that USP18 ectopic expression and ISG15 deficiency inhibit STING expression and STING-mediated induction of innate immune responses. Mechanistically, the accumulation of misfolded p53 impaired STING expression and activate in the presence of USP18 or knockout of ISG15.

The activity of STING is critically regulated by posttranslational modifications. Here we show that STING is modified by ISG15 in response to cytoplasmic DNA challenge and viral infection. Mechanistically, inhibition of STING ISGylation at K289 decreases STING-mediated-type I IFN induction by reducing its oligomerization. Additionally, the elimination of ISGylation of STING is sufficient to repress IFN production in cells with STING-dependent interferonopathies.

Our findings thus reveal an important role of p53 in regulating innate immune response at the STING level. Further, we not only reveal an important role of ISGylation in STING-dependent innate immune defense and autoimmune

disorders but also provide important knowledge on how induction of IFN is mechanistically regulated.

List of abbreviations

| | |
|-------------------|--|
| 4EHP | eIF4E homologous protein |
| ABCC2 | ATP binding cassette subfamily C member 2 |
| ACBD3 | Acyl-coenzyme a binding domain containing 3 |
| AIM2 | Absent in melanoma 2 |
| AMFR | Autocrine motility factor receptor |
| APS | Ammonium persulphate solution |
| AML1-ETO | Acute myeloid leukemia 1 (AML1)-eight twenty-one (ETO) |
| ARIH1 | Ariadne RBR E3 ubiquitin protein ligase 1 |
| ATCC | American Type Culture Collection |
| BAF1 | Barrier-to-autointegration factor 1 |
| Baf A1 | Bafilomycin A1 |
| BECN1 | Beclin-1 |
| BFA | Brefeldin A |
| BSA | Bovine serum albumin |
| CDKN1A/p21 | Cyclin-dependent kinase inhibitor 1A |
| cGAMP | 2',3'-cyclic-GMP-AMP |
| cGAS | Cyclic GMP–AMP synthase |
| CLRs | C-type lectin receptors |
| c-MYC | Cellular myelocytomatosis oncogene |
| COP-II | Coat protein complex-II |
| CREB | cAMP response element binding |
| CTD | C-terminal domain |
| CTT | C-terminal tail |
| DAMPs | Damage-associated molecular patterns |
| DBD | DNA-binding domain |
| DC | Dendritic cell |
| DDX3X | DEAD-Box Helicase 3 X-Linked |
| DDX41 | DEAD-box helicase 41 |
| DDX60 | DEAD-box helicase 60 |
| DHX9 | DEAH-box helicase 9 |

| | |
|---------------------------------|---|
| DMEM | Dulbecco's modified eagle complete medium |
| DMSO | Dimethyl sulfoxide |
| DNA-PK | DNA-dependent protein kinase |
| DNase2 | Deoxyribonuclease 2 |
| dNTP | Deoxynucleoside triphosphate |
| DPBS | Dulbecco's phosphate-buffered saline |
| DUBs | Deubiquitinating enzymes |
| EFP | Estrogen-responsive finger protein |
| eIF4E | Eukaryotic translation initiation factor 4E |
| ER | Endoplasmic reticulum |
| ERGIC | Endoplasmic reticulum–Golgi intermediate compartment |
| ESCC | Esophageal squamous cell carcinoma |
| ESCRT-III | Endosomal sorting complexes for transport-III |
| FMDV | Foot-and-mouth disease virus |
| Gag | Group-specific antigen |
| GATA-1 | GATA-binding factor 1 |
| h | Hour |
| HDAC6 | Histone deacetylase 6 |
| HERC5 | HECT domain and RCC1-like domain containing protein 5 |
| HERC6 | HECT domain and RCC1-like domain containing protein 6 |
| HIF-1α | Hypoxia-inducible factor 1-alpha |
| HIV | Human immunodeficiency virus |
| HIV-1 | Human immunodeficiency virus type 1 |
| HS-DNA | Herring sperm DNA |
| IFI16 | Interferon gamma inducible protein 16 |
| IFIT1 | IFN-induced protein with tetratricopeptide repeats-1 |
| IFIT3 | IFN-induced protein with tetratricopeptide repeats-3 |
| IFNAR2 | Type I IFN receptor subunit 2 |
| IFNAR | IFN- α/β receptor |
| IFN-β | Interferon beta |
| IFNγ | Interferon- γ |

| | |
|-----------------|---|
| IL-10 | Interleukin-10 |
| IL-6 | Interleukin-6 |
| IRF3 | Interferon regulatory factor 3 |
| IRF7 | Interferon regulatory factor 7 |
| IRF9 | Interferon regulatory factor 9 |
| ISGs | Interferon-stimulated genes |
| ISRE | Interferon-stimulated response element |
| JAK1 | Janus kinase 1 |
| JAK-STAT | Janus kinase signal transducer and activator of transcription |
| kDa | Kilodalton |
| LB | luria-bertani |
| LC3 | Microtubule-associated protein 1A/1B-light chain 3 |
| LFA1 | Lymphocyte function-associated antigen 1 |
| Lpro | leader proteinase |
| LPS | Lipopolysaccharide |
| LRRC25 | Leucine rich repeat containing 25 |
| LRRC59 | Leucine rich repeat containing 59 |
| M | Mole |
| MAVS | Mitochondrial antiviral signaling |
| MDA5 | Melanoma differentiation-associated protein 5 |
| MDM2 | Murine double minute |
| MDMX | Murine double minute X |
| MEFs | Mouse embryonic fibroblasts |
| MG132 | Carbobenzoxy-Leu-Leu-leucinal |
| min | Minute |
| ml | Milliliter |
| mM | Millimolar |
| min/kb | Kilobase per minute |
| MRP2 | Multidrug resistance-associated protein 2 |
| MVA | Modified vaccinia virus ankara |

| | |
|------------------------|---|
| Native SDS–PAGE | Native polyacrylamide gel electrophoresis |
| NEDD4 | Neuronal precursor cell expressed developmentally downregulated 4 |
| NEMO | NF-kappa-B essential modulator |
| NF-κB | Nuclear factor kappa B |
| ng | Nanogram |
| NK | Natural killer |
| NLRs | NOD-like receptors |
| nm | Nanometer |
| NP-40 | Octylphenoxy polyethoxyethanol |
| NRF2 | Nuclear factor-like 2 |
| NS1 | Nonstructural protein 1 |
| p53 | Tumor protein p53 |
| PAMPs | Pathogen-associated molecular patterns |
| PCNA | Proliferating cell nuclear antigen |
| PKR | Protein kinase R |
| PLpro | Papain-like proteases |
| Pol III | RNA polymerase III |
| poly I:C | Polyinosinic:polycytidylic acid |
| PRRs | Pattern recognition receptors |
| PTM | Post-translational modification |
| PVDF | Polyvinylidene fluoride |
| RA | Retinoic acid |
| rcf | Relative centrifugal force |
| RIG-1 | Retinoic acid-inducible gene I |
| RLRs | RIG-I-like receptors |
| RNF115 | Ring finger protein 115 |
| rpm | Revolutions per minute |
| RPMI | Roswell Park Memorial Institute |
| RT | Room temperature |

| | |
|--------------------------------|---|
| s | Second |
| SAMHD1 | SAM and HD domain-containing deoxynucleoside triphosphate triphosphohydrolase 1 |
| SAVI | STING-associated vasculopathy with onset in infancy |
| SDS | Sodium dodecyl-sulfate |
| SDS-PAGE | Sodium dodecyl-sulfate polyacrylamide gel electrophoresis |
| SARS-CoV-2 | Severe acute respiratory syndrome coronavirus 2 |
| SKP2 | S-phase kinase-associated protein 2 |
| SOX9 | SRY-box transcription factor 9 |
| STING | Stimulator of interferon genes |
| SUMO | Small ubiquitin-related modifier |
| TAK1/TAB1 | Transforming growth factor β -activated kinase 1/TAK binding protein 1 |
| TEMED | N, N, N', N'-Tetramethylethylenediamine |
| TLRs | Toll-like receptors |
| TNF-α | Tumor necrosis factor alpha |
| TREX1 | Three prime repair exonuclease 1 |
| TRIM32 | Tripartite motif containing 32 |
| TRIM38 | Tripartite motif containing 38 |
| TRIM56 | Tripartite motif containing 56 |
| Tris-HCl | Tris (hydroxymethyl) aminomethane |
| TSG101 | Tumor susceptibility 101 |
| U/ml | Unit per milliliter |
| UbcH6 | Ubiquitin-conjugating enzyme H6 |
| Ube1L | Ubiquitin-activating enzyme 1-like |
| UBE2L6/UbcH8 | Ubiquitin conjugating enzyme E2 L6 |
| Ubl | Ubiquitin-like protein |
| UBP | Ubiquitin-specific protease |
| ULK1 | Unc-51-like autophagy activating kinase 1 |
| URM1 | Ubiquitin-related modifier-1 |
| USP13 | Ubiquitin specific peptidase 13 |

| | |
|--------------------|--------------------------------------|
| USP14 | Ubiquitin specific peptidase 14 |
| USP18/UBP43 | Ubiquitin specific peptidase 18 |
| USP20 | Ubiquitin specific peptidase 20 |
| V | Voltage |
| ZBP-1/DAI | Z-DNA binding protein 1 |
| ZEB1 | Zinc finger E-box-binding homeobox 1 |
| μg | Microgram |
| μg/ml | Microgram pro milliliter |
| μl | Microliter |
| μM | Micromolar |

Table of contents

| | |
|--|-----------|
| 1 Introduction | 1 |
| 1.1 Immunity and innate immunity..... | 1 |
| 1.1.1 Pattern recognition receptors | 2 |
| 1.1.2 Sensing of Human immunodeficiency virus (HIV)..... | 3 |
| 1.1.3 cGAS-STING pathway..... | 4 |
| 1.1.3.1 Regulation of DNA level | 6 |
| 1.1.3.2 Regulation of cGAS | 7 |
| 1.1.3.3 Regulations of cGAMP..... | 8 |
| 1.1.3.4 Regulation of STING..... | 9 |
| 1.2 Interferon stimulated gene 15 (ISG15)..... | 11 |
| 1.2.1 ISGylation | 12 |
| 1.2.1.1 The function of ISGylation..... | 14 |
| 1.2.2 Unconjugated extracellular and intracellular ISG15 | 17 |
| 1.2.2.1 The function of unconjugated extracellular ISG15..... | 18 |
| 1.2.2.2 The function of unconjugated intracellular ISG15..... | 19 |
| 1.3 Ubiquitin-specific protease 18 (USP18) | 21 |
| 1.3.1 USP18 as a deISGylation enzyme | 21 |
| 1.3.2 USP18 as a deubiquitinating enzyme..... | 22 |
| 1.3.3 Deconjugating activity-independent role of USP18 | 24 |
| 1.4 Tumor protein p53 (TP53)..... | 24 |
| 1.4.1 Regulation of p53 stability | 25 |
| 1.4.2 p53 acts as a transcription factor..... | 27 |
| 1.4.3 The role of p53 in immunity | 28 |
| 1.5 Aims of thesis | 29 |
| 2 Material and Methods | 30 |
| 2.1 Molecular biology | 30 |
| 2.1.1 Plasmid construction | 30 |
| 2.1.1.1 Polymerase chain reaction (PCR)..... | 35 |
| 2.1.1.2 Agarose gel electrophoresis and gel extraction..... | 35 |
| 2.1.1.3 Double restriction enzyme digestion reaction | 36 |
| 2.1.1.4 Ligation of vector and insert | 36 |
| 2.1.1.5 E. coli transformation..... | 36 |

| | |
|---|-----------|
| 2.1.1.6 DNA extraction..... | 37 |
| 2.1.1.7 Verification the plasmid..... | 38 |
| 2.1.2 Quantitative real-time PCR..... | 38 |
| 2.1.2.1 RNA isolation..... | 38 |
| 2.1.2.2 cDNA synthesis | 39 |
| 2.1.2.3 Real-time PCR | 39 |
| 2.2 Cell culture and virological methods..... | 40 |
| 2.2.1 Cell culture of continuous immortalized cell lines | 40 |
| 2.2.2 Transfection of plasmid | 41 |
| 2.2.3 Transfection of herring sperm DNA (HS-DNA) | 41 |
| 2.2.4 Virus production and transduction..... | 41 |
| 2.2.5 HIV-1 luciferase activity assay | 42 |
| 2.2.6 Generation of reconstituted STING THP-1 cells..... | 43 |
| 2.2.7 Type I interferon production assay..... | 44 |
| 2.3 Protein biochemistry..... | 44 |
| 2.3.1 Cell lysis and micro volume protein concentration determination | 44 |
| 2.3.2 Western blotting assay | 45 |
| 2.3.3 Native-PAGE assay | 47 |
| 2.3.4 Immunoprecipitation for ISGylation assay | 48 |
| 2.4 Statistical analysis..... | 48 |
| 3 Results..... | 50 |
| 3.1 USP18 engages STING-mediated cytosolic DNA sensing pathway in a p53-dependent manner | 50 |
| 3.1.1 Ectopic expression of USP18 promotes HIV-1 infection..... | 50 |
| 3.1.2 Ectopic expression of USP18 represses HIV-1 sensing signaling..... | 50 |
| 3.1.3 Ectopic expression of USP18 represses sensing of cytosolic DNA..... | 51 |
| 3.1.4 USP18 deficiency upregulates sensing of HIV-1 and cytosolic DNA | 53 |
| 3.1.5 USP18 inhibits STING expression and counteracts STING activation..... | 54 |
| 3.1.6 USP18 deficiency promotes STING expression and its activation | 56 |
| 3.1.7 USP18 destabilizes STING not at protein level..... | 57 |
| 3.1.8 USP18 regulates STING at the mRNA level | 58 |
| 3.1.9 USP18 catalytic activity regulates STING expression and STING mediated signaling activation | 59 |
| 3.1.10 USP18 catalytic activity regulates the stability of STING mRNA..... | 60 |

| | |
|---|----|
| 3.1.11 Ectopic expression of USP18 or ISG15 deficiency inhibit STING expression in a p53-dependent manner | 61 |
| 3.1.12 Misfolded p53 inhibits STING expression and STING-dependent immune signaling | 63 |
| 3.2 Regulation of STING activity in viral DNA sensing by ISG15 modification | 65 |
| 3.2.1 ISG15 deficiency promotes HIV-1 infection by inhibiting sensing of HIV-1 | 65 |
| 3.2.2 ISG15 deficiency impairs STING-dependent DNA-sensing | 66 |
| 3.2.3 STING is modified by ISG15 | 68 |
| 3.2.4 K224, K236, K289, K338, K347, and K370 of STING are modified by ISG15 | 69 |
| 3.2.5 K289 of STING is vital to induce type I IFN production | 71 |
| 3.2.6 ISGylation at K289 of STING promotes its activation | 73 |
| 3.2.7 ISGylation of STING facilitates its dimerization and oligomerization..... | 74 |
| 3.2.8 SAVI–STINGs require ISGylation for their activity..... | 75 |
| 4 Discussion..... | 78 |
| 5 Reference list | 86 |

1 Introduction

1.1 Immunity and innate immunity

The innate immune response constitutes the first line of host defense against invading pathogens and harmful substances. The initiation of innate immunity relies on the sensing of conserved structures termed pathogen-associated molecular patterns (PAMPs) and damage-associated molecular patterns (DAMPs) through multiple cellular pattern recognition receptors (PRRs) [1-3]. Upon PAMP recognition, activated PRRs rapidly trigger the activation of a multitude of intracellular signaling cascades, culminating in the induction of proinflammatory cytokines and interferons against pathogens [2, 3]. The sensing of microbes or danger signals has been attributed to numerous cells that mediate the innate immune response, including dendritic cells, phagocytes, basophils, eosinophils, monocytes, and natural killer (NK) cells [4].

Innate immune immunity, without immunologic memory, cannot recognize or “memorize” the same pathogen should the body be exposed to it in the future [5]. However, the adaptive immune system can memorize and respond to diverse pathogens from past encounters [6]. Therefore, the innate immune system together with the adaptive immune system provides highly efficient recognition and clearance of pathogens: the innate immune system is not specific to a particular pathogen, sensing microbes through pattern recognition receptors and initiating inflammatory response, whereas adaptive immunity relies on cells with specific receptors to recognize pathogens enabling pathogen-specific responses [7]. In fact, the presence of the innate immune response plays a crucial role in shaping the activation of adaptive immunity. For example, macrophages present antigens to help the activation of T and B lymphocytes and stimulate the expression of numerous proinflammatory cytokines that have a direct impact on the responses of T and B cells [8-10].

1.1.1 Pattern recognition receptors

PPRs are a class of germline-encoded host sensors, that recognize PAMPs and DAMPs, including glycoconjugates, microbial nucleic acids, and molecules released during tissue damage [11]. Such molecular patterns possess common characteristics: first, PAMPs are a set of highly constrained molecular structures from microbial components, that are essential functional components for the survival of microorganisms and are extremely difficult for microbes to lose through evolution. Second, PPRs are germline-encoded, nonsomatic recombination, nonclonally distributed biological macromolecules that are expressed constitutively by immune and nonimmune cells. Third, host cells detect microorganisms in an immunologic memory independent manner and regardless of their life-cycle stage [1, 12]. Most importantly, innate immunity is highly conserved in living organisms, from plants and fruit flies to mammals [13, 14].

Generally, Toll-like receptors (TLRs) and the C-type lectin receptors (CLRs) are responsible for the recognition of extracellular PAMPs, such as structural elements from viruses or bacteria, as well as nucleic acids [15, 16]. In most cases, intracellular PAMPs are sensed by cytoplasmic or nuclear sensors, including NOD-like receptors (NLRs), RIG-I-like receptors (RLRs), and a group of cytosolic DNA sensors that contain cyclic GMP–AMP synthase (cGAS), absent in melanoma 2 (AIM2), interferon- γ (IFN γ)-inducible protein 16 (IFI16), Z-DNA binding protein 1 (ZBP-1 or DAI), DEAD-box helicase 41 (DDX41), DEAH-box helicase 9 (DHX9), DEAD-box helicase 60 (DDX60), DNA-dependent protein kinase (DNA-PK), RNA polymerase III (Pol III), and heterogeneous nuclear ribonucleoprotein A2B1 (hnRNPA2B1) [17, 18]. RLRs detect several different cytosolic RNA species and trigger the activation of mitochondrial antiviral signaling (MAVS) protein, whereas DNA sensors including cGAS, IFI16, and DDX41 cooperate with stimulator of interferon genes (STING), resulting in the activation of downstream signal transduction through different adaptor proteins and various transcription factors, including nuclear factor- κ B (NF- κ B), interferon regulatory factor 3 (IRF3) and 7 (IRF7) [19-21]. Activation of transcription factors leads to the induction of type I IFN, cytokines and chemokines against pathogenic organisms. In addition, IFN- α

and interferon beta (IFN- β) interact with the IFN- α/β receptor (IFNAR) and induce transcription of interferon-stimulated genes (ISGs) via the Janus kinase signal transducer and activator of transcription (JAK-STAT) pathway [22, 23].

1.1.2 Sensing of Human immunodeficiency virus (HIV)

HIV falls into a group of enveloped viruses called retroviruses. Retroviruses are a unique class of viruses that use RNA as genomic material for reverse transcription to produce DNA copies that integrate their DNA into the host cell genome [24]. The replication cycle, of HIV can be divided into seven stages, including binding, fusion, reverse transcription, integration, replication, assembly, and budding [25]. Upon HIV infection, the HIV genome, consisting of two genomic single-stranded (ss) RNAs and the viral core formed by capsid proteins, is introduced into the cytoplasm of cells. HIV viral RNA as well as viral DNA produced during the reverse transcription of HIV can be sensed by multiple families of PRRs [26]. The cytoplasmic RNA sensors retinoic acid-inducible gene I (RIG-I), melanoma differentiation-associated protein 5 (MDA5), and DEAD-Box Helicase 3 X-Linked (DDX3X) are localized within the cytoplasm and are responsible for detecting human immunodeficiency virus type 1 (HIV-1) RNA in infected cells, leading to triggering of the MAVS-dependent signaling cascade [27-29]. Within the incoming viral core, HIV-1 reverse transcribes the single-stranded genomic RNA into different DNA forms, including RNA:DNA hybrids, ssDNA, and dsDNA. This viral DNA is potentially recognized by the cytoplasmic DNA sensors cGAS, interferon gamma inducible protein 16 (IFI16), and DDX41, thus leading to the activation of STING-dependent antiviral immune responses [30-32].

In HIV infection, cGAS-STING signaling is the best-studied pathway to mount the antiviral immune response. During HIV infection, HIV utilizes its capsid to protect viral reverse transcripts from detection by the DNA sensor cGAS [33]. However, recent studies have demonstrated that the cGAS protein is recruited to the viral core in a polyglutamine-binding protein-1 or non-POU (Pit-Oct-Unc) domain-containing octamer-binding protein-dependent manner in the cytosol and nucleus

respectively, enabling cGAS to recognize the HIV-1 reverse-transcribed DNA and enhancing innate signaling in response to infection by HIV [34-36].

1.1.3 cGAS-STING pathway

cGAS is an essential DNA sensor that detects a diverse array of cytosolic dsDNA, including DNA from bacterial infection, viral infection or self-DNA (Fig. 1) [37]. Structural and biochemical studies showed that the C-terminus of cGAS mediates its interaction with DNA as well as dimerization and that the N-terminus part of cGAS contributes to the enhancement of cGAS enzymatic activity [38]. Upon binding dsDNA, cGAS undergoes a conformational change to rearrange the catalytic pocket of the enzyme for its activation [39]. cGAS utilizes ATP and GTP as substrates to synthesize the secondary messenger 2',3'-cyclic-GMP-AMP (cGAMP) [40].

cGAMP binds and activates the downstream adaptor STING, leading to driving signaling cascade activation for the induction of type I IFNs [41, 42]. STING is an endoplasmic reticulum (ER) membrane protein that contains four transmembrane helices followed by a cytoplasmic ligand-binding domain that binds cGAMP (Fig. 1) [43, 44]. STING has a C-terminal tail (CTT) that contains a highly conserved PXPLRXD (X: any residue) motif for binding with TBK1 [45]. Under steady-state conditions, STING is located at the ER membrane and forms a dimer so that two ligand-binding domains create a deep butterfly-shaped ligand-binding pocket for one cyclic dinucleotide molecule that can be buried at its bottom [42, 46, 47]. Upon binding to cGAMP, the STING dimer undergoes a conformational change, which induces a 180° clockwise rotation of its LBD in relation to the transmembrane region, thus leading to closure of the dimer pocket and causing higher-order multimerization of STING. STING traffics from the ER membrane to the endoplasmic reticulum–Golgi intermediate compartment (ERGIC) and Golgi via coat protein complex-II (COP-II) vesicles [48]. COP-II contains five cytosolic proteins, including secretion-associated ras-related GTPase 1, protein transport protein sec23, protein transport protein sec24, protein transport protein sec13, and

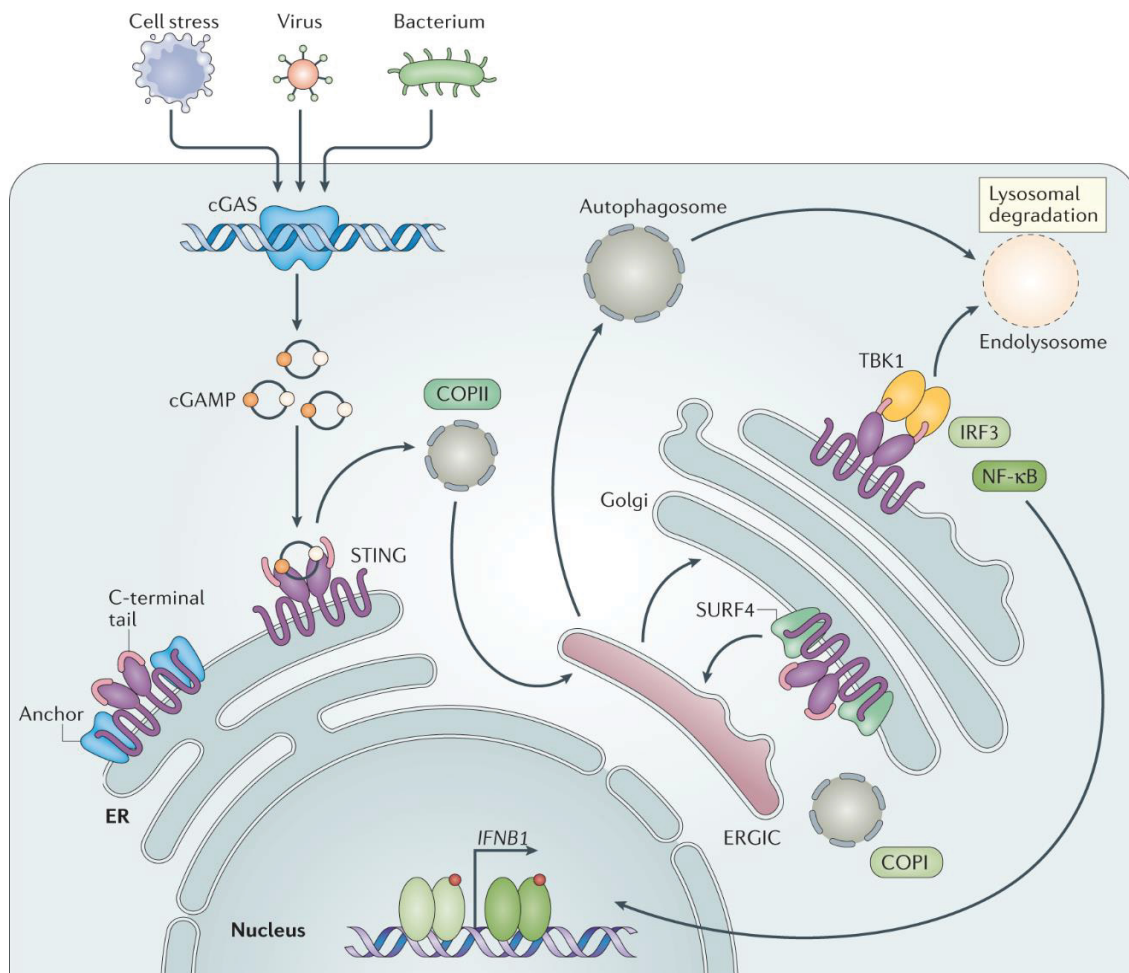


Fig. 1: The cGAS-STING signaling pathway [49]. The presence of various cytoplasmic DNAs can be sensed by the innate immune sensor cyclic GMP-AMP synthase (cGAS). Upon binding of dsDNA, cGAS undergoes a conformational change that leads to its enzymatic activation, resulting in the production of the second messenger 2',3'-cyclic-GMP-AMP (cGAMP). Upon cGAMP binding, stimulator of interferon genes (STING) translocates from the endoplasmic reticulum (ER) to the Golgi apparatus via coat protein complex-II (COP-II) vesicles, where it recruits TANK-binding kinase 1 (TBK1), promoting TBK1 autophosphorylation and STING phosphorylation. Phosphorylated STING recruits interferon regulatory factor 3 (IRF3), which is further phosphorylated by TBK1. In addition to IRF3, TBK1 also activates nuclear factor kappa B (NF-κB) signaling. Subsequently, nuclear translocation of IRF3 and NF-κB induces the expression of type I interferons and inflammatory cytokines. Activation of STING also leads to the formation of microtubule-associated protein 1A/1B-light chain 3 (LC3⁺) vesicles by autophagy. Figure from: Decout, A., Katz, J.D., Venkatraman, S. et al. The cGAS–STING pathway as a therapeutic target in inflammatory diseases. *Nature Reviews Immunology*. Volume 21, 548–569. Published 2021 by Springer Nature, reproduced with permission from Springer Nature.

protein transport protein sec31 [50]. Upon cGAMP binding to STING, SEC24C-mediated STING exits the ER to COP-II vesicles, which then form ERGIC [51]. Some STING-containing ERGIC vesicles further act as a membrane source for microtubule-associated protein 1A/1B-light chain 3 (LC3) lipidation and autophagosome biogenesis, which is important for clearing DNA and viruses in the cytosol (Fig. 1) [51]. In parallel, other STING-coated ERGIC vesicles translocate to Golgi and postGolgi endosomes, at which STING recruits downstream TBK1 via the CTT of STING [45]. The stable oligomer platform of STING provides a solution for multiple TBK1 dimers, resulting in two TBK1 dimers activating one another via intermolecular trans-autophosphorylation [38, 44, 45, 52]. TBK1 binds to the CTT of STING, resulting in the CTT of neighboring STING proteins can be phosphorylated by CTT-bound TBK1. The phosphorylated CTT from STING molecules that are not bound to TBK1 provides a binding site for IRF3, which can then be efficiently phosphorylated by nearby TBK1 [44, 53]. Subsequently, phosphorylated IRF3 dimerizes and traffics into the nucleus to initiate the transcription of type I IFN and other cytokines [53]. After activation by STING, TBK1 acts redundantly with its homolog I κ B kinase epsilon to drive activation of the transcription factor NF- κ B [44, 53-55]. NF- κ B cooperates with IRF3 to drive high levels of type I IFN and inflammatory cytokines [56].

1.1.3.1 Regulation of DNA level

In general, an abnormal DNA damage response can cause cytoplasmic DNA accumulation, which can activate immune signaling through cytosolic DNA sensors [57]. cGAS recognizes dsDNA regardless of its sequence but is a length-dependent mechanism; therefore, it can sense self-DNA and foreign DNA and activate the immune response [58]. Therefore, several DNA binding factors including three prime repair exonuclease 1 (TREX1) and deoxyribonuclease 2 (DNase2), play essential roles in controlling the DNA level in normal cells and preventing the cGAS-dependent autoimmune response [59, 60]. Mutations in the *TREX1* gene are unable to degrade cytosolic DNA and lead to constitutive

production of cGAS-mediated type I IFN, causing autoimmune diseases such as familial chilblain lupus, aicardi-goutières syndrome, retinal vasculopathy with cerebral leukodystrophy and systemic lupus erythematosus [61, 62]. TREX1-deficient/mutant mice exhibit systemic inflammation, however, TREX1-deficient mice lacking cGAS fail to develop autoimmune disorders [63]. Barrier-to-autointegration factor 1 (BAF1) is a conserved protein that can detect foreign DNA and prevent chromosomal integration [64]. The lack of BAF1 induces the accumulation of cytosolic DNA that activates cGAS-STING-IRF3-mediated inflammation and the cellular ISG response [65]. Upon viral infection, spermine contributes to cGAS-triggered antiviral defense by condensing viral DNA, but not host nucleosome DNA [66]. Mechanistically, spermine condenses viral DNA and stabilizes cGAS-DNA binding to activate cGAS, however, depletion of spermine attenuates cGAS-dependent signaling [66]. Collectively, the accumulation of abnormal DNA leads to the activation of the cGAS-dependent signaling pathway in various pathological conditions.

1.1.3.2 Regulation of cGAS

Previous studies have shown that cGAS is a general cytoplasmic DNA sensor. More evidence reveals that nuclear cGAS interacts with the nucleosome, which abolishes cGAS dimerization to maintain it in an inactive format [67, 68]. cGAS is activated by interacting with long dsDNA (>20 bp) rather than short dsDNA, as longer DNA can efficiently form dsDNA 2:2 cGAS-DNA complexes, thereby promoting cGAS dimerization [58]. The expression of cGAS is upregulated by interferon stimulation, and this regulation provides positive feedback to type I IFN induction [69]. cGAS expression is frequently absent in many tumor cell lines, therefore these cells are unable to produce interferons upon cytosolic DNA stimulation [70]. DNA methylation inhibitors can restore synthase cGAS expression in some of these cells through epigenetic mechanisms [71].

The location, DNA binding, enzymatic activity and protein stability of cGAS are mainly regulated by the posttranslational modifications (PTMs), including

phosphorylation, SUMOylation, ubiquitination, acetylation, glutamylation and ISGylation [62, 70, 72, 73]. For example, B-lymphoid tyrosine kinase phosphorylates cGAS at Y215 to control its cytoplasmic localization [74]. Phosphorylation of human cGAS at S305 by protein kinase B and T68, and S213 by DNA-PK both suppress its enzymatic activity [75, 76]. The acetylation of cGAS at K384, K394, and K414 contributes to keeping cGAS inactive; however, lysine acetyltransferase 5 catalyzes the acetylation of cGAS at K47, K56, K62, and K83 to promote the cGAS-dependent immune program [77, 78]. cGAS can be glutamylated by tubulin tyrosine ligase like 6 and tubulin tyrosine ligase like 4, and this modification inhibits its cytosolic dsDNA-binding ability and enzymatic activity, respectively, whereas cytosolic carboxypeptidase 6 and cytosolic carboxypeptidase 5 catalyze deglutamylation of cGAS leading to restoration of the DNA binding and enzymatic activity of cGAS, respectively [79]. Tripartite motif containing 56 (TRIM56) and ring finger protein 185 are E3 ubiquitin ligases that positively modulate cGAS activity [80, 81]. In addition, tripartite motif containing 38 (TRIM38) can induce SUMOylation of cGAS to promote the stability of cGAS in the early stage of viral infection, and catalyze ubiquitination of cGAS in the late stage of viral infection to increase the immune defense [82]. A recent study revealed that ISGylation is involved in regulating oligomerization of cGAS [72]. Together, the activity of cGAS is regulated by many factors.

1.1.3.3 Regulations of cGAMP

cGAS uses ATP and GTP to produce cGAMP by sensing dsDNA [40]. cGAMP contains the 2',5' phosphate bond and the 3',5' phosphate bond [83]. It has been reported that ecto-nucleotide pyrophosphatase/phosphodiesterase family member 1 can block STING activation in the innate immune system by hydrolyzing the phosphodiester bond of 2',3' cGAMP [84, 85]. cGAMP can be transferred to neighboring cells via gap junctions, where it activates the STING-mediated immune response [86]. An example is that after cGAMP is packaged into HIV-1 virions, cGAMP is delivered by virions to next infected cells and activates STING-

dependent antiviral defenses. This might be particularly important for infected cells to rapidly eradicate viral infection [87, 88].

1.1.3.4 Regulation of STING

STING forms a dimer on the ER membrane and generates a butterfly-shaped ligand-binding pocket for one cyclic dinucleotide molecule recognition [47]. Upon binding cGAMP, STING undergoes a conformational change to induce dimer closing. Human STING R232H is the most common *STING* allele, which significantly decreases dimer closing after binding with cGAMP [89]. Based on studies of the structure of STING, many STING agonist molecules were developed, including SR-717, which functions as a direct cGAMP mimetic that induces the same “closed” conformation of STING [90]. Several STING mutations induce a very rare autoinflammatory disease called STING-associated vasculopathy with onset in infancy (SAVI) [91-94]. For example, SAVI patients with N154S and V155M caused an upregulation of the type I IFN response in the body [91]. Mechanistically, V155M and N154S, located in the tightly packed connector region, are assumed to induce STING oligomerization by promoting the 180° rotation of the ligand-binding domain, thus resulting in STING activation in the absence of ligand binding [91, 92].

Similar to cGAS, STING activity is regulated by various PTMs. TBK1 phosphorylates STING at Ser358 and Ser366, which activates STING [44]. In contrast, unc-51-like autophagy activating kinase 1 (ULK1)-triggers STING phosphorylation, facilitating the degradation of STING and repressing persistent innate immune signaling [95]. TRIM38 mediates SUMOylation of STING to enhance its stability and oligomerization in the early stage of viral infection, and in the last stage, SUMO-specific peptidase 2 cleaves the small ubiquitin-related modifier (SUMO) chain from STING to promote the degradation of STING [82]. Palmitoylation of STING at Cys88 and Cys91 is essential for its activation at the Golgi apparatus, and disruption of the palmitoylation of STING by inducing two cysteine residue mutations or the palmitoylation inhibitor 2-bromopalmitate, thus

abolishing the STING-triggered type I IFN response [96]. Dolichyl-diphosphooligosaccharide–protein glycosyltransferase noncatalytic subunit mediates DNA virus infection-induced N-glycosylation of STING, thus promoting STING oligomerization and increasing STING-mediated antiviral defense [97].

Accumulating evidence indicates that STING is regulated by ubiquitination. E3 ligases include TRIM56, tripartite motif containing 32 (TRIM32), and autocrine motility factor receptor (AMFR), which mediates the linkage of the polyubiquitin chain toward STING, leading to an increase in the recruitment of TBK1 and boosting the innate antiviral response [98-100]. In particular, AMFR-catalyzed polyubiquitin of STING can be abolished by ubiquitin specific peptidase 13 (USP13), thus impairing STING-TBK1 binding [101]. Moreover, ring finger protein 115 (RNF115) and mitochondrial E3 ubiquitin ligase 1 promote STING trafficking to the Golgi by catalyzing K63-linked polyubiquitination of STING [102, 103]. Conversely, STING signaling is dampened by the expression of myb like, SWIRM and MPN domain 1, which removes K63-linked polyubiquitination of STING [104]. Tripartite motif containing 29, tripartite motif containing 30 alpha, and ring finger protein 5 promote the degradation of STING through K48-linked polyubiquitination [103, 105, 106]. In turn, several deubiquitinating enzymes can cleave K48-linked polyubiquitin chains on STING and boost the STING-mediated immune response, including eukaryotic translation initiation factor 3 subunit 5, ubiquitin specific peptidase 44 and ubiquitin specific peptidase 20 (USP20) [107-109]. STING oligomerization is required for its activation, and ubiquitin specific peptidase 49 eliminates K63-linked polyubiquitin chains from STING and represses STING oligomerization [110].

COP-II is responsible for the generation of membrane vesicles budding from the ER and facilitates the translocation of STING [48]. Knockdown of components of COP-II reduces STING translocation and activation of STING-dependent downstream signaling [51, 111-113]. Various other factors associated with COP-II have been proposed to be involved in STING signaling, such as inactive rhomboid protein 2, transmembrane emp24 domain-containing protein 2, transmembrane

emp24 domain-containing protein 10, and yip1 domain family member 5, and stimulate membrane curvature formation and subsequent endoplasmic reticulum exit site [48]. A recent study revealed that the Golgi-resident protein acyl-coenzyme a binding domain containing 3 (ACBD3) mediates STING transport from the ER to the Golgi in a nonnormative mechanism [114]. ACBD3 forms a transient bridging complex with ligand-bound STING at the ER-Golgi interface [114]. Studies employing the protein transport inhibitor brefeldin A (BFA) have shown that it inhibits the translocation of STING from the ER to the Golgi [115].

On the other hand, studies have shown that the STING promoter is regulated by several transcription factors. cAMP response element binding (CREB), cellular myelocytomatosis oncogene (c-MYC) and NF- κ B positively regulate the expression of endogenous *STING* [116, 117]. GATA-binding factor 1 (GATA-1) and Sp3 transcription factor are responsible for the modulation of the mouse *STING* promoter [118]. Activation of the tumor protein p53 (p53) increases both the mRNA and protein level of STING in A549 cells [119]. Moreover, nuclear factor-like 2 (NRF2) activation decreases STING-mediated antiviral cytosolic sensing by decreasing the repression of *STING* mRNA stability [120]. Taken together, a series of studies have established the basic framework and mechanisms of the cGAS-cGAMP-STING pathway. However, the regulation of this pathway is still largely unknown and remains to be learned in the future.

1.2 Interferon stimulated gene 15 (ISG15)

ISG15 is an antimicrobial protein expressed at low levels under physiological conditions in normal cells and tissues [121]. The expression of ISG15 is strongly induced by type I IFN via the binding of the transcription factor complex ISGF3 to the interferon-stimulated response element (ISRE) located in the ISG15 promoter (Fig. 2) [122]. In addition, ISG15 expression is induced in lipopolysaccharide (LPS)-stimulated and retinoic acid (RA) treated cells in a type I IFN-dependent manner (Fig. 2) [123, 124]. In contrast, foreign dsRNA can induce the expression of ISG15 by IRF3 in an IFN-independent mechanism [125]. Bacterial DNA-

mediated ISG15 induction depends on STING, TBK1, IRF3 and IRF7 in a cytosolic surveillance pathway [126]. Furthermore, the expression of both mRNA and protein levels of ISG15 is upregulated by p53 via DNA-damaging agents, such as doxorubicin, camptothecin or ultraviolet light [127, 128]. ISG15 was first identified in 1979 in a study of IFN-treated cells [129]. Furthermore, ISG15 was first recognized as a member of the ubiquitin-like protein (Ubl) family in 1987 due to its cross-reactivity with anti-ubiquitin antibodies, which contains two ubiquitin-like β -grasp domains separated by a short linker, and both domains share approximately 30% sequence homology with ubiquitin [130, 131]. The *ISG15* gene comprises two exons and encodes a 17 kilodalton (kDa) precursor (Fig. 2). Under physiological conditions, ISG15 precursor can be cleaved into the mature form of the 15-kDa ISG15 peptide by removing eight C-terminal amino acids, retaining a shared C-terminal amino acid motif LRLRGG, which allows ISG15 to covalently bind to lysine residues of the substrate [132].

1.2.1 ISGylation

Ubl proteins encompass a family of small proteins with sequence and structural similarity to ubiquitin that are involved in posttranslational modifications of target substrates in cells, including ISG15, SUMO, neural precursor cell expressed developmentally downregulated 8, autophagy-related protein 8, autophagy-related protein 12, ubiquitin-related modifier-1, ubiquitin fold modifier 1, and human leukocyte antigen-F adjacent transcript 10 [133, 134]. As a ubiquitin-like modifier, ISG15 is covalently conjugated to cellular proteins in a process called ISGylation (Fig. 2). Protein ISGylation requires the coordinated activities of three modification enzymes, involving E1-activating enzyme, E2-conjugating enzyme, and E3-ligase enzyme. In the first step, ubiquitin-activating enzyme 1-like (UbE1L) activates ISG15 by forming a high-energy thioester bond between the active-site cysteine residue and the C-terminal glycine of ISG15 in an ATP-dependent manner [131, 135]. Following activation, ISG15 is transferred from UbE1L to the active-site cysteine residue on the E2-conjugating enzyme ubiquitin conjugating enzyme E2

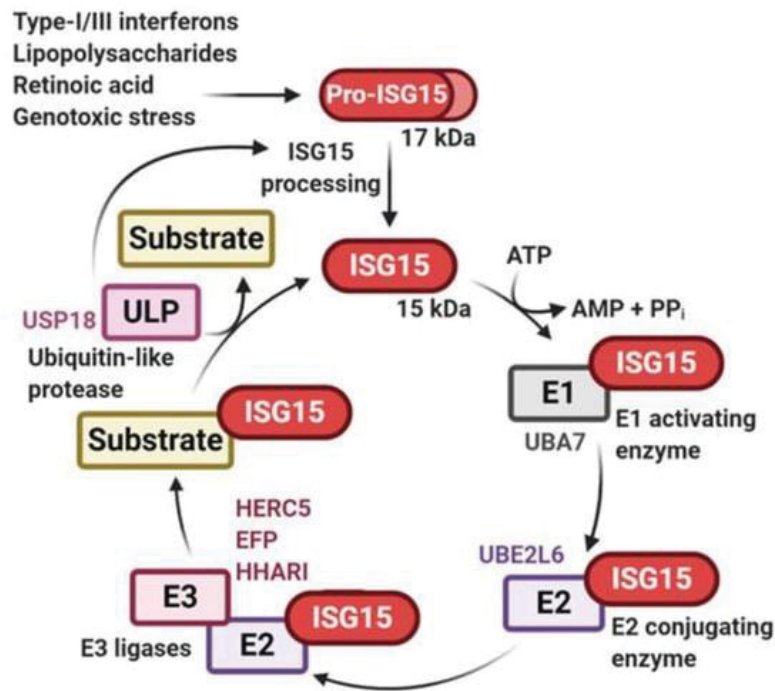


Fig. 2: Processing of ISG15 and mechanism of ISGylation [136]. Interferon-stimulated gene 15 (ISG15) is induced by type I/III interferons, lipopolysaccharides, retinoic acid, genotoxic stress, and various pathogen infections. The 17 kilodalton (kDa) precursor protein (Pro-ISG15) can be cleaved into a mature 15-kDa form via protease cleavage. ISG15 is conjugated to target proteins through a stepwise enzymatic reaction which is activated by the E1 enzyme ubiquitin-activating enzyme 1-like (UbE1L), conjugated by the E2 enzyme ubiquitin-conjugating enzyme E2 L6 (UBE2L6), and ligated by E3 enzymes such as estrogen-responsive finger protein (EFP), ariadne RBR E3 ubiquitin protein ligase 1 (ARIH1), and HECT domain and RCC1-like domain-containing protein 5 (HERC5). ISG15 can be deconjugated from target proteins by the protease ubiquitin specific peptidase 18 (USP18). Figure was reproduced with permission from Sandy, Z., Da Costa, I.C. and Schmidt, C.K.. More than meets the ISG15: emerging roles in the DNA damage response and beyond. *Biomolecules*, 10(11), p.1557. Published by MDPI,2020.

L6 (UBE2L6, Ubch8) in humans or ubiquitin-conjugating enzyme H6 (Ubch6) in mice [137-139]. Ultimately, E3 ligases, including estrogen-responsive finger protein (EFP, TRIM25), ariadne RBR E3 ubiquitin protein ligase 1 (ARIH1), HECT domain and RCC1-like domain containing protein 5 (HERC5) or its murine counterpart HECT domain and RCC1-like domain containing protein 6 (HERC6), bind to the UBE2L6-ISG15 thioester complex and the target protein, facilitating the conjugation of ISG15 to lysine residues of the substrate [140-145]. Similar to

ubiquitination, ISGylation is also reversible by ubiquitin-specific protease 18 (USP18), which can cleave ISG15 from the targeted substrate (Fig. 2) [146].

The expression of the ISGylation process requires E1, E2 and E3 enzymes, which are all robustly induced by type I IFN [135, 137, 139, 140]. UBE1L was identified as an E1 enzyme that catalyzes the first step of ISGylation in the search for proteins interacting with the nonstructural protein 1 (NS1) protein of influenza B virus [135]. UBE1L-deficient mice fail to produce ISG15 conjugates upon stimulation [147]. ISGylated-proteins from LPS-treated macrophages and IFN-treated mouse embryonic fibroblasts (MEFs) derived from UBE1L-deficient mice are completely abrogated, confirming that UBE1L is a specific ISG15-activating E1 enzyme [147]. Both Ubch8 and Ubch6 have been reported to function as E2 enzymes for ISGylation [138, 139]. However, Ubch8 may be the major E2-conjugating enzyme for ISG15 because the amount of the thioester intermediate formed by Ubch8 is much higher than that formed by Ubch6. In addition, Ubch8 also functions as E2 ubiquitin enzyme that binds other ubiquitin E3 ligases, such as Parkin, and Staring [148, 149]. HERC5 is an ISG15 E3 ligase that uses its RLD domain to recognize and interact with a wide range of substrates and is the only human E3 ligase to conjugate ISG15 to host and viral substrates [140, 150, 151]. Depletion of HERC5 dramatically attenuates the total level of ISGylated cellular proteins upon type I IFN treatment [140]. EFP serves as an E3 ligase for ISG15 that can be ISGylated after interferon treatment and this autoISGylation negatively regulates EFP activity [152].

1.2.1.1 The function of ISGylation

Cellular proteins after their biosynthesis often undergo PTMs involved in ubiquitination, ISGylation, and SUMOylation that regulate the structure and function of proteins. Using mass spectrometry analysis, although hundreds of putative targets for ISGylation have been identified, only a subset of these have been experimentally validated [153, 154]. Relative to ubiquitin, the consequence of ISGylation is still poorly understood, but ISGylation appears to play a role in a

variety of cellular processes, such as protein translation, the DNA repair response, autophagy, exosome secretion, tumor progression and immune regulation [148]. For example, ISGylation suppresses multidrug resistance-associated protein 2 (MRP2) expression at the protein level through ISGylation of huRNPA2B1. ISGylated huRNPA2B1 fails to recruit ATP binding cassette subfamily C member 2 (ABCC2) mRNA and thereby inhibits the translation of ABCC2 [155]. Moreover, the covalent combination of ISG15 and protein kinase R (PKR) can inhibit protein translation by phosphorylation of eukaryotic initiation factor 2 α [156]. In response to DNA damage, the E3 ligase EFP enhances the ISGylation of proliferating cell nuclear antigen (PCNA), which is required for PCNA binding to ubiquitin specific peptidase 10 for its deubiquitination and in turn triggers the release of polymerase- η from PCNA for translesion DNA synthesis termination [128]. Furthermore, ISGylation plays an important role in autophagy. IFN treatment-induced ISG15 promotes beclin-1 (BECN1) ISGylation, blocks its ubiquitination and attenuates BECN1-enhanced autophagy [157]. ISGylation can decrease exosome secretion by modifying tumor susceptibility 101 (TSG101) protein for its aggregation and degradation [158].

Increasing evidence has demonstrated that ISGylation functions in pathogen defense and immune modulation. ISG15-deletion mice were more susceptible to influenza A virus, influenza B virus, herpes simplex virus, chikungunya virus, and other pathogens than their wild-type counterparts, showing that ISG15 has a protective effect against viral infection [159]. One of the best described ways ISG15 is conjugated to a wide range of viral proteins to influence various steps of the virus life cycle. ISGylation of NS1 protein of influenza A virus decreases the ability of NS1 to bind to importin- α , which mediates NS1 import into the nucleus [160]. NS1 of IBV is modified by ISG15 and this modification blocks the nuclear localization of the NS1 protein and inhibits virus replication and RNA processing [161]. Beyond NS1, influenza virus matrix protein, hemagglutinin protein and nucleoprotein (NP) have been reported as substrate proteins for ISG15 [162, 163]. ISGylated NP decreased NP oligomerization, inhibiting the formation of viral RNPs [162]. ISGylation inhibits HA protein trafficking to the cell surface [163]. ISGylation

of the human cytomegalovirus pUL26 protein inactivates its function and reduces viral gene expression and virion release [164]. Some newly synthesized viral protein will be ISGylated during replication. ISGylation of HIV-1 group-specific antigen (Gag) protein prevents the ubiquitylation of Gag and inhibits the release of HIV by disrupting the interaction of Gag with TG101 [165]. ISG15 can restrict viral replication by interfering with cellular proteins involved in the translation and exocytosis machinery. For example, the binding of eukaryotic translation initiation factor 4E (eIF4E) with the m7GDP of the mRNA cap allows translation initiation [166]. The eIF4E homologous protein (4EHP) is thought to suppress both cellular and viral mRNA translation by competing with eIF4E [167]. The E3 ligase HHARI promotes the ISGylation of 4EHP and thus enhances its cap structure-binding activity in translational control [142]. Furthermore, ISG15 blocks retrovirus release by binding to endosomal sorting complexes for transport-III (ESCRT-III) complex proteins [168]. Taken together, these studies demonstrate that ISG15 inhibits viral in multiple ways by regulating both host and viral proteins, viral protein translocation, budding, and release.

ISG15, as a PTM, can bind to proteins related to immune signaling pathways and regulate their activity. ISGylation is involved in regulating the activity of RNA sensors and DNA sensors during viral infection. HERC5 ligase-mediated ISGylation of MAD5 is important for its oligomerization and activation in cell and mouse models [169]. In contrast, ISGylation of RIG-I and MDA5 enhances ubiquitin-linked proteasomal degradation [170]. ISG15 can also activate PKR and further promote IFN production in the absence of viral RNA [156]. Recently ARIH1 was reported to be a cGAS-interacting E3 ligase that directly catalyzes ISGylation of cGAS at lysine 187 and enhances its oligomerization after HSV-1 infection [72].

ISGylation can prevent proteasomal-mediated degradation by competing with ubiquitin for conjugation site on a protein. For example, during Sendai virus infection, IRF3 is ISGylated and this modification enhances the stability of IRF3 by inhibiting its ubiquitylation-mediated degradation [171]. ISGylation can regulate ISG production by modulating STAT1 activities. In brief, ISG15 competes with

ubiquitin of STAT1, inhibits the proteasomal degradation of STAT1, and preserves its phosphorylation and continuous activation of downstream signaling [172]. These studies revealed that ISGylation plays a role in regulating the stability of proteins. In addition, ISGylation of Janus kinase 1 (JAK1) was identified by Donger Zhang's laboratory, but the functional importance of ISGylation remains unknown [173]. Induction of ISGylation resulted in increased expression levels of antiviral proteins, such as IFN-induced protein with tetratricopeptide repeats-1 (IFIT1) and IFN-induced protein with tetratricopeptide repeats-3 (IFIT3) [174]. In summary, the covalent form of ISG15 is implicated as a central player in the host antiviral innate immunity and the process of viral infection.

ISG15 was reported to crosstalk with ubiquitin and SUMO chains. K48-linked ubiquitination serves as the most prevalent proteasome-targeting signal to target the substrate protein for degradation; however, ISG15-conjugated mutant K48R ubiquitin protein reduced cellular protein degradation [175]. ISGylation can occur in a SUMO-dependent manner; in this mechanism, SUMO-modified E3 ligase TRIM25 increased protein ISGylation in IFN α -treated SUMO3 cells [176]. Thus, these studies unveil an unanticipated function of PTM crosstalk in coordinating protein homeostasis.

1.2.2 Unconjugated extracellular and intracellular ISG15

Unconjugated form ISG15, as a free molecule, exists in two different forms: released into the serum and unconjugated within the cell [177]. Although ISG15 is deficient in signal peptide for secretion, it has been detected in the serum of type I IFN-treated patients and in virally infected mice [178-181]. Free ISG15 protein was detected in the cell culture medium of type I IFN-treated human lymphocytes, monocytes, neutrophils, plasmablasts, and immune and nonimmune cell lines [177, 182]. Only a few studies have investigated potential ISG15 secretion pathways. It has been reported that exosome, neutrophilic granule, secretory lysosome, neutrophilic granule and microparticle release may provide an alternate means of secretion for ISG15 (Fig. 3) [177, 182-184]. Alternatively, infection of iPSC

macrophages with severe acute respiratory syndrome coronavirus 2 (SARS-CoV-2) induces ISG15 secretion in an LC3-dependent extracellular vesicle loading and secretion pathway [185]. Another potential explanation is that ISG15 is passively released by damaged cells during infection.

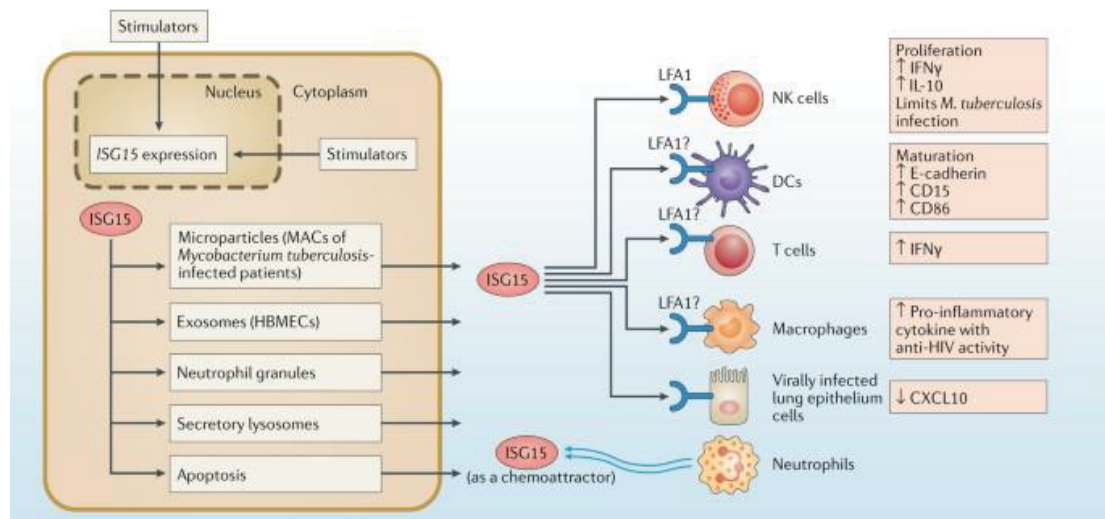


Fig. 3: Functions of extracellular ISG15 [177]. Interferon-stimulated gene 15 (ISG15) can be released from cells via microparticles, secretory lysosomes, exosomes, neutrophilic granules, and apoptosis. Extracellular free ISG15 stimulates natural killer (NK) cells, where it binds to the lymphocyte function-associated antigen 1 (LFA1) receptor and induces the secretion of interferon- γ (IFN γ) and interleukin-10 (IL-10). ISG15 stimulates the secretion of IFN- γ in T lymphocytes and proinflammatory cytokines in macrophages. In addition, ISG15 induces dendritic cell (DC) maturation and inhibits human rhinovirus (HRV)-16-induced CXC-chemokine ligand 10 (CXCL10) protein production. Figure from: Perng, Yi-Chieh, and Deborah J. Lenschow. ISG15 in antiviral immunity and beyond. *Nature Reviews Microbiology*. Volume 16, 423–439. Published 2018 by Springer Nature, reproduced with permission from Springer Nature.

1.2.2.1 The function of unconjugated extracellular ISG15

Lymphocyte function-associated antigen 1 (LFA1) is the receptor for extracellular ISG15 [186]. The direct interaction of extracellular ISG15 with LFA1 initiates the activation of Src-family kinases, stimulating IFN- γ and interleukin-10 (IL-10) secretion in NK cells (Fig. 3) [186]. Additionally, ISG15 constitutively produced by

type I IFN-treated monocytes and lymphocytes can induce the release of IFN- γ from T lymphocyte cells [187]. Human ISG15 increases the proliferation and lysis of NK cells [188]. Extracellular free ISG15 can act as an adjuvant for CD8⁺ cytotoxic T cells, thus enhancing the magnitude and quality of CD8⁺ T-cell responses to modulate antitumor immunity [189]. Another property of ISG15 is the induction of e-cadherin expression on human dendritic cells, which possibly influences their migratory behavior (Fig. 3) [190]. With respect to the impact of ISG15 on neutrophils, ISG15 acts as a chemoattractant and an activator of neutrophils (Fig. 3) [191]. ISG15-included exosomes and microparticles contribute to stimulate macrophages to regulate the transmission of anti-HIV activity and release proinflammatory cytokines, respectively (Fig. 3) [183, 184]. Conflicting results have been obtained regarding the effect of ISG15 on macrophage phagocytosis and the generation of nitric oxide and reactive oxygen species [174, 192]. Free ISG15 secreted from SARS-CoV-2-infected cells correlates with the expression of inflammatory genes and cytokines and polarization of macrophages to the M1 state [185].

1.2.2.2 The function of unconjugated intracellular ISG15

The main role of free intracellular ISG15 is to interact with intracellular proteins and regulate their function. Several groups have now demonstrated that ISG15 inhibits the enzymatic activities of enzymes [182]. For instance, leucine rich repeat containing 25 (LRRC25) recognizes ISG15-associated RIG-I to mediate RIG-I degradation by p62-targeted selective autophagy, leading to inhibition of type I IFN signaling during RNA virus infection [193]. Further study revealed that leucine rich repeat containing 59 (LRRC59) positively regulates the antiviral response by interacting with ISG15-associated RIG-I and blocking its association with LRRC25 (Fig. 4) [194]. ISG15 linked to histone deacetylase 6 (HDAC6) promotes the autophagic clearance of ubiquitin-prone aggregates (Fig. 4) [195]. Moreover, E3 ligase neuronal precursor cell-expressed developmentally downregulated 4 (NEDD4) catalyzes the ubiquitination of the matrix protein of ebola virus VP40,

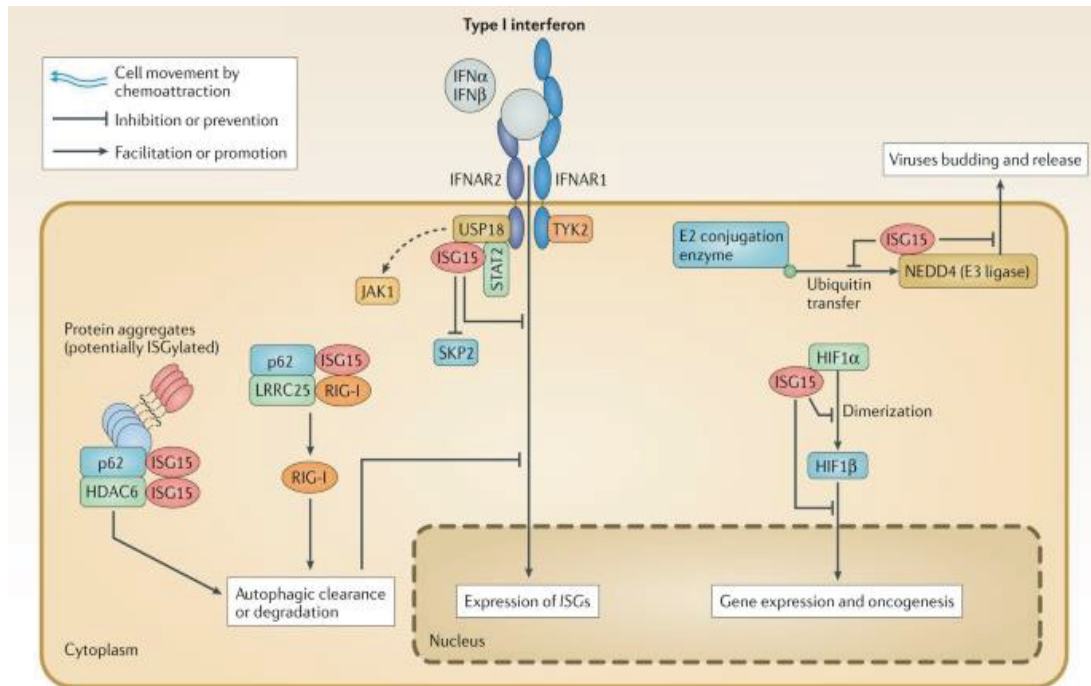


Fig. 4: Functions of intracellular ISG15 [177]. The binding of ubiquitin-specific protease 18 (USP18) with free intracellular interferon-stimulated gene 15 (ISG15) inhibits S-phase kinase-associated protein 2 (SKP2)-mediated USP18 ubiquitylation and proteasomal-mediated USP18 degradation. ISG15 promotes selective autophagy of retinoic acid-inducible gene I (RIG-I) through association with leucine-rich repeat-containing protein 25 (LRRIC25). Intracellular ISG15 regulates S autophagic clearance or degradation of proteins by binding to ubiquitin-binding protein p62 and histone deacetylase 6 (HDAC6). ISG15 interacts with E3 ligase neuronal precursor cell-expressed developmentally downregulated 4 (NEDD4) and suppresses its interaction with E2 conjugation enzymes, thereby disrupting ubiquitin transfer and enhancing the innate antiviral response. Intracellular ISG15 inhibits hypoxia-inducible factor 1-alpha (HIF-1 α) induced gene expression as well as tumorigenic growth. Figure from: Perng, Yi-Chieh, and Deborah J. Lenschow. ISG15 in antiviral immunity and beyond. *Nature Reviews Microbiology*. Volume 16, 423–439. Published 2018 by Springer Nature, reproduced with permission from Springer Nature.

facilitating the release of virus-like particles (Fig. 4) [196]. However, ISG15 binds to NEDD4 ubiquitin ligase and decreases ubiquitination of VP40 to inhibit virion egress [197]. The binding of ISG15 with hypoxia-inducible factor 1-alpha (HIF-1 α) impairs HIF-1 α -targeted gene expression and cancer cell proliferation (Fig. 4) [198]. USP18 is a crucial negative feedback regulator of type I interferon signaling by inhibiting JAK-STAT signaling [199]. S-phase kinase-associated protein 2 (SKP2)

is an E3 ligase that mediates the ubiquitination of USP18 and subsequently promotes its proteasomal degradation [200]. However, noncovalent binding of free intracellular ISG15 with USP18 inhibits SKP2-mediated USP18 degradation (Fig. 4) [200, 201]. These results suggest that free intracellular ISG15 is essential for maintaining the long-term stabilization of USP18. In contrast, mouse USP18 stability is independent of ISG15 [202].

1.3 Ubiquitin-specific protease 18 (USP18)

USP18, a member of the ubiquitin-specific protease (UBP) family with a molecular mass of 43-kDa, was first identified from mice expressing acute myeloid leukemia 1 (AML1)-eight twenty-one (ETO) (AML1-ETO) and later confirmed in virus-infected porcine alveolar macrophages and type I IFN-treated-human melanoma cell lines [203-205]. USP18 expression is strongly induced by type I and type III IFNs and robustly upregulated following LPS, polyinosinic:polycytidylic acid (poly I:C), or tumor necrosis factor alpha (TNF- α) stimulation [206]. In line with this, viral or bacterial infection increases the expression of USP18 in cells [207-209]. USP18 functions as a protease to cleave ISG15 molecules from substrate proteins by isopeptide bonds and as a negative regulator of type I IFN signaling.

1.3.1 USP18 as a deISGylation enzyme

Deubiquitinating enzymes (DUBs) are proteases that can deconjugate ubiquitin or Ubl proteins from target substrates [210]. A few deubiquitinases from the USP family such as ubiquitin specific peptidase 2, ubiquitin specific peptidase 5, USP13, USP14, and ubiquitin specific peptidase 21 have been described to show cross-reactivity against ISG15 and ubiquitin [211]. In contrast with the promiscuous member of cross-reactivity deubiquitinases, USP18 is the only reported ISG15-specific protease that shows no ubiquitin cross-reactivity (Fig. 5A) [212]. Moreover, USP18 constitutes the major ISG15-specific protease in mice [213]. USP18 depleted mice showed highly enhanced and prolonged type I IFN-induced ISGylation without any ubiquitination level changes compared to wild-type mice

[214]. ISG15 conjugation is known to hinder viral infection [177]. However, some viral-encoded specific enzymes are often multifunctional enzymes with protease activity to process deISGylation activity, including foot-and-mouth disease virus (FMDV) leader proteinase (Lpro), coronavirus papain-like proteases (PLpro), and the ovarian tumor domain-containing proteases from nairoviruses and arteriviruses [215-217]. This has led to the hypothesis that these proteases alter the innate immune response to increase efficient infection by the virus. For example, SARS-CoV-2 PLpro enzymatically removes MDA5 and IRF3 ISGylation to evade antiviral immunity and promote viral spread [169, 218].

1.3.2 USP18 as a deubiquitinating enzyme

Contrary to original findings, USP18 has been described to remove ubiquitin from ubiquitin-targeted proteins. Many studies have described that USP18 functions as a deubiquitination enzyme in the regulation of other signaling pathways. USP18 inhibits NF- κ B signaling-mediated regulation of T cell proliferation and IL-2 production by catalyzing deubiquitination of the TGF β -activated kinase/TAK binding protein (TAB1/TAK1) complex, which supports evidence for USP18 regulation of T cell-mediated autoimmunity (Fig. 5B) [219]. Further studies revealed that USP18, but not its protease inactive form USP18 (C64S), abolished the K63-linked polyubiquitination of TAK1, suggesting that in USP18 deubiquitinates of TAK1 in a protease-dependent mechanism [220]. However, USP18 blocks the K63-linked ubiquitination of NF-kappa-B essential modulator (NEMO) in a protease-independent manner [220]. Recently, studies demonstrated the role of USP18 in the regulation of cancer proliferation, migration, and invasion. USP18 promoted glioblastoma cell invasion and migration by removing the ubiquitination of twist-related protein 1, thereby preventing its degradation [221]. USP18 enhanced the proliferation of colorectal cancer cell by modulating ubiquitination of zinc finger protein SNAI1 [222]. Additionally, USP18 acts as a positive regulator of reactive astrogliosis by directly interacting with SRY-box transcription factor 9 (SOX9) and removing ubiquitin from SOX9, thus stabilizing

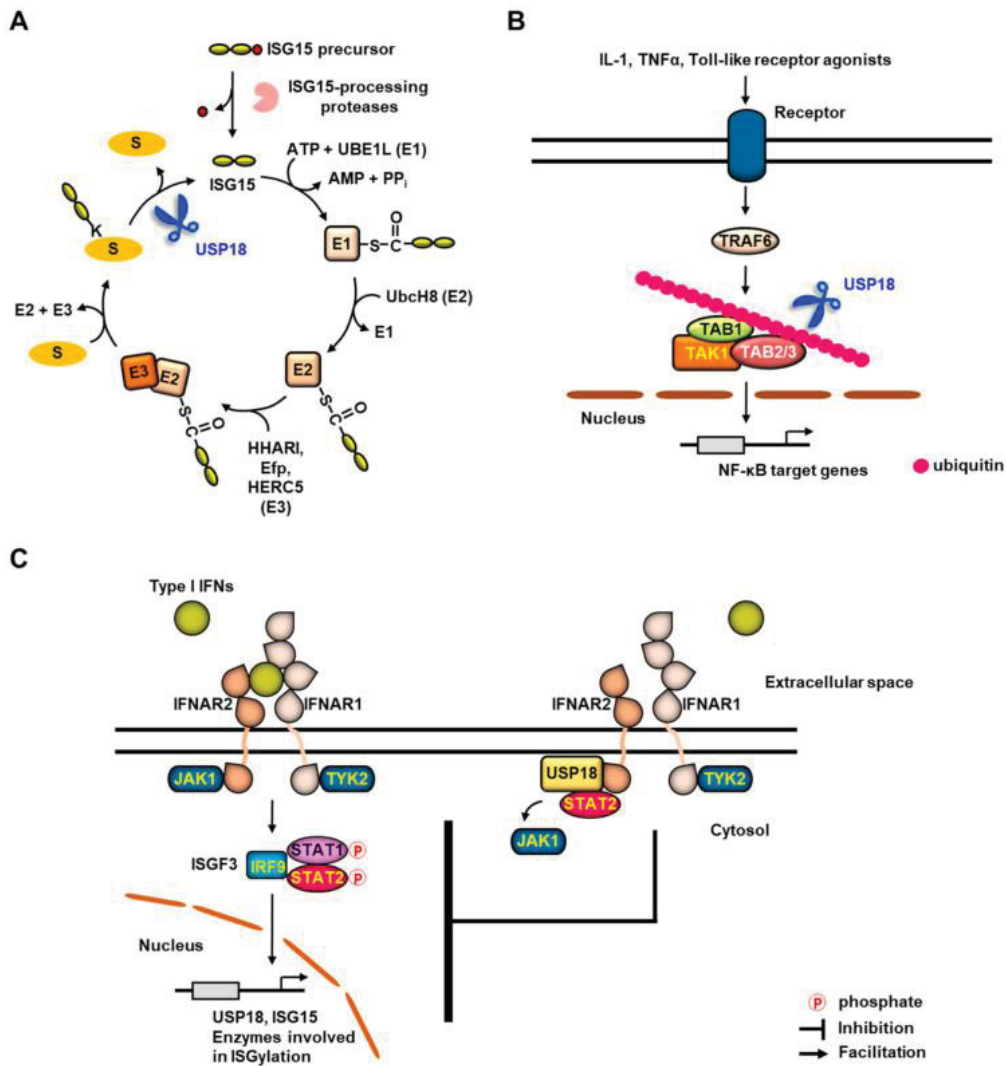


Fig. 5: Multiple functions of USP18 [223]. (A) Ubiquitin-specific protease 18 (USP18) functions as a deISGylation enzyme. USP18 deISGylates target proteins by cleaving conjugated interferon-stimulated gene 15 (ISG15) from the lysine residue of the substrate. (B) USP18 functions as a deubiquitinating enzyme. USP18 negatively regulates nuclear factor κ B (NF- κ B) signaling by deubiquitinating the transforming growth factor β (TGF β)-activated kinase 1/TAK binding protein 1 (TAK1/TAB1) complex. (C) Regulation of type I interferon signaling by USP18. USP18 plays a negative role in regulating type I IFN signaling by competing with Janus kinase 1 (JAK1) for the association with type I IFN receptor subunit 2 (IFNAR2). Figure was reproduced with permission from Kang, Ji An, and Young Joo Jeon. *Emerging roles of USP18: From biology to pathophysiology*. *International Journal of Molecular Sciences*, 21(18), p.6825. Published by MDPI, 2020.

the SOX9 protein [224]. Interestingly, USP18 expression has been shown to be upregulated in the esophageal squamous cell carcinoma (ESCC) patients. USP18

enhances the protein stability of zinc finger E-box-binding homeobox 1 (ZEB1) via decreased ubiquitination of ZEB1, which increasing the migration and invasion abilities of ESCC cells [225].

1.3.3 Deconjugating activity-independent role of USP18

USP18 is a negative regulator of type I IFN signaling, independent of its ISG15 isopeptidase activity. Humans and mice with USP18 deficiency develop severe interferonopathies associated with upregulated interferon signaling [226, 227]. In mechanism, signal transducer and activator of transcription (STAT2) recruits USP18 to bind with type I IFN receptor subunit 2 (IFNAR2), resulting in competition with JAK1 for the associates with IFNAR2, thereby downregulating IFN signaling and IFN-stimulated gene expression (Fig. 5C) [199, 228]. Disruption of the STAT2-USP18 interaction promotes the activation of IFN signaling [228]. In addition, USP18 stability is dependent on free intracellular ISG15 [202]. Notably, human cells lacking ISG15 exhibit prolonged ISG expression due to the loss of USP18 stabilization by ISG15 [202].

On the other hand, the deubiquitinating enzyme USP18 can also indirectly regulate innate immune responses. USP18 upregulates innate antiviral immunity by facilitating TRIM31-catalyzed-ubiquitination of MAVS in an enzymatic-independent manner [229]. USP18 can also recruit the deubiquitinase USP20 to deconjugate the ubiquitination of STING and enhance the stability of STING and the induction of type I IFN and inflammatory cytokines during DNA virus infection [108]. Recently, a study demonstrated that USP18 is located in the nucleus and regulates both typical ISG and noncanonical ISG expression without interacting with IFNAR2 [230].

1.4 Tumor protein p53 (TP53)

p53 was initially discovered as a cellular protein interacting with the large T-antigen in simian virus 40 infected cells and was recognized as a tumor suppressor in 1989 [231-234]. The p53 protein, encoded by the human gene *TP53*, consists of 393 amino acids and four major functional domains, including an amino-terminal

transactivation domain, a core sequence-specific DNA-binding domain, an oligomerization domain, and a regulatory domain [235]. The importance of the tumor suppressor p53 is irrefutable and is commonly referred to as the "guardian of the genome". The tumor suppressor p53 is a complex, multifunctional sequence-specific DNA-binding transcriptional regulator that transactivates dozens of target genes involved in cell cycle arrest, DNA repair, apoptosis, and differentiation in damaged cells [236]. Accordingly, due to somatic mutations in the *TP53* gene, mutations in the p53 protein are observed in a large fraction of many different types of human cancers [237]. Mutations in *TP53* lead to loss of its tumor suppression function and gain of functions, which that may promote tumor growth [238]. The majority of TP53 mutations can be classified into genetic alterations and structural mutations. Some genetic alterations in the DNA-binding domain usually result in inhibition of p53 binding with DNA, such as R248Q and R273H. The second group comprises mutations that destabilize the secondary structure of p53 [239].

1.4.1 Regulation of p53 stability

p53 is maintained at a low level by the E3 ubiquitin-protein ligase murine double minute 2 (MDM2) and murine double minute X (MDMX) [240]. In unstressed cells, MDM2 can bind to the transactivation domain of p53 and inhibit p53 activity [241, 242]. In addition, MDM2 catalyzes the polyubiquitination of p53, thus targeting p53 for degradation through the 26S proteasome and maintaining the stability of p53 (Fig. 6) [241, 242]. On the other hand, MDM2 itself is a transcriptional target of p53, thus forming a negative-feedback loop [243]. The p53-MDM2 feedback loop is vital to control p53 activity to rapidly terminate the p53 response once a p53-activating stress signal has been effectively addressed. Mouse studies have shown that MDM2 null mice exhibit embryonic death in a p53-dependent manner [244, 245]. On the other hand, early embryonic lethality was rescued in *mdm2*-deficient mice by concomitant knockout of p53 [244, 245]. Further study showed that increased MDM2 expression leads to constitutive inhibition of p53 and thereby promotes cancer progression without a need to alter the p53 gene itself [246]. MDMX, a

homolog of MDM2 without E3 ligase activity, is a critical negative regulator of p53 transcriptional activity in a different mechanism from MDM2. MDMX interacts with the transactivation domain of p53 and thereby blocks the

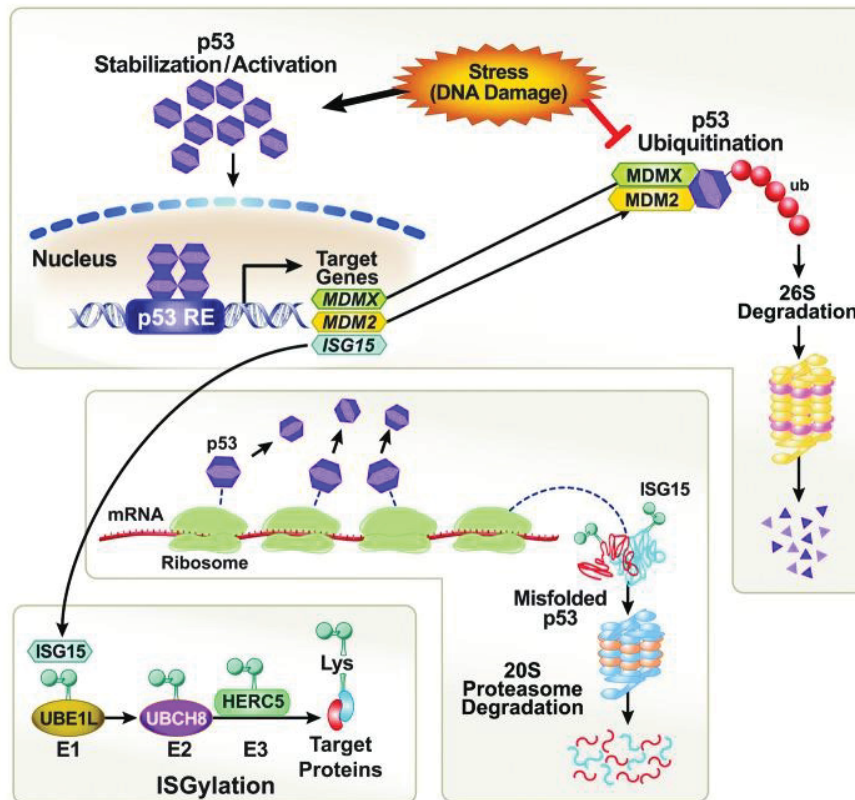


Fig. 6: Regulation of p53 stability [247]. Murine double minute 2 (MDM2) and murine double minute X (MDMX) catalyze the ubiquitination of tumor protein P53 (p53) and promote p53 degradation through the 26S proteasome. Interferon-stimulated gene 15 (ISG15) conjugates to misfolded p53, resulting in misfolded p53 for degradation through the 20S proteasome. Figure from: Anderson, C.W.. p53 vs. ISG15: stop, you're killing me. *Cell Cycle*, 13(14), pp.2160-2161. and © copyright # [2014], reprinted by permission of Informa UK Limited, trading as Taylor & Taylor & Francis Group, <http://www.tandfonline.com>.

transcriptional activity of p53 (Fig. 6) [248]. MDMX mediates regulation of p53 activity by inhibiting the acetylation of p53 [249]. Important insight was obtained in studies showing that the stability and activity of p53 is modulated by ISGylation mediated through ISG15 (Fig. 6). Unlike MDM2, which targets the native form of p53 for ubiquitination, ISG15 is covalently conjugated to lysine residues of misfolded p53, thus promoting misfolded p53 degradation through the 20S

proteasome and maintaining a total p53 activity [250]. It has been confirmed that deletion of ISG15 induced accumulation of both misfolded and native forms of p53 in V-Src transformed MEFs [251]. In dendritic cells, a significant accumulation of misfolded p53 was detected in ISG15 knockout and USP18 overexpressing THP-1 cells, which apparently inactivated the native forms of p53 function [252]. Notably, ISGylation of p53 can be catalyzed by different E3 ligases. HERC5 acts as an E3 ligase interacting with p53 for 20S proteasome mediated degradation [250]. Another study demonstrated that DNA-damaging agents induced E3 ligase EFP-targeted p53 ISGylation, and this modification plays a crucial role in enhancing p53 binding to the promoters of its target genes [253].

1.4.2 p53 acts as a transcription factor

p53 controls transcription genes by interacting with its recognition elements of regulatory genes. Two functionally specialized transactivation domains, including a sequence-specific DNA-binding domain (DBD) and a sequence-independent C-terminal domain (CTD), are associated with the regulatory functions of p53 [254]. The DNA binding assay demonstrated that high affinity binding of the p53 DBD to the consensus RE, whereas the CTD has been shown to bind DNA without sequence specificity [255]. Mutations in DBD, such as R273, can disrupt the binding ability of p53 by directly destabilizing protein-DNA contacts, while some other mutations, such as R175, R249, and R282, can eliminate binding by destabilizing the structure of p53. [254]. It has been described that p53 CTD phosphorylation or acetylation regulates p53 binding to consensus REs [256, 257]. CTD deletion or point mutations at K320 and K382 inhibit p53-mediated transcription in the context of DNA [257]. The well-studied example is the binding of p53 to elements in the cyclin-dependent kinase inhibitor 1A (CDKN1A/p21) promoter upon DNA damage or other stressors [258]. The p21 protein then blocks the activity of several cyclin-CDK complexes and inhibits both of their kinase activities [259]. ISG15 knockout leads to the accumulation of misfolded p53 in myeloid cells, which decreases both the mRNA and protein levels of p21, thus abrogating the antiviral activities of p21 and enhancing HIV-1 infection [252, 260].

1.4.3 The role of p53 in immunity

p53 is considered a regulator of both innate and adaptive immunity by directly transactivating key regulators of immune signaling pathways. The expression of several immune response genes expression is activated by p53, such as ISG15, PKR, interferon regulatory factor 5, IFN regulatory factor 9 (IRF9), and Toll-like receptor 3, which are involved in driving IFN production [234]. Ectopic expression of p53 stimulates the expression of STING, IFIT1, and IFIT3, which are antiviral effector proteins [119]. Activation of wild-type p53 upregulates both the mRNA and protein levels of UL16 binding protein 2 and then results in promotes NK cell-mediated target recognition and the antitumour response [261]. In addition, p53 inhibits the transcription of cluster of differentiation 43 in nonhaematopoietic cells [262]. Lack of p53 in mice led to decreased expression of antiviral gene responses and impaired dendritic cell activation upon AIV infection [263].

In recent years, evidence has indicated that p53 plays a protective role against the development of various autoimmune diseases by decreasing the production of proinflammatory factors. A dominant negative mutation of p53 in rheumatoid arthritis synovial tissue has been associated with increased local expression of interleukin-6 (IL-6) [264]. However, native p53 perfectly inhibits the IL-6 promoter [265]. Other evidence has shown that p53 expressed in T cells acts as a suppressor for the control of autoimmunity by inducing Treg differentiation [266].

The cGAS-STING pathway plays a powerful role in antitumor immunity by promoting the induction of type I IFN [267]. More recent studies have demonstrated that wild-type p53 activates cGAS/STING/IRF3-mediated apoptosis and type I IFN induction by enhancing proteasome degradation of TREX1 [268]. TREX1 degradation through the proteasome. Loss of TREX1 results in the accumulation of cytosolic DNA and activation of cGAS-STING sensing for tumor suppression. On the other hand, mutant p53, but not wild-type p53, hijacks TBK1 and blocks the formation of the STING-TBK1-IRF3 complex, thereby suppressing the activation of innate immune signaling and promoting cancer growth [269].

1.5 Aims of thesis

The cDNA of HIV-1 can be recognized by cGAS. cGAS-cDNA interaction induces cGAMP production, which binds and activates STING. cGAS-STING activation drives interferon induction. The interferon signals back via the type I IFN receptor, inducing a plethora of ISGs, including ISG15 and USP18.

USP18 overexpression and ISG15 deletion support HIV-1 infection by the accumulation of misfolded p53 in cells, which negatively regulates the antiviral function of p21. Both wild-type p53 and misfolded p53 function as master regulators of the cGAS-STING pathway. The mechanisms behind the regulation of HIV-1 infection by misfolded p53 is unknown. In addition, USP18 regulates cellular innate antiviral signaling through the inhibition of IFN and NF- κ B signaling. Therefore, the first study was to examine whether USP18 expression contributes to HIV-1 infection and innate immune sensing escape and whether USP18 regulates HIV-1 sensing in a p53-dependent manner. To this purpose, the HIV-1-DNA sensing signaling was monitored in USP18 overexpression THP-1 cell lines in the context of HIV-1 infection.

In addition, ISG15 exhibits antiviral activity by activating cellular factors required to block viral infection through ISGylation, such as cGAS and IRF3. USP18 regulates cellular innate antiviral signaling through the deISGylation of key antiviral proteins. It is unknown whether HIV-1 infection induces ISGylation on cellular factors. The second aim of this study was to describe the function of ISGylation in modulating HIV-1 infection and innate sensing.

2 Material and Methods

2.1 Molecular biology

2.1.1 Plasmid construction

Plasmid construction was performed by digesting DNA fragments with restriction enzymes at restriction sites and then ligating the resulting fragments. Briefly, DNA fragments were amplified by polymerase chain reaction (PCR), separated by gel electrophoresis and purified by gel extraction. The digested vector and insert fragments were ligated by T4 ligase. Subsequently, ligated DNA constructs were transformed into *E.coli* and single colonies were selected by LB agar plates containing antibiotics. Finally, positive plasmids were identified by double restriction digestion reaction and Sanger sequencing.

STING-FLAG plasmid was obtained from Renate König (Paul-Ehrlich-Institut, Langen, Germany). For generation of reconstituted STING THP-1 cells and ISGylation assay, we constructed a pLOC lentiviral vector (Thermo Fisher Scientific, Waltham, USA) encoding HA-tagged wild-type and various mutant STING (STING-HA). These plasmids included a synonymous mutation on the PAM sequence with forward primer, disrupting the PAM motif associated with the guide RNA target [270]. For pLOC-STING-HA plasmid generation, the STING-FLAG plasmid was used as a template. The insert sequence was amplified using primer pairs containing forward primer (primer A here) that introduced a synonymous mutation on the PAM sequence with a Spe I (Thermo Fisher Scientific, Waltham, USA) restriction enzyme at the 5' end and a reverse primer (primer B here) that introduced an HA tag with an Asc I (Thermo Fisher Scientific, Waltham, USA) restriction enzyme at the 3' end of the insert.

The overlap PCR method was used for the generation of single and multiple mutations of STING-HA with the pLOC vector. PCR primers (primer C and primer D) containing both a point mutation and 10-15 bases of overlapping sequence were designed (Fig. 7). In the first round of PCR, using the pLOC-STING-HA plasmid as a template, primers A and C were used to amplify fragment 1, and primers B and D were used to amplify fragment 2. Both fragments 1 and 2 were

separated by gel electrophoresis and purified by gel extraction. In the second round of PCR, using both fragments 1 and 2 as templates, primers A and B were used to amplify full-length single mutant inster. Subsequently, the DNA fragments were separated by gel electrophoresis and proceeded to the next step. Similarly, multiple STING mutants were introduced in the same way. Plasmids were generated and used for this study, as shown in Table 1. The oligo nucleotide primers for plasmid generation are shown in Table 2. Oligo nucleotide primers were synthesized at Eurofines company (Eurofines, Luxembourg).

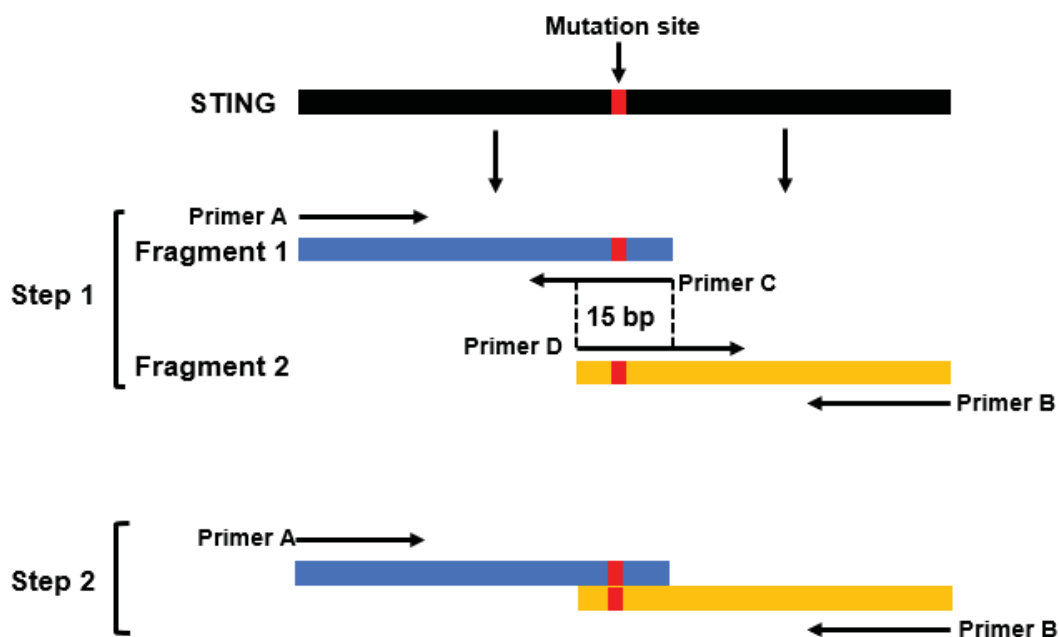


Fig. 7: Schematic illustration of overlap PCR-based construction of the STING single mutation. The desired mutation should be in the middle of the primer (primers C and D) with 10–15 bases of correct sequence on both sides. Step 1 uses PCR to generate PCR fragments that contain a 15 bp overlap at the 3' end of fragment 1 and the 5' end of fragment 2. Step 2 used fragment 1 and fragment 2 to generate full-length STING with a single mutation using overlap PCR.

Table 1: List of plasmids.

| Plasmid | Resistance gene | Reference/Origin |
|---------------------|-----------------|---|
| pcDNA3.1-STING-FLAG | Ampicillin | Renate König, Paul-Ehrlich-Institute, Langen, Germany |
| pLOC vector | Ampicillin | Thermo Fisher Scientific, Waltham, USA |

| Plasmid | Resistance gene | Reference/Origin |
|--|------------------------|-------------------------|
| pLOC-STING-HA | Ampicillin | This work |
| pLOC-STING-K0-HA (A20, A137, A150, A224, A236, A289, A338, A347, A370) | Ampicillin | This work |
| pLOC-STING-K0-K20-HA (Replace A20 to K20 at pLOC-STING-K0-HA) | Ampicillin | This work |
| pLOC-STING-K0-K137-HA | Ampicillin | This work |
| pLOC-STING-K0-K150-HA | Ampicillin | This work |
| pLOC-STING-K0-K224-HA | Ampicillin | This work |
| pLOC-STING-K0-K236-HA | Ampicillin | This work |
| pLOC-STING-K0-K289-HA | Ampicillin | This work |
| pLOC-STING-K0-K338-HA | Ampicillin | This work |
| pLOC-STING-K0-K347-HA | Ampicillin | This work |
| pLOC-STING-K0-K370-HA | Ampicillin | This work |
| pLOC-STING-K224R-HA (Replace K224 to R224 at pLOC-STING-HA) | Ampicillin | This work |
| pLOC-STING-K236R-HA | Ampicillin | This work |
| pLOC-STING-K289R-HA | Ampicillin | This work |
| pLOC-STING-K338R-HA | Ampicillin | This work |
| pLOC-STING-K347R-HA | Ampicillin | This work |
| pLOC-STING-K370R-HA | Ampicillin | This work |
| pLOC-STING-K6R-HA (R224, R236, R289, R338, R347, R370) | Ampicillin | This work |
| pLOC-STING-K5R-R224K-HA (Replace R224 to K224 at pLOC-STING-K6R-HA) | Ampicillin | This work |
| pLOC-STING-K5R-R236K-HA | Ampicillin | This work |
| pLOC-STING-K5R-R289K-HA | Ampicillin | This work |
| pLOC-STING-K5R-R338K-HA | Ampicillin | This work |
| pLOC-STING-K5R-R347K-HA | Ampicillin | This work |
| pLOC-STING-K5R-R370K-HA | Ampicillin | This work |
| pLOC-STING-S366A-HA | Ampicillin | This work |

| Plasmid | Resistance gene | Reference/Origin |
|---------------------------|------------------------|---|
| pLOC-STING-V155M-HA | Ampicillin | This work |
| pLOC-STING-K6R-V155M-HA | Ampicillin | This work |
| pLOC-STING-K289R-V155M-HA | Ampicillin | This work |
| pLOC-USP18 | Ampicillin | [260] Carsten Münk, Heinrich-Heine-Universität Düsseldorf, Düsseldorf, Germany |
| pLOC-USP18-C64A | Ampicillin | [260] Carsten Münk, Heinrich-Heine-Universität Düsseldorf, Düsseldorf, Germany |
| pLOC-USP18-C64S | Ampicillin | [260] Carsten Münk, Heinrich-Heine-Universität Düsseldorf, Düsseldorf, Germany |
| pLOC-USP18-V5 | Ampicillin | [260] Carsten Münk, Heinrich-Heine-Universität Düsseldorf, Düsseldorf, Germany |
| pLOC-ISG15 | Ampicillin | [260] Carsten Münk, Heinrich-Heine-Universität Düsseldorf, Düsseldorf, Germany |
| pLOC-E1 (UBE1L) | Ampicillin | [252] Carsten Münk, Heinrich-Heine-Universität Düsseldorf, Düsseldorf, Germany |
| pLOC-E2 (UBCH8) | Ampicillin | [252] Carsten Münk, Heinrich-Heine-Universität Düsseldorf, Düsseldorf, Germany |
| pMDLg/pRRE | Ampicillin | [271] Luigi Naldini, Cell Genesys, Foster City, California, USA |
| pRSV-Rev | Ampicillin | [271] Luigi Naldini, Cell Genesys, Foster City, California, USA |
| pMD.G | Ampicillin | [271] Luigi Naldini, Cell Genesys, Foster City, California, USA |
| pSIN.PPT.CMV.Luc.IRES.GFP | Ampicillin | [272] Carsten Münk, Heinrich-Heine-Universität Düsseldorf, Düsseldorf/Germany |
| pcDNA6/myc-His-VPX | Ampicillin | [273] Nathaniel R Landau, New York University School of Medicine, New York, USA |
| pMDLx | Ampicillin | [273] Nathaniel R Landau, New York University School of Medicine, New York, USA |
| psPAX2 | Ampicillin | Obtained from the NIH, AIDS Reagent Program repository |

Table 2: List of oligo primers for plasmid generation.

| Primer | Forward 5' to 3' | Reverse 5' to 3' |
|----------------------------|--|--|
| STING-HA (with PAM mutant) | GGACTAGTATGCCCCACTCCAG CCTGCATCCATCCATCCCCTGT CCCAGGAGTCACGGGGCCCA | AAGGCGCGCCTCAAGCGTAATC TGGAACATCGTATGGGTAAGAG AAATCCGTGCGGAGAG |
| STING K20R | GCCCAGACGGCAGCCTTGGT | GGCTGCCCTCTGGGCCCCGT |
| STING K137R | TGGGCCTCAGGGGCCTGGC | AGGCCCTGAGGCCCAGG |
| STING K150R | GTGTGAAAGAGGGAATTTCA | TTCCCTCTTTCACACACTG |
| STING K224R | CTGGATAGACTGCCCCAGCA | GGGCAGTCTATCCAGGAAGCGA |
| STING K236R | CTGGCATCAGGGATCGGGT | GATCCCTGATGCCAGCAT |
| STING K289R | AGCAGGCCAGACTCTTCTG | AGAGTCTGGCCTGCTCAAG |
| STING K338R | AGGAGGAAAGGGAAGAGGT | TCTTCCCTTTCCTCCTGC |
| STING K347R | CAGCTTGAGGACCTCAGCGGT | GAGGTCCTCAAGCTGCCCA |
| STING K370R | TGAGCTCCTCATCAGTGGAATG GAAAGGCCCTCCCTCTCCG | GAGGGGCCTTTCATTCCA |
| STING-K20 | GCCCAGAAGGCAGCCTTGGT | CCAAGGCTGCCTTCTGGGCCCC GT |
| STING-K137 | GCCTCAAGGGCCTGGCCCCA | CAGGCCCTTGAGGCCCAGGA |
| STING-K150 | GTGTGAAAAAGGGAATTTCAAC GTGG | TCCCTTTTTTACACACTGCAGAG |
| STING-K224 | TCCTGGATAAACTGCCCCAGC | GCAGTTTATCCAGGAAGCGA |
| STING-K236 | GCTGGCATCAAGGATCGGGT | CGATCCTTGATGCCAGCATGGT |
| STING-K289 | CAGGCCAAACTCTTCTGCCGGA | AGAAGAGTTTGGCCTGCTCAAG C |
| STING-K338 | CAGGAGGAAAAGGAAGAGGTTA CTGT | ACCTCTTCCCTTTCCTCCTGCC |
| STING-K347 | CAGCTTGAAGACCTCAGCGGT | TGAGGTCTTCAAGCTGCCCAC |
| STING-K370 | AGTGGAATGGAAAAGCCCCTCC CTCT | AGGGGCTTTCATTCCACTGAT |
| STING-S366A | TCATCGCAGGAATGGAAAAGC | CCATTCCTGCGATGAGGAGCT |
| STING-V155M | TTCAACATGGCCCATGGGCTGG C | CCAGCCCATGGGCCATGTTGAA AT |

2.1.1.1 Polymerase chain reaction (PCR)

PCR was used to synthesize new DNA fragments for several purposes, including cloning the DNA sequence into an expression vector. Q5[®] High-Fidelity DNA polymerase (New England Biolabs, Ipswich, USA) was used to amplify DNA fragments according to the manufacturer's instructions. A 50 microliter (µl) reaction mixture contained nuclease-free water, 10 µl 5X reaction buffer, 10 micromolar (µM) of forward primer, 10 µM of reverse primer, 0.3 µl Q5 High-Fidelity DNA polymerase, 10 millimolar (mM) deoxynucleoside triphosphate (dNTP) (New England Biolabs, Ipswich, USA), and 10 nanogram (ng) template from plasmid or DNA genomic. Gently mix the reaction and transfer the PCR tube to a PCR machine (Bioer GeneTouch™ Thermal Cycler, Hangzhou, China) with the following program: (i) initial denaturation, 30 seconds (s) at 98°C; (ii) 30 cycles of denaturation for 15s at 95°C, annealing at 50-70°C for 20 s, extension at 72°C for 1 kilobase per minute (min/kb); and (iii) final extension at 72°C for 10 minutes (min).

2.1.1.2 Agarose gel electrophoresis and gel extraction

DNA fragments can be separated by gel electrophoresis according to their size. After PCR, PCR products premixed with DNA gel loading buffer and an 1 kilobase plus DNA ladder (Thermo Fisher Scientific, Waltham, USA) were loaded into agarose gel wells. Electrophoretic separation of DNA was performed with a constant 150 voltage (V) for 30 min. Use the camera to capture the image and cut the DNA fragment from agarose gel based on the DNA ladder. The DNA-containing agarose gel was purified by using a modified protocol of the QIAquick gel extraction kit (QIAGEN, Venlo, Netherlands). Add 300-500 milliliter (ml) QG buffer into tubes and incubate in a shaker at 500 revolutions per minute (rpm) for 10 min at 50°C. Transfer all solution into a QIAquick spin column and centrifuge at full speed for 1 min. Add 600 µl of PE buffer and centrifuge at full speed for 1 min and repeat one time. Add 25 µl EB buffer to columns and centrifuge at full speed for 1 min to elute DNA. The DNA concentration was photometrically measured at 260 nanometers (nm).

2.1.1.3 Double restriction enzyme digestion reaction

1 microgram (μg) of purified insert and 1 μg of donor plasmid backbone were digested by using double-restriction enzymes according to the manufacturer's instructions. The 20 μl reaction system contained 1 μg of purified insert or donor plasmid backbone, 1X or 2X of an enzyme-specific buffer according to the recommendation from the double digest calculator, 1 μl of each restriction enzyme, and nuclease-free water. The components were mixed by pipetting and incubated at 37°C for 1-2 hours (h). After incubation, the digested DNA can be evaluated by gel electrophoresis and purified by gel extraction.

2.1.1.4 Ligation of vector and insert

The ligation system was performed with T4 DNA ligase according to the manufacturer's instructions. The 20 μl ligation system was performed by adding 2 μl 10X T4 DNA ligase buffer, 1 μl T4 ligase, nuclease-free water, and purified sticky-end insert and vector in a molar ratio of 1:3 into a 1.5 ml microcentrifuge tube. Mix thoroughly, spin briefly, and incubate at room temperature (RT) for 1 h. Use 10 μl of the mixture to transform an aliquot of competent cells.

2.1.1.5 *E. coli* transformation

The ligated DNA constructs were transformed into Top10 and Stbl2 chemically competent cells (Thermo Fisher Scientific, Waltham, USA) according to the manufacturer's instructions. Thaw an aliquot of competent cells on ice. Mix 10 μl of ligated DNA constructs with competent cells by pipette and incubate on ice 10 min for Top10 or 30 min for Stbl2. Following heat shock at 42 °C for 1 min, the cells were placed on ice for 2 min for Top10 or 10 min for Stbl2. Then, 500 μl fresh Luria-Bertani (LB) liquid medium was added to the mixture of DNA and competent cells and subsequently cultured in a shaker at 500 rpm for 1 h at 37°C for Top10 or 30°C for Stbl2. The resulting cells were spread on LB agar plates containing 100 $\mu\text{g/ml}$ ampicillin or 100 $\mu\text{g/ml}$ kanamycin and were grown overnight at 37°C for Top10 or 30°C for Stbl2. Single colonies were

inoculated into 4 ml of LB medium containing ampicillin (100 µg/ml) or kanamycin (100 µg/ml) with vigorous shaking at 180 rpm overnight at 37°C for Top10 or 30°C for Stbl2.

2.1.1.6 DNA extraction

DNA extraction from bacteria was performed by using a modified protocol of the ZR Plasmid Miniprep-Classic kit (Zymo Research Irvine, USA). 2 ml bacterial cultures were harvested by centrifugation for 20 sec at full speed. Pelleted bacteria were then resuspended in 200 µl of P1 buffer. Then, 200 µl of P2 buffer was added and the tube was mixed by inverting 2-4 times and incubated for 2 min. Then, 400 µl of P3 buffer was added, mixed gently but thoroughly, and incubated at RT for 2 min before centrifuging the samples for 2 min at full speed. Following centrifugation, the supernatant was transferred into a Zymo-Spin™ IIN column and centrifuged at full speed for 1 min. After discarding the effluent in the collection tube, 200 µl endo-wash buffer was added to the column and centrifuged at full speed for 1 min. Then, 400 µl plasmid wash buffer was added to the column and centrifuge at full speed for 1 min. Finally, the column was dissolved in 30 µl nuclease-free water and plasmids were transferred into a 1.5 ml microcentrifuge tube by centrifugation for 1 min at full speed. The DNA concentration was photometrically measured at 260 nm. PureYield™ Plasmid Maxiprep system (Promega, Madison, USA) was used for large-scale purification of plasmids according to the manufacturer's instructions.

DNA genomic extraction from cells was carried out using the protocol of the DNeasy Blood & Tissue kit (QIAGEN, Venlo, Netherlands). Cells resuspended in 200 µl of dulbecco's phosphate-buffered saline (DPBS) (PAN-Biotech, Aidenbach, Germany). After adding 20 µl Proteinase K, add 200 µl buffer AL, mix by vortexing, and incubate at 56°C for 10 min. After incubation, add 200 µl 96% ethanol and mix by vortexing. Transfer the mixture into the DNeasy Mini spin column, centrifuge at 12,000 rpm for 1 min, and discard the flow-through. Add 500 µl buffer AW1, discard the flow-through by centrifugation at 12,000 rpm for 1 min. Add 500 µl buffer AW2,

dry the DNeasy membrane by centrifugation at at 14,000 rpm for 2 min. Finally, 50 µl of total DNA was eluted by centrifugation at 12,000 rpm for 1 min.

2.1.1.7 Verification the plasmid

After purifying the DNA, 300 ng of plasmid was verified by double restriction digestion. A 10 µl reaction mixture containing 300 ng of plasmids, 1X or 2X of an enzyme-specific buffer according to the recommendation from the double digest calculator, 0.25 µl of each restriction enzyme, and nuclease-free water. Mix components by pipetting, spin briefly and incubate at 37°C for 1 h. Plasmids can be verified by gel electrophoresis according to this size. Plasmids were identified by Sanger sequencing at Eurofines company (Eurofines, Luxembourg) and pairwise sequence alignment was carried out by using DNASTAR Lasergene (DNASTAR, Inc., Madison, USA).

2.1.2 Quantitative real-time PCR

2.1.2.1 RNA isolation

Total RNA was purified from cells using the QIAGEN RNeasy® Mini Kit (QIAGEN, Venlo, Netherlands). Add 350 µl of RLT buffer and vortex to lyse the cells. Add 350 µl 70% ethanol before transfer. Transfer up to 700 µl of sample to an RNAeasy spin column with a 2 ml collection tube, centrifuge at 12,000 rpm for 1 min, and discard the flow-through. Add 700 µl of RW1 buffer to the spin column, centrifuge at 12,000 rpm for 1 min, and discard the flow-through. Wash the spin column twice with 500 µl REF buffer, centrifuge at 12,000 rpm for 1 min, and discard the flow-through. Add 30 µl RNase-free water to the spin column and centrifuge at full speed for 1 min to elute RNA into a new 1.5 ml collection tube. Total RNA was stored at -80°C for further usage.

2.1.2.2 cDNA synthesis

For each sample, 1,500 ng RNA was reverse transcribed by using the RevertAid H Minus First Strand cDNA Synthesis kit (Thermo Fisher Scientific, Waltham, USA). For cDNA synthesis, a 20 µl reaction mix containing 1500 ng RNA, 1 µl primer oligo (dT)18 primer, 4 µl 5X Reaction Buffer, 1 µl RiboLock RNase inhibitor, 1 µl RevertAid H Minus M-MuLV reverse transcriptase, 2 µl 10 mM dNTP mix, and nuclease-free water was mixed and incubated at 42°C for 1 h, at 70°C for 5 min. cDNA was stocked at -80°C for further usage.

2.1.2.3 Real-time PCR

Real-time PCR was used to analyze gene expression. cDNA was dissolved in nuclease-free water. Dilute cDNA at a concentration of 10 ng/µl in nuclease-free water. A 20 µl real-time PCR mixture containing 1 µl cDNA, 1 µl primer pair mix (10 pmol/µl each primer), 8 µl nuclease-free water, and 10 µl SYBR™ Green PCR Master Mix (Thermo Fisher Scientific, Waltham, USA) was mixed into each reaction tube. Amplification was carried out on the ABI PRISM 7700 with the following program: 95°C hold for 10 min, 40 cycles of 95°C for 15 s and 60°C for 1 min, followed by 95°C for 10 min. Relative quantification was performed by the 2(-Delta Delta C(T)) method using GAPDH as a housekeeping gene [274]. qPCR primers were used for this study, as shown in Table 3. qPCR primers were synthesized at Eourfines company (Eourfines, Luxembourg).

Table 3: List of qPCR primers.

| Gene | Forward (5' to 3') | Reverse (5' to 3') |
|---------------|-------------------------|---------------------------|
| <i>IFNB1</i> | CCTGTGGCAATTGAATGGGAGGC | CCAGGCACAGTGAAGTGTACTCCTT |
| <i>ISG54</i> | TCAGGTCAAGGATAGTCTGGAG | AGGTTGTGTATTCCCACACTGTA |
| <i>TNF-α</i> | CTGCACTTTGGAGTGATCGG | TCAGCTTGAGGGTTTGCTAC |
| <i>ISG15</i> | GTGGACAAATGCGACGAACC | TCGAAGGTCAGCCAGAACAG |
| <i>CXCL10</i> | ACGCTGTACCTGCATCAGCAT | CTCAACACGTGGACAAAATTGG |
| <i>GAPDH</i> | CAACAGCGACACCCACTCCT | CACCCTGTTGCTGTAGCCAAA |

2.2 Cell culture and virological methods

2.2.1 Cell culture of continuous immortalized cell lines

HEK293T and HEK293A cells were obtained from the American Type Culture Collection (ATCC) and maintained with Dulbecco's modified eagle complete medium (DMEM) (PAN-Biotech, Aidenbach, Germany), supplemented with 10% fetal bovine serum (FBS) (PAN-Biotech, Aidenbach, Germany), 2 mM L-glutamine (PAN-Biotech, Aidenbach, Germany), and 100 units per milliliter (U/ml) penicillin-streptomycin (PAN-Biotech, Aidenbach, Germany). Human monocytic THP-1 cells were obtained from ATCC and STING ckout THP-1 cells were obtained as a gift from Veit Hornung [270], cultured in Roswell Park Memorial Institute (RPMI) 1640 (Thermo Fisher Scientific, Waltham, USA) containing 10% FBS, 2 mM L-glutamine, and 100 U/ml penicillin-streptomycin. USP18KO THP-1 cells, ISG15KO THP-1 cells, THP-1-pLV2 cells, THP-1 cells expressing pEV, USP18, and its mutants C64A were generated as described before [252, 260]. HEK-Blue™ IFN- α/β cells (Invivogene, San Diego, USA) were cultured in DMEM supplemented with 10% FBS, 2 mM L-glutamine, 100 U/ml penicillin-streptomycin, 30 $\mu\text{g/ml}$ of blasticidin S hydrochloride (Sigma-Aldrich, Carlsbad, USA) and 100 $\mu\text{g/ml}$ of Zeocin™ (Invivogene, San Diego, USA). All cells grew at 37°C and 5% CO₂ and were handled under sterile conditions. For serial passaging, adherent cells were washed with DPBS and then incubated with 0.05% trypsin (PAN-Biotech, Aidenbach, Germany) for 1-2 min at 37°C. Suspension cells were harvested by centrifugation at 500 relative centrifugal force (rcf) for 5 min and resuspended in fresh medium. For long-term storage, cells were centrifuged at 500 rcf for 5 min and then resuspended in 1 ml 10% dimethyl sulfoxide (DMSO) (PanReac AppliChem, Chicago IL, USA) in FBS per cryo vial. Vials were placed in a Nalgene Mr. Frosty freezing container containing 100% isopropyl alcohol at -80°C for 48 h and transferred into liquid nitrogen.

2.2.2 Transfection of plasmid

HEK293T or HEK293A cells were seeded into 6-well/12-well plates (Sigma-Aldrich, Carlsbad, USA) and grown to 80% confluence before transfection. PolyJet™ in vitro DNA transfection reagent (SignaGen Laboratories, Frederick, USA) was used according to the instructions. For each well of a 6-well/12-well plate, dilute 2000/600 ng DNA into 100/50 µl DMEM and vortex gently. Dilute 4/2 µl of PolyJet™ reagent into 100/50 µl DMEM and vortex gently. Add diluted PolyJet™ reagent to dilute DNA solution and vortex gently followed by incubation for 10 min at RT. PolyJet™/DNA transfection complexes were added to cells.

2.2.3 Transfection of herring sperm DNA (HS-DNA)

To induce STING-mediated signaling activation, undifferentiated and PMA-differentiated THP-1 cells were transfected with 4 µg/ml herring sperm DNA (HS-DNA) (Thermo Fisher Scientific, Waltham, USA) using PolyJet™ reagent. Before transfection, the required 1.0×10^6 THP-1 cells per well were centrifuged in a 6-well plate at 150 rcf at room temperature for 10 min. The supernatant was completely removed, 200 µl pre-warmed fresh complete cell growth medium was added, and the plate was incubated at 37°C. For each well of a 6-well plate, dilute 8 µg HS-DNA into 100 µl DMEM and vortex gently. Dilute 6 µl of PolyJet™ reagent into 100 µl DMEM and vortex gently. Add diluted PolyJet™ reagent to diluted the DNA solution and vortexed gently, followed by incubation for 10 min at room temperature. PolyJet™/DNA transfection complexes were added to the cells and incubated at 37°C and 5% CO₂ for 30 min. At the end of incubation, 1.6 ml of pre-warmed fresh complete cell growth medium was added to each well, and the plate was incubated at 37°C with 5% CO₂ for the indicated time.

2.2.4 Virus production and transduction

HIV-1 luciferase reporter viruses were produced by transfecting 6-well-contained HEK293T cells with 600 ng of pMDLg/pRRE or pMDLx g/pRRE, 150 ng of pMD.G, 250 ng of pRSV-Rev, and 600 ng of pSIN.PPT.CMV.Luc.IRES.GFP with or without

pcDNA6/myc-His-VPX using PolyJet™ transfection reagent. The production of HIV-1-based lentiviruses for the generation of stable expression cell lines relied on cotransfection of HEK293T cells with 750 ng of packaging plasmid psPAX2, 200 ng of pMD.G, 250 ng of pRSV-Rev together with 750 ng of pLOC empty vector or pLOC vector containing insert gene using PolyJet™ transfection reagent. Supernatants were harvested 48 h posttransfection, purified by centrifugation at 5,000 rpm for 10 min at 4°C to remove cells, concentrated by ultracentrifugation at 14,000 rpm for 4 h at 4°C, resuspended in RPMI, and stored at -80°C.

For generation of stable expression THP-1 cell lines, THP-1 cells were transfected with HIV-1-based lentiviruses and spinoculated with 1,200 rcf for 2 h at 30°C. In reporter virus infection assays, THP-1 cells were spin-infected with HIV-1 luciferase reporter viruses at 1200 rcf for 2 h at 30°C. Two hours prior to infection, the cells were incubated at 37°C and 5% CO₂ for the indicated time.

Modified vaccinia virus ankara (MVA) is a gift from Prof. Dr. Ingo Drexler, Heinrich-Heine-Universität Düsseldorf, Düsseldorf, Germany. In briefly, MVA (cloned isolate F6) at 582nd passage on chicken embryo fibroblasts (CEF) were routinely propagated, purified by two consecutive ultracentrifugation steps through a 36 % (wt/vol) sucrose cushion and titrated following standard methodology [275].

2.2.5 HIV-1 luciferase activity assay

To determine the regulation of proteins of interest in HIV-1 infection, undifferentiated and differentiated THP-1 cells were infected with HIV-1 luciferase reporter viruses and the efficiency of HIV-1 infection was analyzed by a steady-glo luciferase assay (Promega, Madison, USA) system according to the manufacturer's instructions. For undifferentiated THP-1 cells, 1.5×10^5 THP-1 cells were seeded in 96 well plates with 60 µl of prewarmed fresh cell medium and cultured overnight. For phorbol-12-myristat-13-acetat (PMA)-differentiated THP-1 cells, 1.5×10^5 THP-1 cells per well were seeded with 60 µl prewarmed fresh cell medium containing 2 µg/ml PMA (Calbiochem, Darmstadt, Germany) for 24 h at 37°C and 5% CO₂. The PMA-containing medium was completely removed, and

the cells were washed one time with prewarmed DPBS, refilled with 60 μ l of prewarmed cell medium, and incubated overnight. Correspondingly, undifferentiated or PMA-differentiated THP-1 cells were infected with 50 μ l of HIV-1 luciferase reporter virus without or with Vpx. THP-1 cells were spinoculated at 1,200 rcf for 2 h at 30°C and then incubated at 37°C and 5% CO₂. After 72 h, infected cells were lysed with 100 μ l luciferase reagent and cell pallets were incubated at room temperature for 15 min in the dark. After incubation, transfer 100 μ l of cell lysate into black 96-well polypropylene microplates (Greiner Bio-One, Kremsmünster, Austria) and luminescence was measured for 10 seconds per well by using a Centro XS3 LB 960 microplate luminometer (Berthold Technologies Bioanalytic, Bad Wildbad, Germany).

2.2.6 Generation of reconstituted STING THP-1 cells

Reconstituted STING THP-1 cells were generated by transduction of STINGKO THP-1 cells with lentiviral vector. HIV-1-based lentiviral vector particles were produced by transfecting HEK293T cells with pLOC vector or pLOC vector containing insert gene, packaging plasmid psPAX2, pMD.G, and pRSV-Rev. At 48 h posttransfection, viral supernatants were harvested and concentrated. STINGKO THP-1 cells were transduced with the HIV-1 pseudovirus for 48 h. Transduced cells were selected in a fresh complete cell growth medium containing 5 μ g/ml blasticidin S for 10 days. The efficiency of reconstituted STING expression of the gene was tested by immunoblot analysis (Fig. 8).

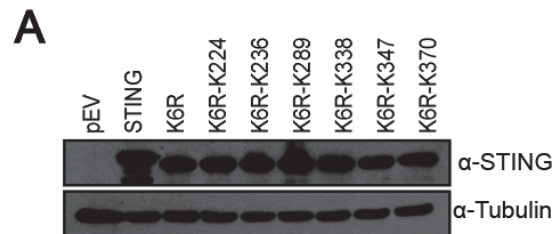


Fig. 8: Generation of reconstituted STING THP-1 cells. (A) Protein lysates from reconstituted STING THP-1 cells were immunoblotted with the indicated antibodies.

2.2.7 Type I interferon production assay

Type I IFN production assay was performed by using HEK-Blue™ IFN- α/β cells as previously described [276]. These cells stably express a reporter gene containing a secreted embryonic alkaline phosphatase (SEAP) under the control of the ISG54 promoter. Briefly, HEK293A cells were transfected with STING and its mutant plasmids for the indicated times. Alternatively, THP-1 cells were infected with HIV-1 or MVA, transfected with 4 $\mu\text{g/ml}$ HS-DNA, or stimulated with 3.6 μM STING agonist SR-717 for indicated times (STING agonist SR-717 is a gift from Prof. Dr. Thomas Kurz, Heinrich-Heine-Universität Düsseldorf, Düsseldorf, Germany). STING agonist SR-717 was synthesized according to the described method [90]. 20 μl of supernatant was added to 180 μl of fresh complete cell growth medium containing 50,000 per well HEK-Blue™ IFN- α/β cells in a flat-bottom 96-well plate (Sigma-Aldrich, Carlsbad, USA). After 20 h of incubation at 37°C and 5% CO₂, 20 μl of reporter cell-induced supernatant was added into 180 μl of resuspended QUANTI-Blue™ solution (Invivogene, San Diego, USA) in a flat-bottom 96-well plate and incubate for 1 h at 37°C. Determine SEAP levels using a Multiskan Spectrum spectrophotometer (Thermo Fisher Scientific, Waltham, USA) at 630 nm.

2.3 Protein biochemistry

2.3.1 Cell lysis and micro volume protein concentration determination

The indicated cells were harvested and washed with cold DPBS and lysed for 20 min on ice with 100 μl of cold mild lysis buffer (50 mM Tris (hydroxymethyl) aminomethane (Tris-HCl) [pH 8], 150 mM natriumchlorid (Carl Roth, Karlsruhe, Germany), 0.8% octylphenoxypolyethoxylethanol (NP-40) (PanReac AppliChem, Chicago IL, USA), 10% glycerol (PanReac AppliChem, Chicago IL, USA), 1mM phenylmethanesulfonyl fluoride solution, a tablet of protease inhibitor cocktail III (Sigma-Aldrich, Carlsbad, USA) and 1% phosphatase inhibitor cocktail I (MedChemExpress, South Brunswick Township, USA). Cell lysis was subsequently cleared by centrifugation at 14,000 rpm for 20 min at 4 °C. Protein concentrations were subsequently calculated using protein A280 application from

the NanoDrop 1000 spectrophotometer (Thermo Fisher Scientific, Waltham, USA). Using water, a blank was established, and 2 μ l sample was pipetted for protein concentration determination.

2.3.2 Western blotting assay

Polyacrylamide gels were prepared according to the instructions in Table 5. For the sodium dodecyl-sulfate polyacrylamide gel electrophoresis (SDS–PAGE) assay, the same amount of protein was mixed with ROTI®Load 1, reduced loading buffer (Carl Roth, Karlsruhe, Germany) and heated at 95°C for 5 min. For the STING dimerization assay, the same amount of protein mixed with NuPAGE LDS sample buffer (Thermo Fisher Scientific Scientific, Waltham, USA). Samples as well as prestained protein molecular weight marker (Thermo Fisher Scientific Scientific, Waltham, USA) were loaded into the gel wells. Electrophoretic separation of proteins was performed on ice for a constant 130 V in 1 X solution of sodium dodecyl-sulfate (SDS) running buffer. Proteins were transferred from gels to a polyvinylidene fluoride (PVDF) membrane (Sigma-Aldrich, Carlsbad, USA) under a constant 20 V for 1 h using a Bio-Rad semidry transfer cell (Bio-Rad, Hercules, USA) in a semi-dry transfer method. Briefly, the semidry transfer method contains the following layers: SDS-containing transfer buffer prewetted filter paper (Bio-Rad, Hercules, USA), methanol (Carl Roth, Karlsruhe, Germany) prewetted PVDF membrane, SDS gel, and SDS-containing transfer buffer prewetted filter paper. Membranes were blocked with 5% nonfat milk (PanReac AppliChem, Chicago IL, USA) solution or 5% bovine serum albumin (BSA) (Thermo Fisher Scientific, Waltham, USA) solution for 1 h at room temperature. The membranes were incubated in the primary antibody solution overnight at 4°C with gentle agitation. The next day, membranes were washed three times for 10 min each with TBST buffer before HRP-linked secondary antibody was incubated for 2 h with gentle agitation at RT. Afterwards, the membranes were washed three times for 10 min each with TBST. Finally, membranes were incubated in the Amersham™ ECL Prime Western-Blot detection reagent (GE Healthcare, Chicago, USA) according

to the manufacturer's directions and signaling was captured with a ChemiDoc MP imaging system (Bio-Rad, Hercules, USA). Antibodies used in this study are shown in Table 5.

Table 4: Pipetting scheme for SDS gels

| | Stacking gel 10% | Separating gel 10% |
|--|-------------------------|---------------------------|
| Rotiphorese® Gel 30 (37.5:1) (Carl Roth, Karlsruhe, Germany) | 840 µl | 5 ml |
| 1.5 mole (M) Tris-HCl pH 8.6 (PanReac AppliChem, Chicago IL, USA) | / | 3.75 ml |
| 1 M Tris-HCl pH 6.8 (PanReac AppliChem, Chicago IL, USA) | 630 µl | / |
| 10% SDS (PanReac AppliChem, Chicago IL, USA) | 50 µl | 150 µl |
| 20% Ammonium persulphate solution (APS) (Sigma-Aldrich, Carlsbad, USA) | 25 µl | 75 µl |
| N, N, N', N'- Tetramethylethylenediamine (TEMED) (VWR, Radnor, PA/USA) | 5 µl | 15 µl |
| H ₂ O | 3.5 ml | 6.1 ml |

Table 5: Antibodies for western blotting

| Antibody | Source & Identifier& Supplier | Dilution |
|-----------------|--|-----------------|
| anti-USP18 | 4813S (Cell Signaling Technology, Danvers, USA) | 1/1,000 |
| anti-ISG15 | 15981-1-AP (Proteintech, Rosemont, USA) | 1/1,000 |
| anti-STING | 13647S (Cell Signaling Technology, Danvers, USA) | 1/1,000 |
| anti-p-STING | 19781S (Cell Signaling Technology, Danvers, USA) | 1/1,000 |
| anti-TBK1 | 3504S (Cell Signaling Technology, Danvers, USA) | 1/1,000 |
| anti-p-TBK1 | 5483S (Cell Signaling Technology, Danvers, USA) | 1/1,000 |
| anti-IRF3 | 4302S (Cell Signaling Technology, Danvers, USA) | 1/1,000 |
| anti-IRF3 | ab238521 (Abcam, Cambridge, UK) | 1/1,000 |
| anti-p-IRF3 | 4947S (Cell Signaling Technology, Danvers, USA) | 1/1,000 |

| Antibody | Source & Identifier& Supplier | Dilution |
|---------------------------------------|---|----------|
| anti-p-IRF3 | ab76493 (Abcam, Cambridge, UK) | 1/1,000 |
| anti-p53 | OP43 (Oncogene, California, USA) | 1/500 |
| anti-GAPDH | EB06377 (Everest Biotech, Bicester, UK) | 1/10,000 |
| anti-Tubulin | T6074 (Sigma-Aldrich, Carlsbad, USA) | 1/10,000 |
| anti-V5 | V8137 (Sigma-Aldrich, Carlsbad, USA) | 1/5,000 |
| anti-HA | 51064-2-AP (Proteintech, Rosemont, USA) | 1/5,000 |
| HRP-conjugated sheep anti-mouse IgG | NA931V (GE Healthcare, Chicago, USA) | 1/10,000 |
| HRP-conjugated donkey anti-rabbit IgG | NA9340V (GE Healthcare, Chicago, USA) | 1/10,000 |
| HRP-conjugated mouse anti-goat IgG | sc-2354 (Santa Cruz Biotechnology, Dallas, USA) | 1/10,000 |

2.3.3 Native–PAGE assay

Native polyacrylamide gel electrophoresis (Native–PAGE) was performed to measure STING oligomerization. Native gels were prepared according to the instructions in Table 6 [277]. Following transfection of plasmids into HEK-293A or stimulation of THP-1 cells, cells were collected by DPBS and lysed by mild lysis buffer on ice. The same amount of protein lysate was mixed with a sample buffer. Run the gel in 1 X running buffer under a constant 100 V for 2 h on ice. The transfer cassette by layering the following: transfer buffer prewetted filter paper, methanol prewetted PVDF membrane, native gel, and transfer buffer prewetted filter paper. After transfer, the membranes were blocked with 5% nonfat milk solution, and the remaining steps were proceed.

Table 6: Pipetting scheme for native gels

| | Stacking gel | Separating gel |
|------------------------------|--------------|----------------|
| Rotiphorese® Gel 30 (37.5:1) | 1 ml | 6 ml |
| 1.5 M Tris-HCl pH 8.6 | / | 9.5 ml |
| 2.5 M Tris-HCl pH 6.8 | 2.5 ml | / |
| 20% APS | 45 µl | 240 µl |
| TEMED | 22.5 µl | 12 µl |
| H ₂ O | 8.3 ml | 8.3 ml |

2.3.4 Immunoprecipitation for ISGylation assay

ISGylation assay was performed as described previously [252]. For analyzing the ISGylation of STING, HEK293A cells transfected with plasmids for STING-HA, STING-HA and USP18, or STING-HA and active-site mutants of USP18 (C64A or C64S) in the presence of ISG15 and its conjugating enzymes E1 (UBE1L) and E2 (UBCH8) for 48 h or reconstituted STING THP-1 cells were stimulated with 500 U/ml IFN- β (PBL Assay Science, New Jersey, USA), infected with HIV-1, stimulated with 3.6 μ M STING agonists SR-717, or transfected with HS-DNA for 48 h. Cells were harvested by cold DPBS and lysed by 400 μ l mild lysis buffer for 20 min on ice. Samples were cleared by centrifugation at 20,000rcf for 30 min at 4°C. 360 μ l of whole cell lysates were gently rotated overnight at 4°C with 10 μ l of anti-HA affinity matrix (Sigma-Aldrich, Carlsbad, USA). Beads were washed three times with 1 ml of mild lysis buffer on ice. Affinity-tagged proteins were eluted by boiling the beads for 5 min at 95°C in a reducing loading buffer. The rest of the lysates were mixed with reducing loading buffer and heated at 95°C for 5 min. Both immunoprecipitates and the the rest cell lysates were subjected to SDS-PAGE.

2.4 Statistical analysis

Statistical analysis was performed with GraphPad Prism 8.0 (GraphPad Software Inc., La Jolla, CA, USA). Data is plotted as individual points and data summary were given as mean \pm standard deviation. For all statistical analyses, an alpha of

0.05 was used as the significance. Unpaired Student's *t*-tests were used for two group comparisons. If sample sizes in both conditions were equal, an unpaired two-tailed Student's *t*-test was applied. If values were normalized to an internal control, one-sample *t*-tests was used. Multiple comparison procedures were used in one-way analysis of variance or two-way analysis of variance.

3 Results

3.1 USP18 engages STING-mediated cytosolic DNA sensing pathway in a p53-dependent manner

3.1.1 Ectopic expression of USP18 promotes HIV-1 infection

To investigate the potential roles of USP18 in HIV-1 infection, recognition, and sensing in innate cells, we examined the effects of ectopic expression of USP18 on HIV-1 infection and induction of type I IFN triggered by HIV-1 infection. We generated ectopic expression of USP18 in THP-1 cells by using the HIV-1-based lentivirus system (Fig. 9A) [260]. Similar to our previous observations [260], we found that ectopic expression of USP18 in undifferentiated and PMA-differentiated THP-1 cells promoted HIV-1 infection compared to vector control cells (Fig. 9B). These results suggested that USP18 enhances HIV-1 infection.

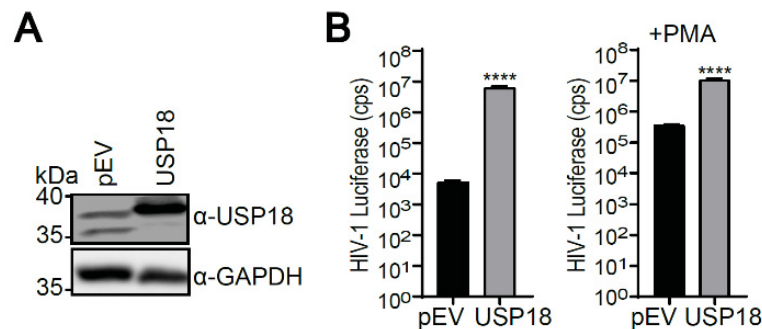


Fig. 9: Ectopic expression of USP18 enhances HIV-1 infection. (A) Protein lysates from undifferentiated THP-1.USP18 and THP-1.pEV cells were immunoblotted with the indicated antibodies. (B) Undifferentiated or PMA-differentiated THP-1.USP18 and THP-1.pEV cells were transduced with HIV-1 luciferase reporter virus for 72 h followed by luciferase activity analysis. Significance was determined using two-tailed Student's *t*-test (Fig. 9B) (**P* < 0.05, ***P* < 0.01, ****P* < 0.001, and *****P* < 0.0001). Data are representative of three independent experiments (graphs show mean ± SD).

3.1.2 Ectopic expression of USP18 represses HIV-1 sensing signaling

Upon HIV-1 infection, nucleic acid and reverse transcription products of HIV-1 can be sensed by cell-expressed cytoplasmic innate immune sensors, leading to the induction of type I IFN and downstream antiviral genes [26]. We next used HEK-

IFN- α/β -reporter cells to measure the induction of type I IFN in HIV-1 infected THP-1.USP18 cells. As shown in Fig. 10A, HIV-1 infection-induced production of type I IFN was markedly attenuated in USP18-expressing THP-1 cells in comparison to vector control cells. Correlating with the decreased type I IFN production observed in the THP-1.USP18 cells, USP18 inhibited the transcription of *IFNB1*, *ISG54* and *TNF- α* genes triggered by HIV-1 infection in undifferentiated and PMA-differentiated THP-1 cells (Fig. 10B). These results suggest that USP18 negatively regulates the activation of sensing signaling of HIV-1.

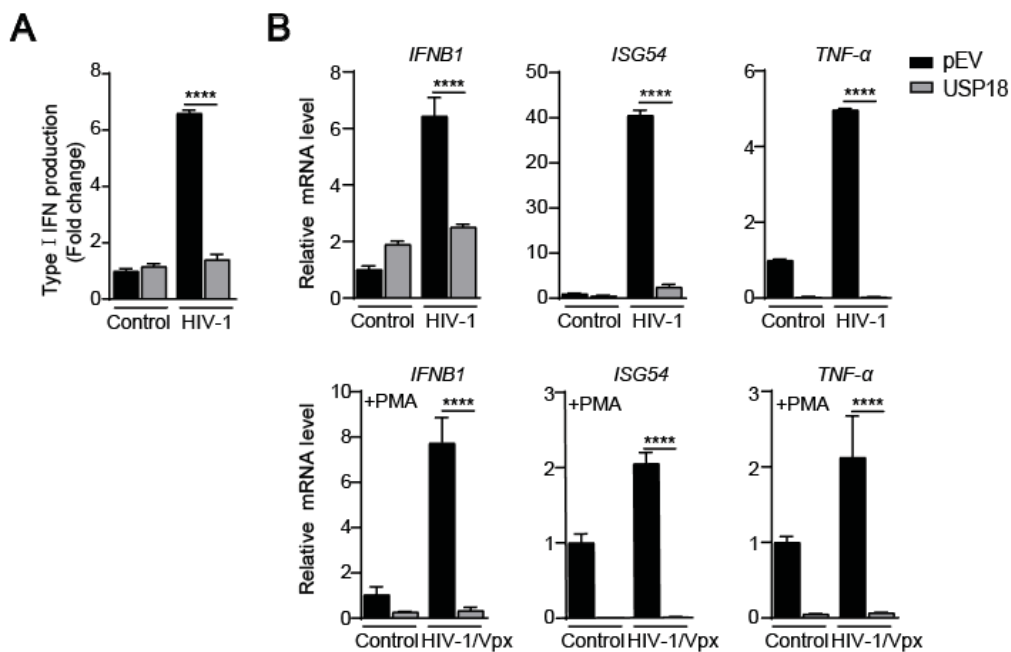


Fig. 10: USP18 suppresses HIV-1 sensing signaling. (A) THP-1.USP18 and THP-1.pEV cells were transduced with HIV-1 luciferase reporter virus for 72 h followed by interferon production analysis. (B) RT-qPCR analysis of *IFNB1*, *ISG54*, and *TNF- α* mRNA in undifferentiated and PMA-differentiated THP-1.USP18 and THP-1.pEV cells infected with HIV-1 or HIV-1/Vpx for 24 h. Significance was determined using two-tailed Student's *t*-test (Figs. 10A-10B) (**P* < 0.05, ***P* < 0.01, ****P* < 0.001, and *****P* < 0.0001). Data are representative of three independent experiments (graphs show mean \pm SD).

3.1.3 Ectopic expression of USP18 represses sensing of cytosolic DNA

Previous studies have demonstrated that USP18 interferes with the DNA sensing pathway [108]. We next investigated the roles of USP18 in sensing DNA viruses

and cytosolic DNA. We examined the production of type I IFN induced by cytosolic DNA-stimulated THP-1 cells. The results indicated that USP18 expression inhibited the induction of type I IFN in response to MVA infection and double strand DNA transfection (Fig. 11A).

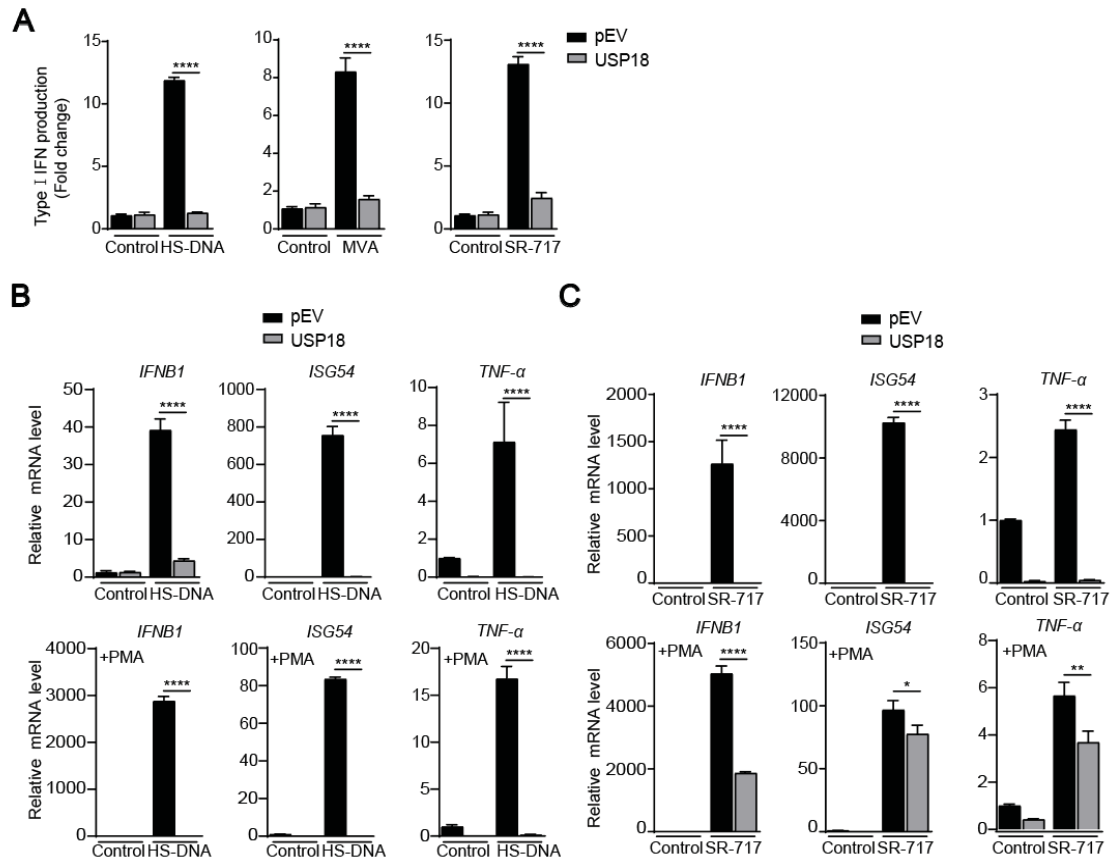


Fig. 11: USP18 inhibits cytosolic DNA sensing signaling. (A) THP-1.USP18 and THP-1.pEV cells infected with MVA, transfected with 4 μ g/ml HS-DNA, or stimulated with 3.6 μ M STING agonist SR-717 for 48 h followed by interferon production analysis. (B and C) RT-qPCR analysis of *IFNB1*, *ISG54*, and *TNF- α* mRNA in undifferentiated and PMA-differentiated THP-1.USP18 and THP-1.pEV cells transfected with 4 μ g/ml HS-DNA for 24 h (B) or stimulated with 3.6 μ M STING agonist SR-717 for 2 h (C). Significance was determined using two-tailed Student's *t*-test (Figs.11A-11C) (**P* < 0.05, ***P* < 0.01, ****P* < 0.001, and*****P* < 0.0001). Data are representative of three independent experiments (graphs show mean \pm SD).

At present, multiple DNA sensors have been proposed to use STING as a key adaptor protein to activate downstream signaling [278]. Furthermore, we evaluated the effect of USP18 in response to STING agonist SR-717-induced type I IFN

production [90]. Consistently, USP18 abolished STING agonist SR-717-induced the production of type I IFN (Fig. 11A). qPCR analysis indicated that cytosolic DNA transfection or STING agonist SR-717 stimulation-induced the expression of *IFNB1*, *ISG54* and *TNF- α* genes was impaired in THP-1.USP18 cells (Figs.11B and 11C). These results indicated that USP18 expression suppresses STING-dependent sensing signaling in innate immune cells.

3.1.4 USP18 deficiency upregulates sensing of HIV-1 and cytosolic DNA

To further characterize the effects of USP18 on cellular DNA sensing signaling, USP18-deficient THP-1 cells were generated by using the CRISPR-Cas9 method (Fig. 12A) [260]. The results from the HIV-1 infection assay showed that the efficiency of HIV-1 infection was impaired in undifferentiated and PMA-differentiated USP18-knockout THP-1 cells (Fig. 12B). In contrast to USP18 overexpressing THP-1 cells, USP18 knockout THP-1 cells potentiated type I IFN production in response to HIV-1 infection (Fig.12C). Similarly, STING agonist stimulation or MVA-induced IFN production was increased in the absence of USP18 (Fig.12C). These observations correlated with increased *IFNB1* mRNA induction in the undifferentiated and differentiated THP-1-USP18KO cells in response to HS-DNA transfection or STING agonist SR-717 stimulation compared to vector control cells (Fig. 12D). In summary, USP18 plays a major role in STING-mediated sensing signaling activation.

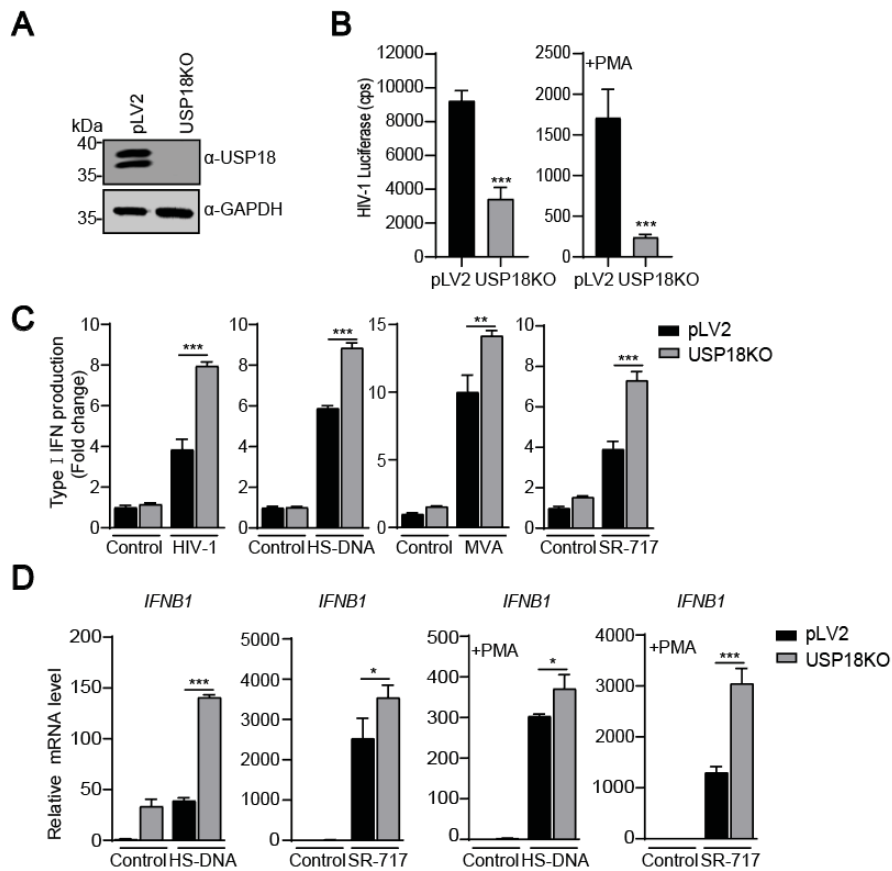


Fig. 12: Deletion of USP18 enhances sensing of HIV-1 and cytosolic DNA. (A) Protein lysates from THP-1.USP18KO and THP-1.pLV2 cells were immunoblotted with the indicated antibodies. (B) Undifferentiated or PMA-differentiated THP-1.USP18KO and THP-1. pLV2 cells were transduced with HIV-1 luciferase reporter virus for 72 h followed by luciferase activity analysis. (C) THP-1.USP18KO and THP-1.pLV2 cells infected with HIV-1 or MVA, transfected with 4 μ g/ml HS-DNA, or stimulated with 3.6 μ M STING agonist SR-717 for 48 h followed by interferon production analysis. (D) RT-qPCR analysis of *IFNB1* mRNA in undifferentiated and PMA-differentiated THP-1.USP18KO and THP-1.pLV2 cells transfected with 4 μ g/ml HS-DNA for 24 h or stimulated with 3.6 μ M STING agonist SR-717 for 2 h. Significance was determined using two-tailed Student's *t*-test (Figs.12B-12D) (**P* < 0.05, ***P* < 0.01, ****P* < 0.001, and *****P* < 0.0001). Data are representative of three independent experiments (graphs show mean \pm SD).

3.1.5 USP18 inhibits STING expression and counteracts STING activation

The induction of type I IFN was significantly dampened in STING agonist SR-717-stimulated THP-1.USP18 cells, whereas deletion of USP18 promoted antiviral

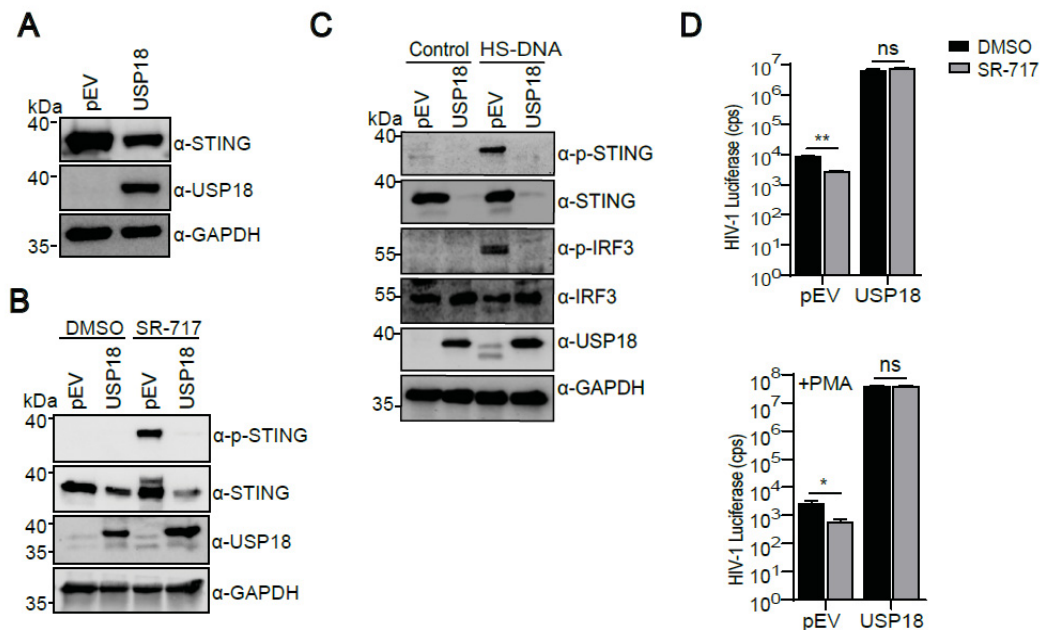


Fig. 13: USP18 inhibits STING expression and STING-dependent antiviral immunity. (A) Protein lysates from THP-1.USP18 and THP-1.pEV cells were immunoblotted with the indicated antibodies. (B and C) THP-1.USP18 and THP-1.pEV cells were stimulated with 3.6 μ M STING agonist SR-717 for 1 h (B) or transfected with 4 μ g/ml HS-DNA for 24 h (C) followed by immunoblotting analysis with the indicated antibodies. (D) Undifferentiated and PMA-differentiated THP-1.USP18 and THP-1.pEV cells were stimulated with 3.6 μ M STING agonist SR-717 or DMSO for 12 h and then infected with HIV-1 for 72 h and analyzed by luciferase activity analysis. Significance was determined using two-tailed Student's *t*-test (Fig. 13D). (**P* < 0.05, ***P* < 0.01, ****P* < 0.001, and *****P* < 0.0001). Data are representative of three independent experiments (graphs show mean \pm SD).

gene expression in response to STING agonist SR-717 stimulation, we reasoned that USP18 inhibited cellular antiviral immune responses at the level of STING. We performed with western blotting assay and found that the expression of STING was markedly attenuated in THP-1.USP18 cells compared with vector control cells (Fig. 13A). In the next step, we evaluated the STING-dependent signaling activation. As shown in Fig.13B, STING agonist SR-717 stimulation or HS-DNA transfection-induced phosphorylation of STING and IRF3 was substantially inhibited in the presence of USP18, suggesting that USP18 negatively regulates cytosolic DNA sensing signaling in a STING-dependent manner (Fig. 13C). The STING agonist

SR-717 acts as a cGAMP mimetic that induces the same “closed” conformation of STING, thus enhancing STING-dependent antitumor immunity and diverse STING-dependent biological processes [90]. Furthermore, we examined the antiviral function of the STING agonist SR-717 in THP-1.USP18 cells and found that the presence of USP18 abrogated the STING agonist SR-717-induced antiviral defense in response to HIV-1 infection (Fig.13D). Together, these data demonstrated that USP18 attenuates STING expression and STING-dependent antiviral defense.

3.1.6 USP18 deficiency promotes STING expression and its activation

Previous study reported that knockout of USP18 promotes induction of type I IFN and inhibition of HIV-1 infection in macrophages [279]. To further confirm the regulatory effect of USP18 on STING expression, we then investigated the expression and activation of STING in USP18 depleted THP-1 cells. As shown in Figs.14A-14C, USP18 knockout promoted the expression of STING as well as the phosphorylation level of STING in response to STING agonist SR-717 or cytosolic DNA stimulation. We next examined the effect of STING agonist-induced antiviral function in the absence of USP18 and found that USP18 deficiency potentiated the induction of type I IFN and dampened the infection of HIV-1 compared with vector control THP-1 cells, which was associated with upregulated expression of STING (Fig.14D). Collectively, these data supported that USP18 negatively regulates cytosolic DNA-triggered innate sensing.

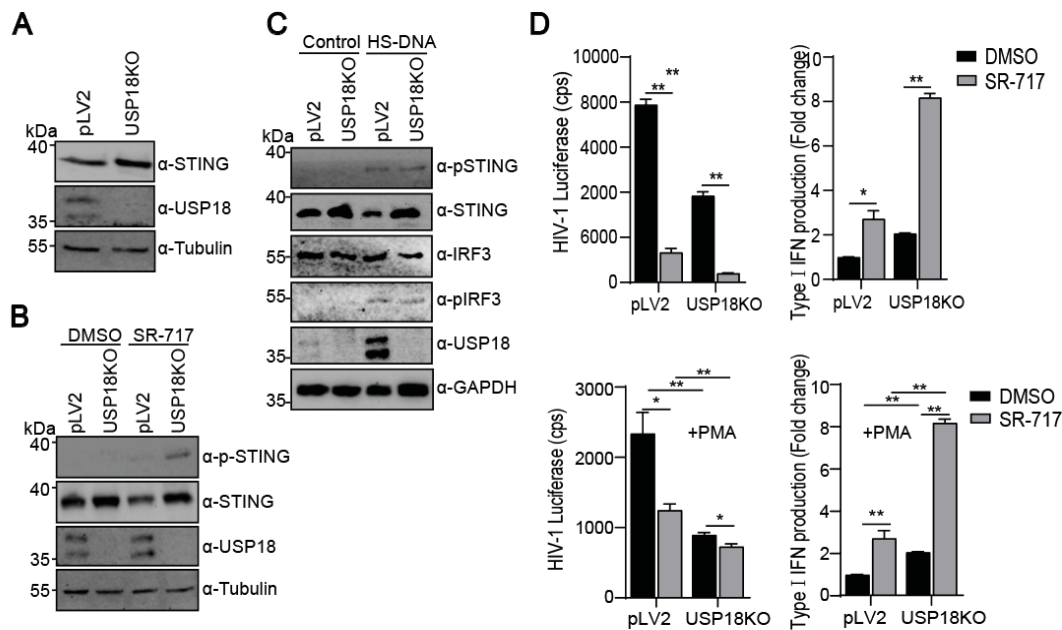


Fig. 14: Deletion of USP18 enhances STING expression and its activation. (A) Protein lysates from THP-1.USP18KO and THP-1.pLV2 cells were immunoblotted with the indicated antibodies. (B and C) THP-1.USP18KO and THP-1.pLV2 cells were stimulated with 3.6 μ M STING agonist SR-717 for 1 h (B) or transfected with 4 μ g/ml HS-DNA for 24 h (C) followed by immunoblotting analysis with the indicated antibodies. (D) Undifferentiated and PMA-differentiated THP-1.USP18KO and THP-1.pLV2 cells were stimulated with 3.6 μ M STING agonist SR-717 or DMSO for 12 h and then infected with HIV-1 for 72 h and analyzed by luciferase activity analysis and interferon production analysis. Significance was determined using two-way ANOVA (Fig.14D) (* $P < 0.05$, ** $P < 0.01$, *** $P < 0.001$, and **** $P < 0.0001$). Data are representative of three independent experiments (graphs show mean \pm SD).

3.1.7 USP18 destabilizes STING not at protein level

To characterize the mechanism of reduced expression of STING in the presence of USP18, we coexpressed STING and USP18 in HEK293A cells. Immunoblot analysis showed that STING expression was not decreased with the increased expression of USP18 (Fig.15A). It has been reported that STING degradation is regulated by both ubiquitin-proteasomal and lysosomal-dependent pathways [95, 103]. As shown in Fig.15B, inhibition of the proteasome pathway by MG132 failed to restore STING expression in the presence of USP18. In addition, treatment with the autophagosome inhibitor bafilomycin A1 (BafA1) did not change the low

expression of STING in THP-1.USP18 cells (Fig.15B), indicating that USP18 destabilizes STING expression, but not at the protein level.

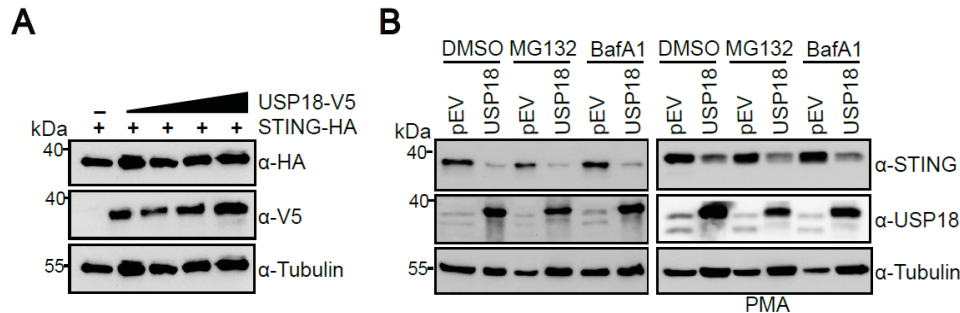


Fig. 15: USP18 suppresses STING but not at the protein level. (A) HEK293A cells were transfected with the indicated plasmids for 30 h followed by immunoblotting analysis with the indicated antibodies. (B) Undifferentiated and PMA-differentiated THP-1.USP18 and THP-1.pEV cells were treated with DMSO, 10 μ M MG132, or 10 nM BafA1 for 24 h followed by immunoblotting analysis with the indicated antibodies. Data are representative of three independent experiments.

3.1.8 USP18 regulates STING at the mRNA level

To explore whether USP18 regulates the mRNA level of STING, *STING* mRNA determined by RT-qPCR assay. As shown in Fig. 16A, the expression level of the *STING* gene was significantly reduced in USP18.TH1 cells, indicating USP18 inhibits STING expression at the mRNA level.

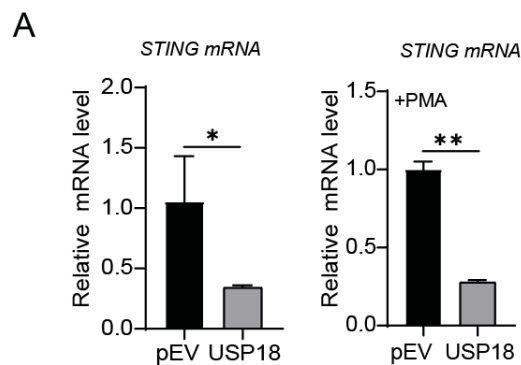


Fig. 16. USP18 regulates STING at the mRNA level. (A) RT-qPCR analysis of *STING* mRNA in undifferentiated and PMA-differentiated THP-1.USP18 and THP-1.pEV cells. Significance was determined using two-tailed Student's *t*-test (Fig.16A) (**P* < 0.05, ***P* < 0.01, ****P* < 0.001, and *****P* < 0.0001). Data are representative of three independent experiments (graphs show mean \pm SD).

3.1.9 USP18 catalytic activity regulates STING expression and STING mediated signaling activation

Considering that USP18 exhibits both enzymatic and nonenzymatic activities, we next asked whether the protease activity of USP18 directly regulates the stability of STING. Interestingly, the variants of USP18 lacking the active site cysteine (USP18-C64A) showed no inhibition of STING protein expression (Fig. 17A).

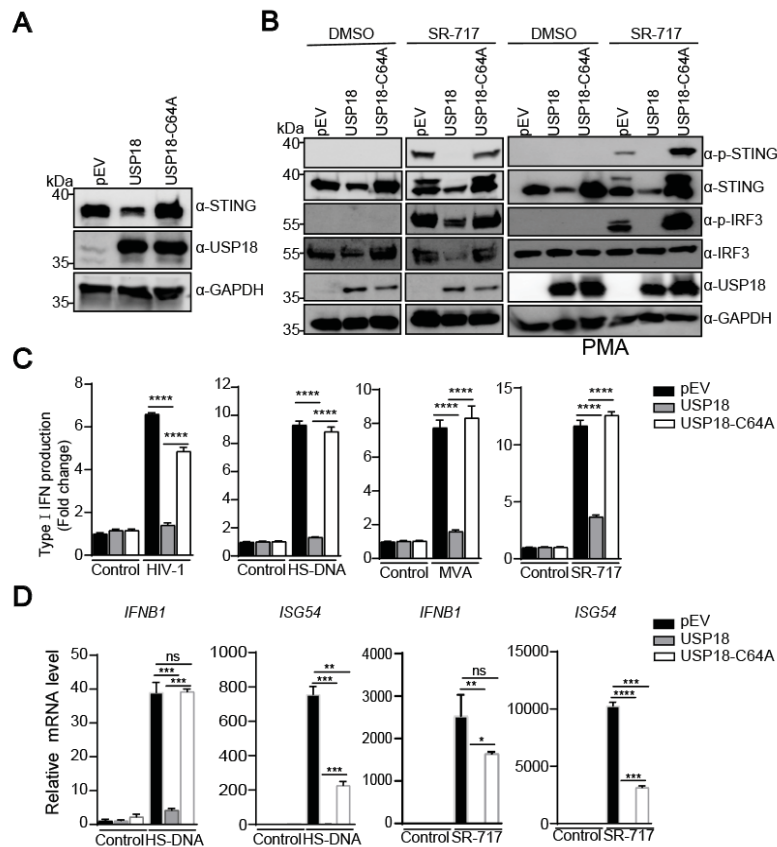


Fig. 17: USP18 catalytic activity is essential for STING expression and its activation. (A) Protein lysates from THP-1.USP18, THP-1.USP18-C64A, and THP-1.pEV cells were immunoblotted with the indicated antibodies. (B) THP-1.USP18, THP-1.USP18-C64A, and THP-1.pEV cells were stimulated with 3.6 μ M STING agonist SR-717 for 1 h followed by immunoblotting analysis with the indicated antibodies. (C) THP-1.USP18, THP-1.USP18-C64A, and THP-1.pEV cells were infected with HIV-1 or MVA, transfected with 4 μ g/ml HS-DNA, or stimulated with 3.6 μ M STING agonist SR-717 for 48 h followed by interferon production analysis. (D) THP-1.USP18, THP-1.USP18-C64A, and THP-1.pEV cells were transfected with 4 μ g/ml HS-DNA for 24 h or stimulated with 3.6 μ M STING agonist SR-717 for 2 h and analyzed by RT-qPCR analysis. Significance was determined using one-way ANOVA (Figs. 17C-17D) (* $P < 0.05$, ** $P < 0.01$, *** $P < 0.001$, and **** $P < 0.0001$). Data are representative of three independent experiments (graphs show mean \pm SD).

Next, We examined key molecules in STING-triggered signaling and found that with restoration of STING protein levels, STING and IRF3 phosphorylation were restored in USP18-C64A THP-1 cells in response to stimulation with the STING agonist SR-717 (Fig. 17B). Consistent with this notion, USP18-C64A THP-1 cells, but not THP-1.USP18 cells, restored the induction of type I IFN in the presence of HIV-1 and MVA infection, HS-DNA transfection, and STING agonist SR-717 stimulation (Fig. 17C). Consistently, USP18 expression inhibited mRNA levels of *IFNB1* and *ISG54* induced by the STING agonist SR-717 or cytosolic DNA stimulation, whereas USP18-C64A cells reversed the expression these genes under stimulation (Fig. 17D). Take together, these data suggest that USP18 catalytic activity is essential for STING expression and STING-dependent signaling activation.

3.1.10 USP18 catalytic activity regulates the stability of STING mRNA

USP18 represses STING expression at the mRNA level in THP-1 cells. Furthermore, we tested whether the mRNA level of STING is regulated by USP18 lacking the active site cysteine. We observed that the mRNA level of STING was restored in THP-1 cells with the USP18-C64A expression compared with THP-1.USP18 cells (Fig. 18A). These results suggest that USP18 catalytic activity is required for the regulation of STING stability.

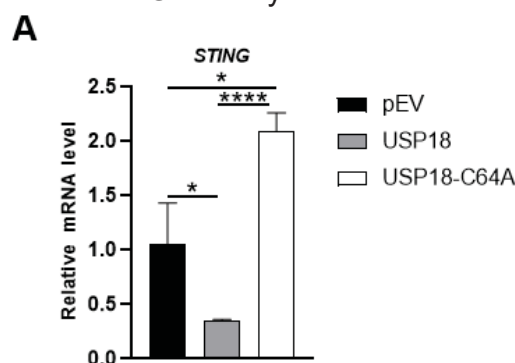


Fig. 18: USP18 catalytic activity regulates STING mRNA stability. (A) RT-qPCR analysis of *STING* mRNA in THP1.USP18, THP1.USP18-C64A, and THP-1.pEV cells. Significance was determined using one-way ANOVA (Fig.18A) (*P < 0.05, **P < 0.01, ***P < 0.001, and ****P < 0.0001). Data are representative of three independent experiments (graphs show mean ± SD).

3.1.11 Ectopic expression of USP18 or ISG15 deficiency inhibit STING expression in a p53-dependent manner

A recent report demonstrated that functional p53 acts as a transcription factor that regulated the expression of the *STING* gene [119]. Our previous studies reported that USP18 wild-type but not USP18-C64A expression leads to the accumulation of dominant negative p53 and inhibition of overall p53 activity [252]. These findings led us to investigate whether STING is regulated in p53-dependent manner. We next performed immunoblot analysis to investigate the relationship between STING and p53 in USP18.THP-1 cells. Notably, the expression of USP18 induced with low expression of STING and accumulation of misfolded p53 in cells (Fig. 19A).

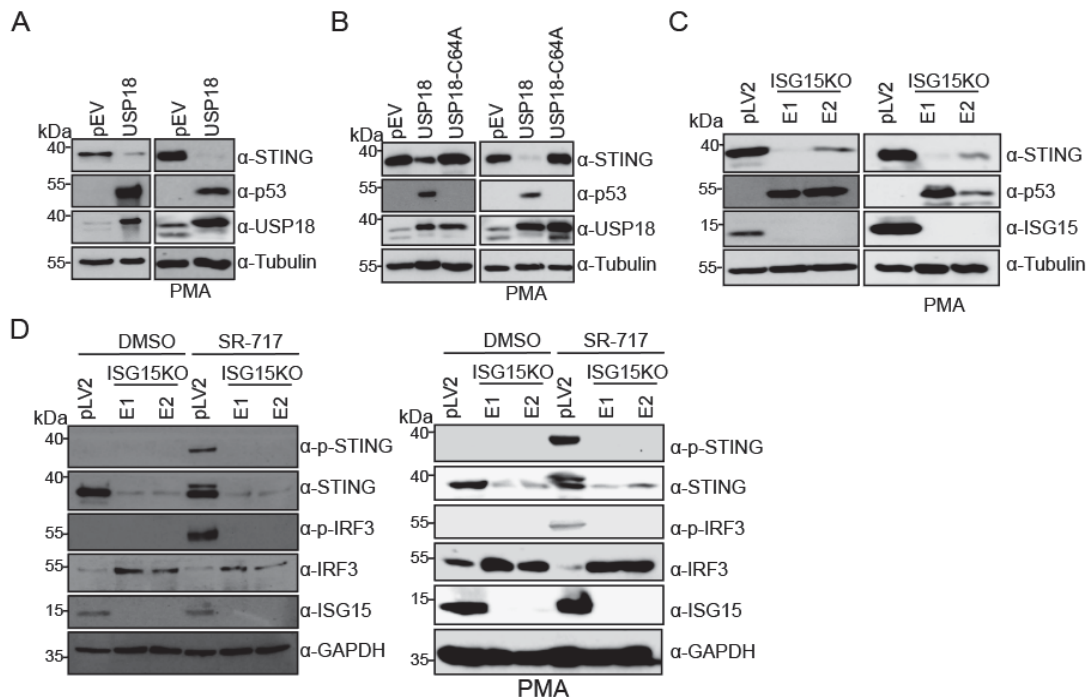


Fig. 19: USP18 or ISG15 deletion represses STING in a p53-dependent manner. (A) Protein lysates from undifferentiated and PMA-differentiated THP-1.USP18 and THP-1.pEV cells were immunoblotted with the indicated antibodies. (B) Protein lysates from undifferentiated and PMA-differentiated THP-1.USP18, THP-1.USP18-C64A, and THP-1.pEV cells were immunoblotted with the indicated antibodies. (C) Protein lysates from undifferentiated and PMA-differentiated THP-1.ISG15KO and THP-1.pLV2 cells were immunoblotted with the indicated antibodies. (D) Protein lysates from undifferentiated and PMA-differentiated THP-1.ISG15KO and THP-1.pLV2 cells were stimulated with 3.6 μ M STING agonist SR-717 for 2 h followed by immunoblotting analysis with the indicated antibodies. Data are representative of three independent experiments.

In nontransformed cells, ISGylation of misfolded p53 serves as a proteasomal degradation signal [247, 250]. Wild-type USP18, but not the active site mutant USP18-C64A acts as a deISGylation enzyme, which cleaves ISG15 from misfolded p53, resulting in the accumulation of dominant negative p53 and the inhibition of wild-type p53 activity [252]. We found that STING expression was restored in the presence of USP18-C64A (Fig. 19B). Indeed, misfolded p53 accumulates in the ISG15-deficient THP-1 cells [252]. To further support this hypothesis, we next performed immunoblot analysis and found that ISG15 deletion induced the accumulation of p53 and attenuated the expression of STING (Fig. 19C). Furthermore, the diminished activation of STING-mediated signaling in response to stimulation with the STING agonist SR-717 was a consequence of ISG15 deletion (Fig. 19D).

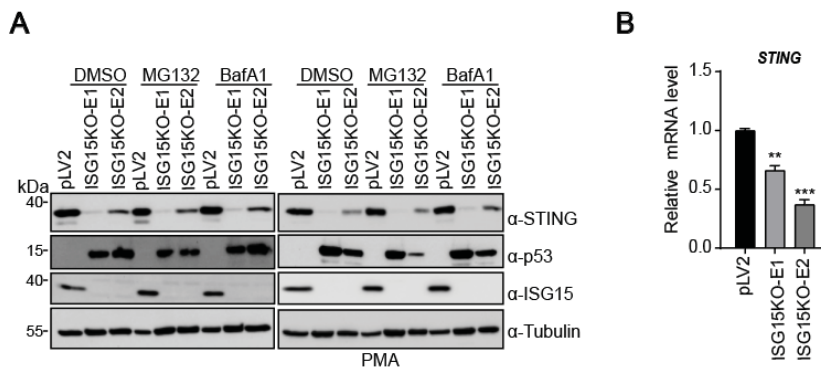


Fig. 20: ISG15 deletion represses the mRNA level of STING. (A) Undifferentiated and PMA-differentiated THP-1.ISG15KO and THP-1.pLV2 cells were treated with DMSO, 10 μ M MG132, or 10 nM BafA1 for 24 h followed by immunoblotting analysis with the indicated antibodies. (B) RT-qPCR analysis of *STING* mRNA in THP-1.ISG15KO and THP-1.pLV2 cells. Significance was determined using one-way ANOVA (Fig. 20B) (*P < 0.05, **P < 0.01, ***P < 0.001, and ****P < 0.0001). Data are representative of three independent experiments (graphs show mean \pm SD).

We then determined whether ISG15 deletion regulates STING expression at the protein level. The immunoblot results showed that the protein level of STING was not restored in the presence of either MG132 or bafilomycin A1 in ISG15-knockout THP-1 cells (Fig. 20A). Consistently, compared with control cells, ISG15-knockout THP-1 cells showed a reduction in the mRNA level of *STING*, suggesting that ISG15 deletion decreases mRNA level of STING in a p53-dependent manner (Fig. 20B).

3.1.12 Misfolded p53 inhibits STING expression and STING-dependent immune signaling

Our previous studies found that THP-1 cells contain two different p53 alleles: wild-type Tp53; the other allele contains a 26-bp deletion in exon 5 (C Δ Tp53) that causes a frameshift resulting in an approximately 25-kDa truncated protein [252]. We next examined both the mRNA and protein levels of STING in wild-type Tp53 and misfolded C Δ Tp53 overexpressing THP-1 cell lines. Compared with vector control THP-1 cells, both mRNA and protein levels were impaired in the presence of misfolded C Δ Tp53, suggesting that misfolded p53 inhibits STING expression (Fig. 21A). Furthermore, we examined the induction of type I IFN induced by cytosolic DNA or STING agonist stimulated-THP-1 cells. The results indicated that the presence of misfolded C Δ Tp53 inhibited the induction of type I IFN (Fig. 21B). Correlating with the decreased type I IFN production observed in the misfolded C Δ Tp53 expressing THP-1 cells, misfolded C Δ Tp53 was highly susceptible to HIV-1 infection (Fig. 21C). Take together, these data suggest that misfolded p53 suppresses STING expression and STING-dependent antiviral signaling.

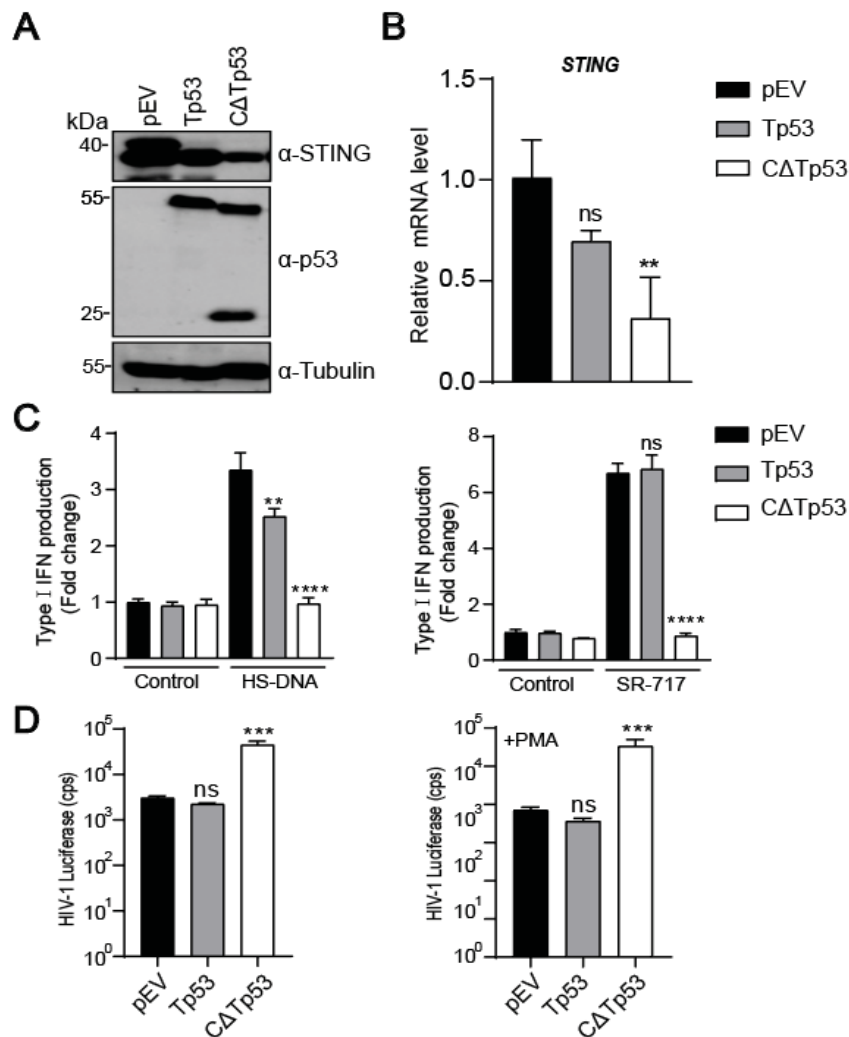


Fig. 21: ISG15 deletion represses the mRNA level of STING. (A) Protein lysates from PMA-differentiated THP-1.pEV, THP-1.Tp53 and THP-1.ΔTp53 cells were immunoblotted with the indicated antibodies. (B) RT-qPCR analysis of *STING* mRNA in THP-1.pEV, THP-1.Tp53 and THP-1.ΔTp53 cells. (C) THP-1.pEV, THP-1.Tp53 and THP-1.ΔTp53 cells were transfected with 4 μg/ml HS-DNA or stimulated with 3.6 μM STING agonist SR-717 for 48 h followed by interferon production analysis. (D) Undifferentiated and PMA-differentiated THP-1.pEV, THP-1.Tp53 and THP-1.ΔTp53 cells were transduced with HIV-1 luciferase reporter virus for 72 h followed by luciferase activity analysis. Significance was determined using one-way ANOVA (Figs.20B-20D) (*P < 0.05, **P < 0.01, ***P < 0.001, and ****P < 0.0001). Data are representative of three independent experiments (graphs show mean ± SD).

3.2 Regulation of STING activity in viral DNA sensing by ISG15 modification

3.2.1 ISG15 deficiency promotes HIV-1 infection by inhibiting sensing of HIV-1

Our previous study showed that ISG15 deficiency supports HIV-1 infection by abrogating p21 and SAM and HD domain-containing deoxynucleoside triphosphate triphosphohydrolase 1 (SAMHD1) antiviral function [252, 260]. Consistent with our previous observations [252], we found that the infection of HIV-1 is enhanced in both undifferentiated and differentiated ISG15-deficient THP-1 cells compared to vector control THP-1 cells (Figs. 22A and 22B).

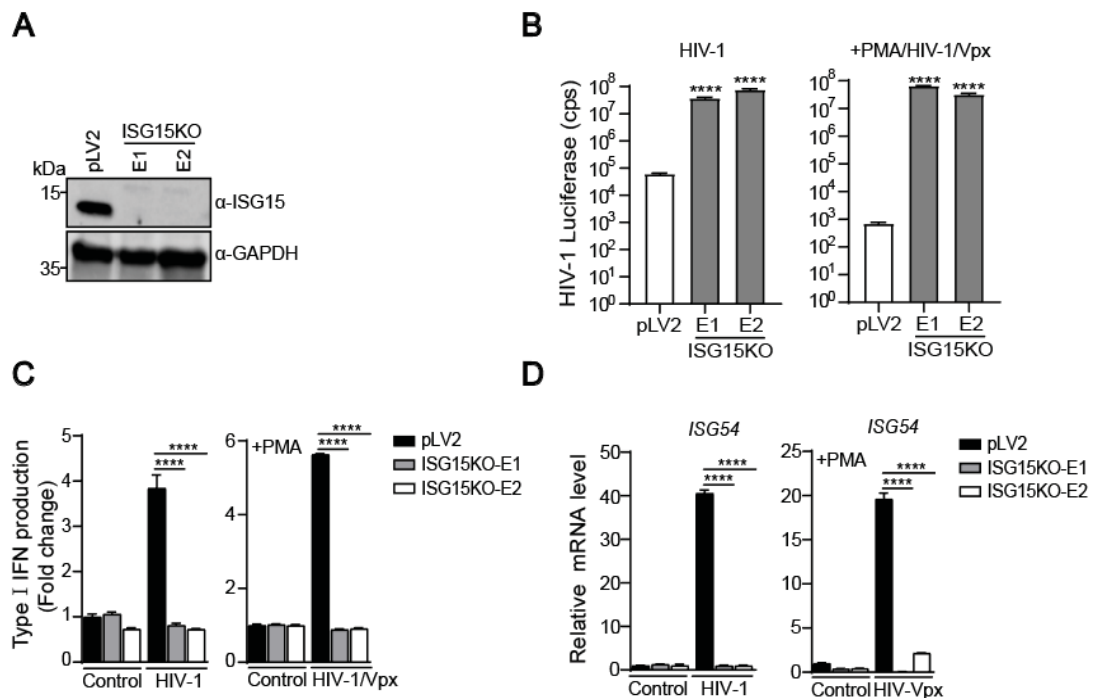


Fig. 22: ISG15 deficiency enhances HIV-1 infection by impairing sensing of HIV-1. (A) Protein lysates from THP-1.ISG15KO and THP-1.pLV2 cells were immunoblotted with the indicated antibodies. (B and C) Undifferentiated and PMA-differentiated THP-1.ISG15KO and THP-1.pLV2 cells were transduced with HIV-1 luciferase reporter virus for 72 h followed by the luciferase activity analysis (B) and interferon production analysis (C). (D) RT-qPCR analysis of *ISG54* mRNA in undifferentiated and PMA-differentiated THP-1.ISG15KO and THP-1.pLV2 cells infected with HIV-1 or HIV-1/Vpx for 24 h. Significance was determined using one-way ANOVA (Figs.22B-22D) (* $P < 0.05$, ** $P < 0.01$, *** $P < 0.001$, and **** $P < 0.0001$). Data are representative of three independent experiments (graphs show mean \pm SD).

However, it is unknown whether ISG15 regulates the sensing of HIV-1. To test this hypothesis, we used ISG15 knockout THP-1 cells and to examine the production of type I IFN in HIV-1 infected ISG15 knockout THP-1 cells. Results from type I IFN production assay showed that ISG15 knockout decreased the induction of type I IFN in response to HIV-1 infection, compared with vector control cells (Fig. 22C). Furthermore, we found that ISG15 deficiency significantly inhibited HIV-1-induced expression of *ISG54*, indicating that ISG15 is vital for the HIV-1-triggered induction of downstream antiviral genes (Fig. 22D). These data suggest that ISG15 deficiency impairs the sensing of HIV-1 and thus promotes HIV-1 infection.

3.2.2 ISG15 deficiency impairs STING-dependent DNA-sensing

Sensing of HIV-1 cDNA by cGAS–STING signaling has emerged as a major sensing pathway in mounting the antiviral immune response towards the infection [26, 31]. We next examined the sensing of cytoplasmic DNA of other sources in the absence of ISG15 in THP-1 cells. Consistent with the observations using HIV-1, ISG15 deficiency inhibited the induction of type I IFN-triggered by infected with MVA or transfected HS-DNA (Fig. 23A). Additionally, depletion of ISG15 substantially inhibited the expression of *IFNB1*, *ISG54* and *TNF- α* genes after transfection of HS-DNA (Fig. 23B). Previous reports identified STING agonists that bypass cGAS to activate innate immune responses [90, 280]. Using the potent STING agonists SR-717 [90], the induction of type I IFN and *IFNB1*, *ISG54* and *TNF- α* mRNAs was almost completely lost in ISG15-knockout THP-1 cells compared to vector control cells (Figs. 23C and 23D). Subsequently, we examined the antiviral function of the STING agonist SR-717 treatment in ISG15-knockout THP-1 cells. The absence of ISG15 abrogated the SR-717-induced inhibition of HIV-1 infection due to the impaired induction type I IFN after HIV-1 infection (Figs. 23E and 23F). These data together suggest that ISG15 is required for STING-dependent induction of innate immune responses.

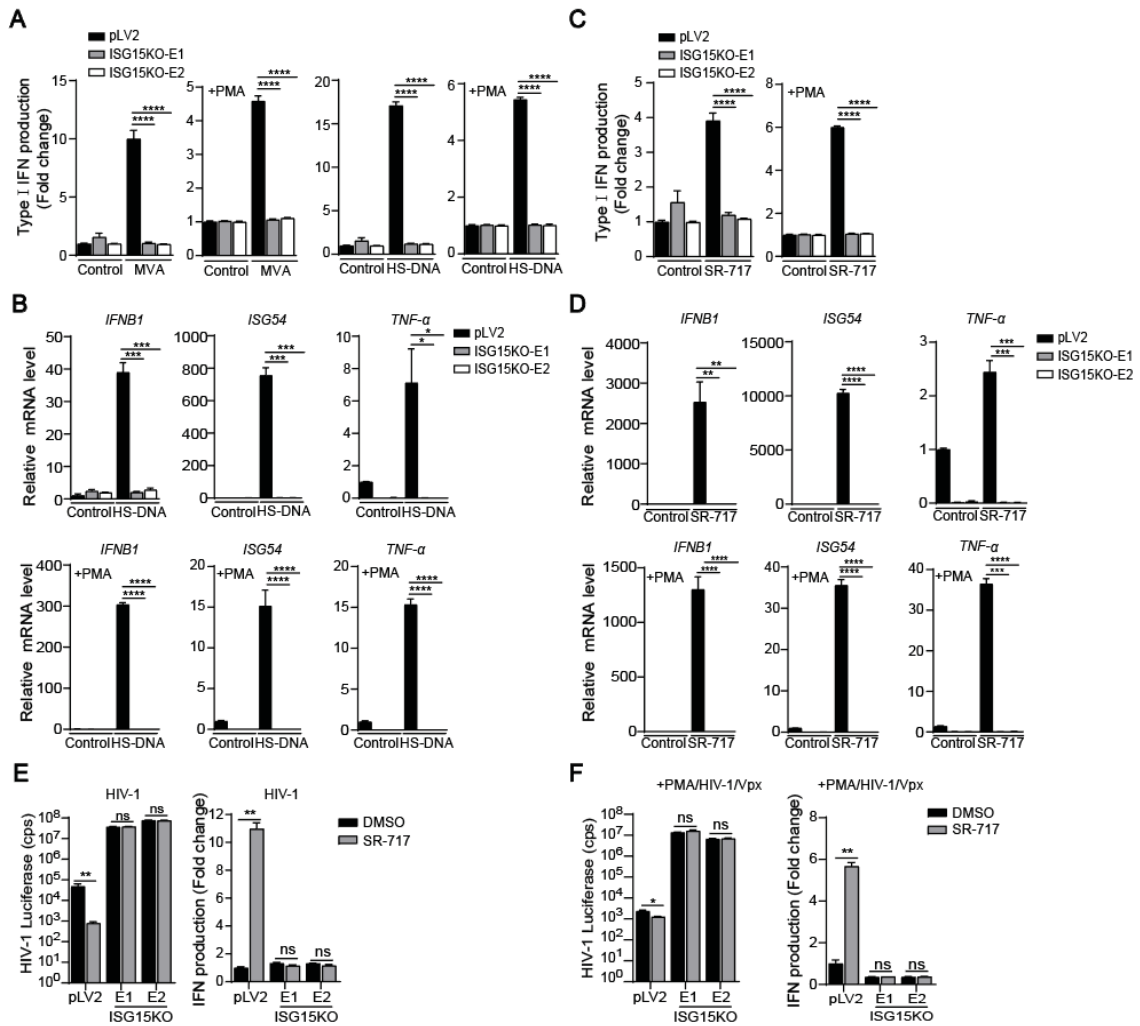


Fig. 23: ISG15 deficiency inhibits STING-dependent DNA-sensing. (A) Undifferentiated and PMA-differentiated THP-1.ISG15KO and THP-1.pLV2 cells were infected with MVA or transfected with 4 μ g/mL HS-DNA for 48 h followed by interferon production analysis. (B) RT-qPCR analysis of *IFNB1*, *ISG54*, and *TNF- α* mRNA in undifferentiated and PMA-differentiated ISG15-knockout and vector control THP-1 cells transfected with 4 μ g/mL HS-DNA for 24 h. (C) Undifferentiated and PMA-differentiated THP-1.ISG15KO and THP-1.pLV2 cells were stimulated with 3.6 μ M SR-717 for 48 h followed by interferon production analysis. (D) RT-qPCR analysis of *IFNB1*, *ISG54*, and *TNF- α* mRNA in undifferentiated and PMA-differentiated THP-1.ISG15KO and THP-1.pLV2 cells stimulated with 3.6 μ M SR-717 for 2 h. (E and F) Undifferentiated (E) and PMA-differentiated (F) THP-1.ISG15KO and THP-1.pLV2 cells were treated with 3.6 μ M SR-717 or DMSO for 12 h and then infected with HIV-1 or HIV-1/Vpx for 72 h and analyzed by luciferase activity assay and interferon production assay. Significance was determined using one-way ANOVA (Figs. 23A-23D) or two-tailed Student's *t*-test (Figs. 23E-23F) (**P* < 0.05, ***P* < 0.01, ****P* < 0.001, and*****P* < 0.0001). Data are representative of three independent experiments (graphs show mean \pm SD).

3.2.3 STING is modified by ISG15

Because ISG15 deficient THP-1 cells failed to induce type I IFN in the presence of STING agonist stimulation, we further investigated the role of ISG15 in regulating innate immune signaling at the level of STING. Considering that the active-site mutant of USP18 failed to inhibit the expression of STING, we determined whether STING can be modified by ISG15. We used HEK293A cells to express STING-HA together with ISG15, UBE1L and UBCH8, in the presence of either USP18 or its mutants. Immunoprecipitation of STING and immunoblotting for ISG15 showed a high-molecular-weight (55 kDa to 70 kDa) species reactive to anti-ISG15 antibody in STING-expressing cells, suggesting that ISG15 was indeed covalently linked to STING (Fig. 24A). Importantly, the ISGylation of STING was reversed by USP18 expression, but not by the active-site mutants USP18-C64A or USP18-C61A (Fig. 24A). In further support of ISGylation of STING, we generated reconstituted STING knockout THP-1 cells with STING that has its C-terminus fused to an HA-tag. These cells were stimulated with IFN β to induce the expression of endogenous ISG15 along with its E1, E2, and E3 enzymes. Interestingly, immunoblot analysis showed that STING was modified by ISG15 in the presence of IFN β in PMA-differentiated THP-1-STING-HA cells (Fig. 24B). To examine whether ISGylation of STING is induced for external stimuli, ISGylation assay was carried out in HS-DNA-transfected or HIV-1-infected-reconstituted STING THP-1 cells. Indeed, STING was modified by ISG15 in response to all the external stimuli tested, indicating that ISGylation is a novel modification of STING in response to cytosolic DNA stimulation or viral infection (Fig. 24C). These data demonstrate that STING is modified by ISG15.

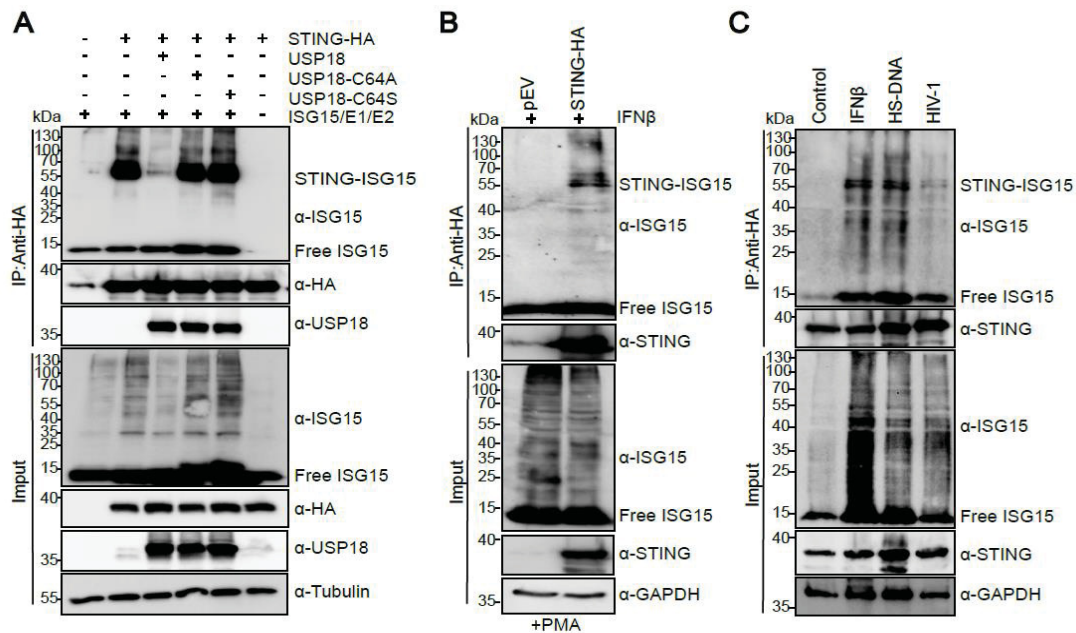


Fig. 24: STING is an ISG15 target protein. (A) HEK293A cells were transfected with the indicated plasmids for 48 h followed by ISGylation assay and immunoblotting analysis. (B) PMA-differentiated reconstituted STING THP-1 cells were stimulated with 500 U/ml IFN- β for 48 h followed by ISGylation analysis and immunoblotting analysis. (C) Reconstituted STING THP-1 cells were stimulated with 500 U/ml IFN- β , transfected with 4 μ g/ml HS-DNA, or infected with HIV-1 for 48 h followed by ISGylation analysis and immunoblotting analysis. Data are representative of three independent experiments.

3.2.4 K224, K236, K289, K338, K347, and K370 of STING are modified by ISG15

ISG15 modifies proteins in a manner similar to ubiquitylation, and is attached to lysine residues in target proteins through a C-terminal Gly-Gly motif. To identify the preferred ISGylation sites on STING, we constructed a plasmid expressing lysine-free STING (STING-K0) by replacing lysines (Ks) with alanines (As), which acted as a negative control. Furthermore, individual single lysine residues were generated back into the STING-K0 plasmid, and these STING mutations were then used to test for STING ISGylation. The Immunoprecipitation assay showed that STING ISGylation was abrogated in the expression of STING-K0. Additionally, we found that six lysine residues (K224, K236, K289, K338, K347, and K370) were modified when the ISG15-modifying system was expressed in cells, and these

modifications were abolished in the presence of USP18 (Fig. 25A). To exclude structural changes in STING due to lysine to alanine mutations, single or multiple lysine to arginine (R) mutations were generated in STING. Upon coexpression of STING mutants and ISG15 conjugation components, the STING-K6R (K224, K236, K289, K338, K347, K370) mutant completely lost the ISGylation signal compared to wild-type STING (Fig. 25B). Meanwhile, the ISGylation of STING reappeared when in STING-K6R single residues were restored to lysine K224, K236, K289, K338, K347, or K370 STING mutants, indicating that these six lysines are associated with ISG15 binding (Fig. 25B).

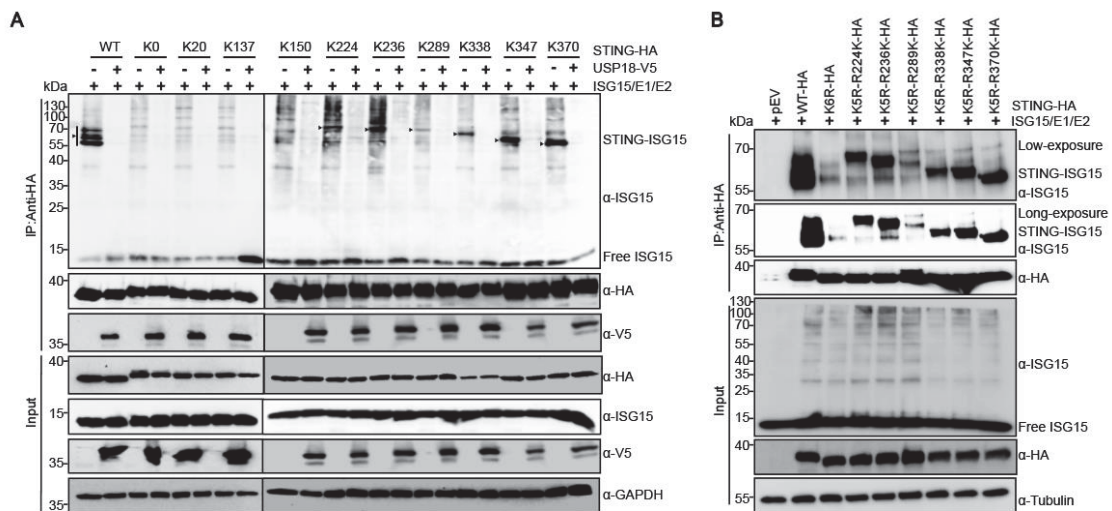


Fig. 25. ISG15 modifies STING on K224, K236, K289, K338, K347 and K370 lysine residues. (A and B) HEK293A cells were transfected with the indicated plasmids for 48 h followed by ISGylation analysis and immunoblotting analysis. Data are representative of three independent experiments.

To further validate this observation in endogenous STING expression, we generated reconstituted STING-K6R together with other mutations of STING in THP-1 cells. In this context, we noted that reconstituted wild-type STING was ISGylated but not STING-K6R after STING agonist stimulation (Fig. 26A). In addition, when six lysines reappeared in reconstituted STING-K6R THP-1 cells, higher molecular weight bands were detected, reminiscent of the covalent linkage

of ISG15 to STING (Fig. 26B). Collectively, these results suggest that lysines 224, 236, 289, 338, 347 and 370 are sites of STING modification by ISG15.

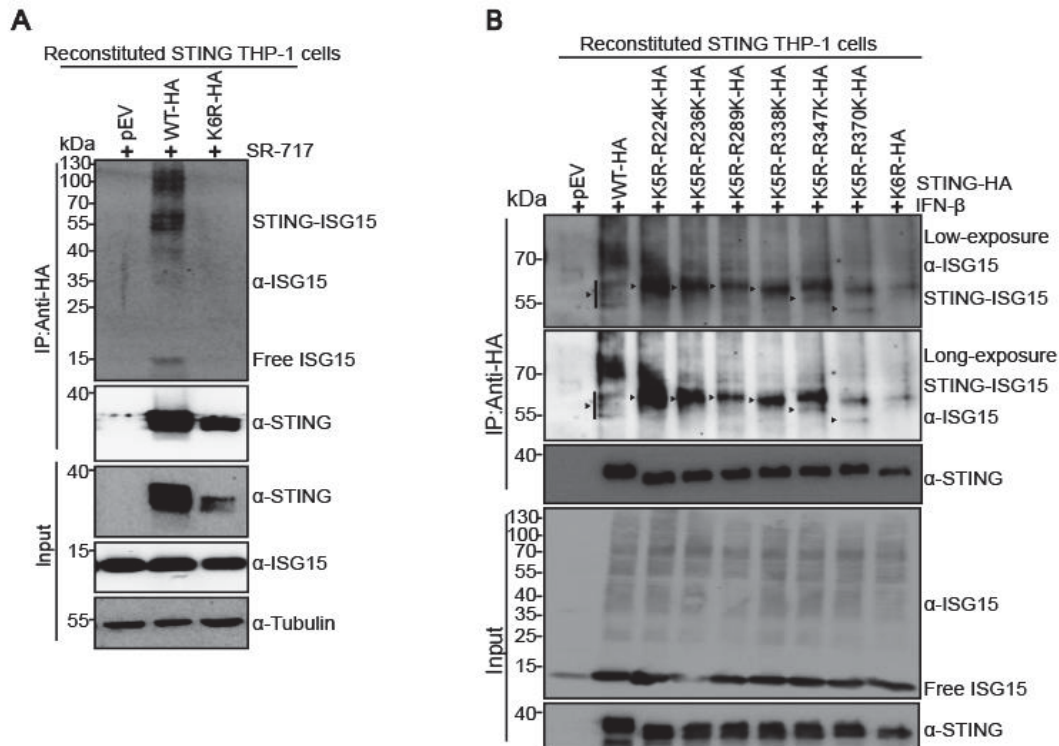


Fig. 26: K224, K236, K289, K338, K347 and K370 of STING are modified by ISG15. (A and B) Reconstituted STING THP-1 cells were stimulated with 3.6 μ M STING agonist SR-717 (A) or 500 U/ml IFN- β (B) for 48 h followed by ISGylation analysis and immunoblotting analysis. Data are representative of three independent experiments.

3.2.5 K289 of STING is vital to induce type I IFN production

Next, we investigated whether and how ISGylation of STING affects STING-triggered innate immune responses against viral infections and cytosolic DNA challenges. Wild-type or mutant STING was expressed in HEK293A cells and the production of interferons was measured. The results showed that the production of type I IFN was significantly damaged in HEK293A cells expressing of the ISGylation sites mutants STING-R289 and STING-K6R as well as the STING phosphorylation site mutant S366A (Fig. 27A). As expected, this impairment could be restored by replacing R289 with K289 in STING-K6R in transfected HEK293A cells (Fig. 27B).

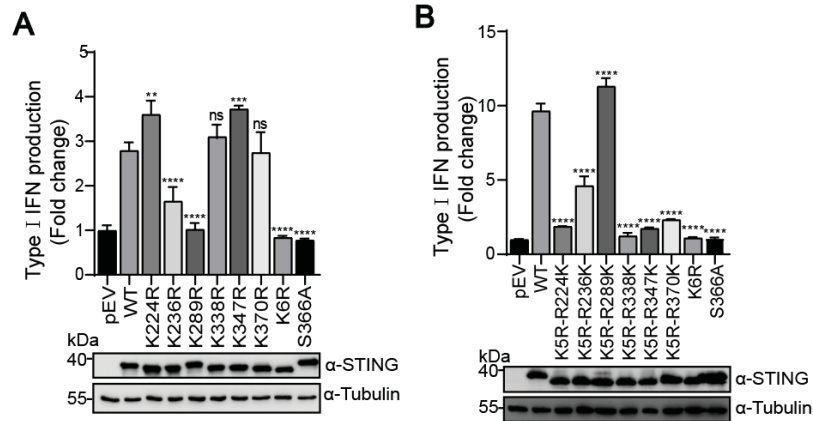


Fig. 27: STING-K6R and STING-R289 failed to induce type I IFN in transfected HEK293A cells. (A and B) HEK293A cells were transfected with the indicated plasmids for 30 h followed by interferon production analysis and immunoblotting analysis. Significance was determined using one-way ANOVA (Figs. 27A-27B) (*P < 0.05, **P < 0.01, ***P < 0.001, and ****P < 0.0001). Data are representative of three independent experiments (graphs show mean ± SD).

To further confirm the above results, reconstituted STING THP-1 cells were transfected with HS-DNA or infected with HIV-1, followed by the interferon production assay. Similarly, reconstitution of STING-K6R failed to induce the expression of type I IFN; however, reconstitution of STING-K5R-R289K THP-1 restored HIV-1 infection and HS-DNA stimulation-induced type I IFN (Fig. 28A). Consistent with these observations, the STING-K6R and STING-R289 produced low levels of *IFNB1*, *ISG15*, and *CXCL10* genes expression after transfection with DNA ligands (Fig. 28B). In addition, STING agonist-induced *IFNB1* and *ISG54* gene expression was reduced in STING-knockout THP-1 cells reconstituted with STING-K6R or STING-R289, suggesting that STING-K289 is the key ISGylation site that regulates the STING-induced innate immune response (Fig. 28C). Together, these results strongly suggest that STING lysine 289 is an important acceptor site for ISGylation and is required for STING activation.

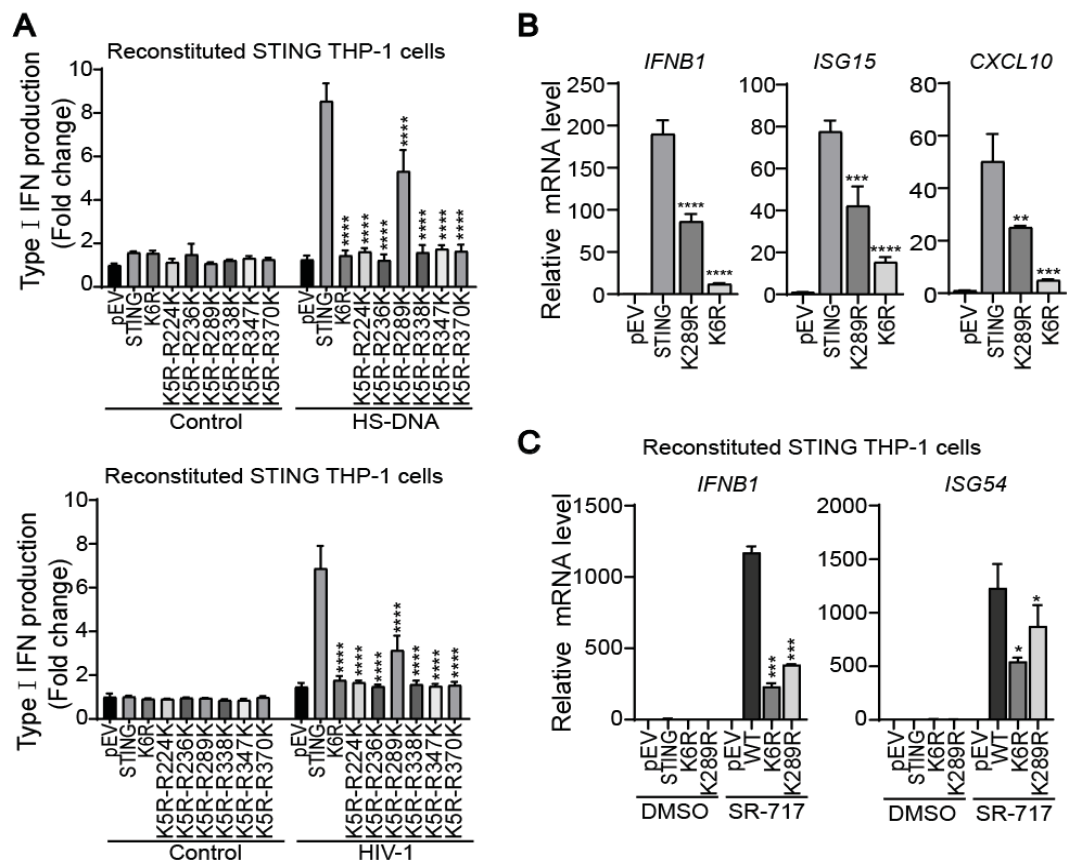


Fig. 28: K289-linked ISGylation on STING is essential for induction of type I IFN. (A) Reconstituted STING THP-1 cells were transfected with 4 $\mu\text{g/ml}$ HS-DNA, or infected with HIV-1 for 72 h followed by interferon production analysis and immunoblotting analysis. (B) RT-qPCR analysis of *IFNB1*, *ISG15*, and *CXCL10* in HEK293A cells transfected with the indicated plasmids for 24 h. (C) RT-qPCR analysis of *IFNB1* and *ISG54* in reconstituted STING THP-1 cells stimulated with 3.6 μM STING agonist SR-717 for 2 h. Significance was determined using one-way ANOVA (Figs. 28A-28C) (* $P < 0.05$, ** $P < 0.01$, *** $P < 0.001$, and **** $P < 0.0001$). Data are representative of three independent experiments (graphs show mean \pm SD).

3.2.6 ISGylation at K289 of STING promotes its activation

The above data suggested that ISGylation site mutations of STING at K289 as well as STING-K6R inhibited STING-mediated cellular antiviral immunity, which prompted us to investigate how K289-linked ISGylation of STING affected STING-mediated signaling activation. We examined STING-triggered signaling activation in reconstituted STING THP-1 cells and observed that accelerated reduction in the

phosphorylation of STING, TBK1, and IRF3 in ISGylation site mutant cells (STING-R289 and STING-K6R) following stimulation with the STING agonist SR-717 (Fig. 29A). We next transfected STING as with STING mutants into HEK293A cells and found that mutation of STING-K6R and STING-R289 dramatically reduced the phosphorylation of STING, TBK1, and IRF3 protein levels, suggesting that ISGylation is involved in the regulation of STING activation (Fig. 29B). In contrast, the impairment was restored by replacing R289 with K289 in STING-K6R in STING agonist SR-717 stimulated reconstituted STING THP-1 cells (Fig. 29C). Further evidence supports that K289-linked ISGylation is important for STING activation in transfected HEK293A cells (Fig. 29D). These results suggest that ISGylation at K289 of STING by ISG15 promotes its activation.

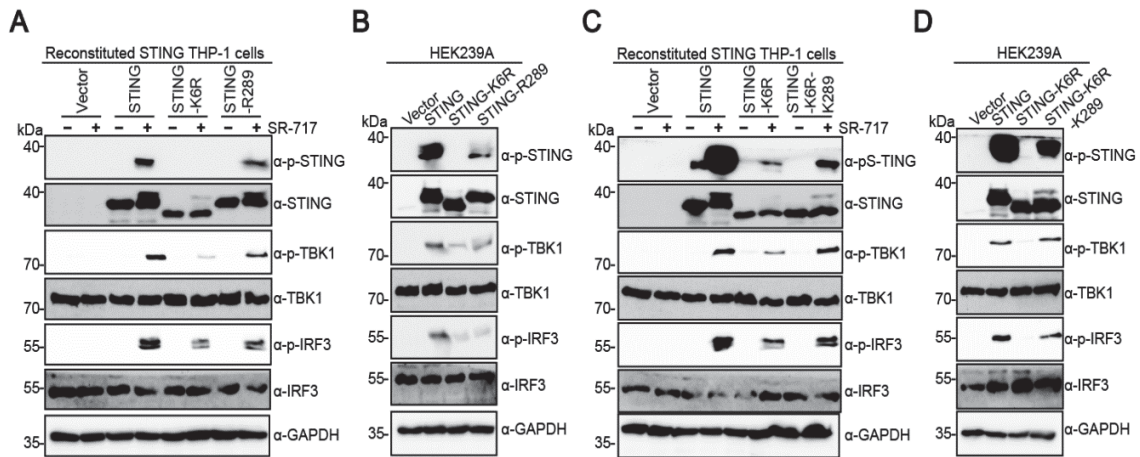


Fig. 29: K289-linked ISGylation of STING regulates STING activation. (A - D) Reconstituted STING THP-1 cells were stimulated with 3.6 μ M STING agonist SR-717 for 2 h (A and C) or HEK293A cells were transfected with the indicated plasmids for 30 h (B and D) followed by immunoblotting analysis. Data are representative of three independent experiments.

3.2.7 ISGylation of STING facilitates its dimerization and oligomerization

To determine the mechanisms, we examined the dimerization and oligomerization of STING, which are critical for TBK1 and IRF3 activation [38, 98]. Immunoblotting assay indicated that both the dimerization and oligomerization of STING (K6R) were markedly damaged in STING agonist SR-717-stimulated reconstituted STING THP-1 cells or transfected HEK293A cells in comparison to wild-type

STING (Figs. 30A and 30B). Additionally, the dimerization of STING (K289R) was comparable but its oligomerization was markedly impaired in comparison to that wild-type STING (Figs. 30A and 30B). Consistently, STING agonist SR-717-induced oligomerization of STING was potentiated and was substantially restored when R289 was mutated into K289 at STING-K6R in reconstituted STING THP-1 cells and transfected HEK293A cells (Figs. 30C and 30D). These results indicate that ISGylation of STING promotes its dimerization and facilitates its oligomerization and STING-dependent innate immunity.

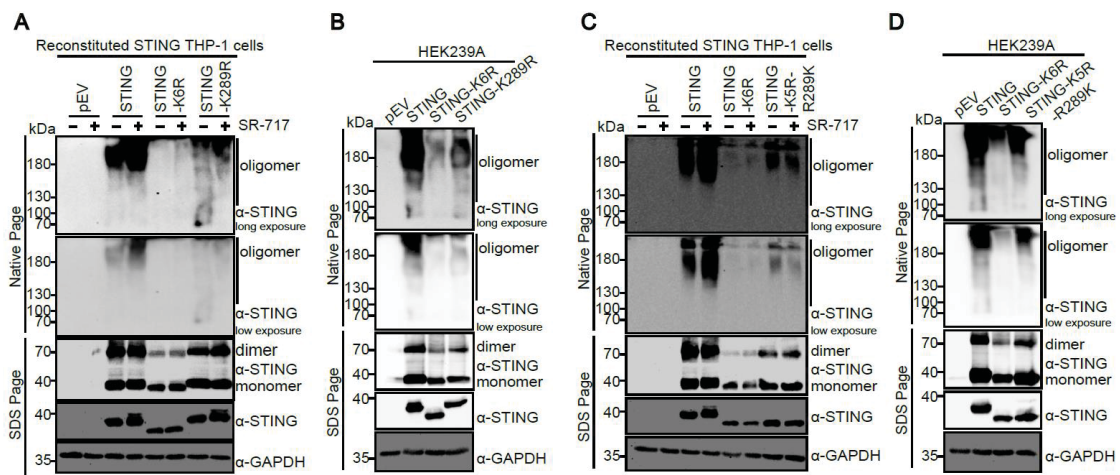


Fig. 30: ISGylation of STING is required for its dimerization and oligomerization. (A - D) Reconstituted STING THP-1 cells were stimulated with 3.6 μ M STING agonist SR-717 for 2 h (A and C) or HEK293A cells were transfected with the indicated plasmids for 30 h (B and D) followed by immunoblotting analysis and STING oligomerization analysis. Data are representative of three independent experiments.

3.2.8 SAVI–STINGs require ISGylation for their activity

Gain-of-function mutations in the STING gene cause a systemic autoinflammatory disease known as SAVI, with STING-V155M being the most prevalent [281]. SAVI patients exhibit a gain-of-function phenotype with a strong transcriptional ISG signature in the peripheral whole blood [92, 93, 282]. We then examined whether ISGylation was required for the activity of the SAVI–STINGs. We transiently expressed wild-type and mutant STING in HEK293A cells and then performed

various analyses. We found that STING-V155M expression exhibited high levels of STING activity measured by type I IFN production, STING and IRF3 phosphorylation, as well as induction of downstream antiviral gene of ISG15 (Fig. 31A). In contrast, the activity of STING-V155M was significantly abolished by the K289R or K6R mutations (Fig. 31A). Additionally, we examined the effect of ISGylation on SAVI-STING in THP-1 cells. We found that STING-V155M reconstituted THP-1 cells showed type I interferon responses and STING and IRF3 phosphorylation, and the induction of ISG15 protein under unstimulated conditions, whereas SAVI-STING with the K289R or K6R mutation lost the constitutive activity (Fig. 31B). STING-V155M is located at the connector helix loop and is assumed to promote the 180° rotation of the ligand-binding domain, thus resulting in the STING oligomerization construct irrespective of the presence of cGAMP [282]. We examined the oligomerization of STING and found that STING-V155M with the K289R or K6R mutation significantly reduced the oligomerization (Fig. 31C). Thus, inhibition of ISGylation could suppress a gain-of-function in SAVI-STING. We therefore conclude that ISGylation is not only required for wild-type STING function but is also required for the constitutive activity of SAVI STING.

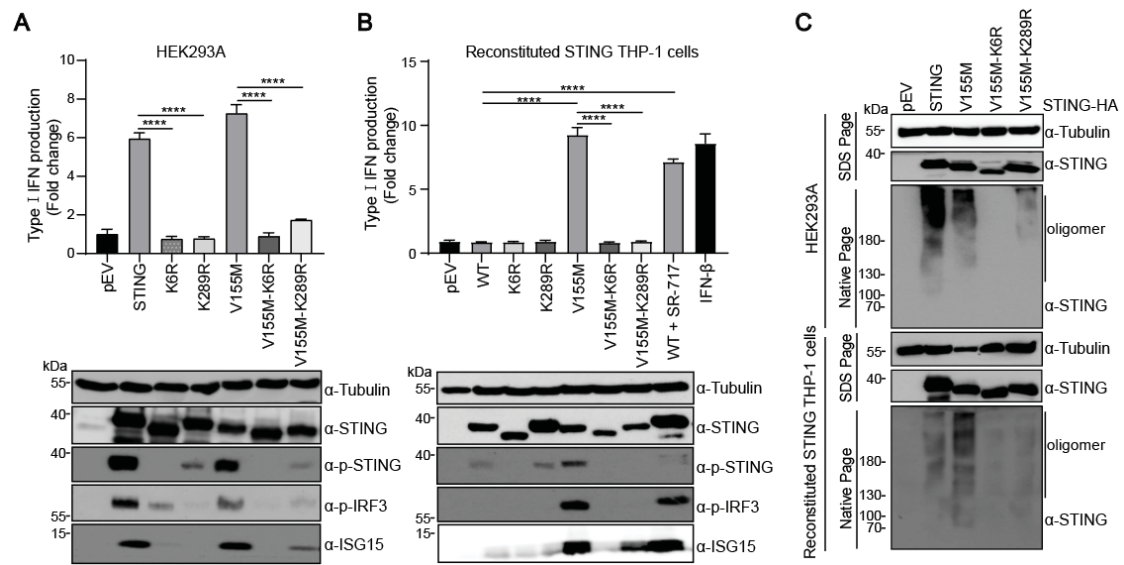


Fig. 31: SAVI–STINGs require ISGylation for their activity. (A) HEK293A cells were transfected with the indicated plasmids for 30 h followed by immunoblot analysis and interferon production analysis. (B) Reconstituted STING THP-1 cells were stimulated or unstimulated with 3.6 μ M SR-717 for 24 h followed by immunoblot analysis and interferon production analysis. (C) Reconstituted STING THP-1 cells or HEK293A cells were transfected indicated plasmids for 24 h followed by immunoblot analysis and STING oligomerization analysis. Significance was determined using one-way ANOVA (Figs. 28A–28B) (* $P < 0.05$, ** $P < 0.01$, *** $P < 0.001$, and**** $P < 0.0001$). Data are representative of three independent experiments (graphs show mean \pm SD).

4 Discussion

The cGAS–STING pathway is not only a highly evolutionarily conserved defense mechanism against infection by DNA-containing microbes but is also involved in sensing tumor-derived DNA and producing intrinsic antitumor immunity [70, 283, 284]. cGAS-STING pathway plays an essential role in maintaining homeostasis and regulating physiological and pathological processes [70, 283, 284]. Monogenic STING gain-of-function mutations and aberrant recognition of self-DNA by cGAS can lead to autoimmune and inflammatory diseases [70, 284]. Therefore, cGAS-STING signaling must be properly regulated.

The activity and stability of STING are regulated by various posttranslational modifications to initiate rapid responses against pathogenic DNA or damaged cellular DNA [285]. In this study, we demonstrate that USP18 represses antiviral cytosolic sensing by suppressing the expression of the adaptor protein STING in a p53-dependent manner. In support of this observation, we describe that ectopic USP18 expression enhances HIV-1 infection and abrogates HIV-1 and cytosolic DNA sensing signaling by decreasing the protein level of STING in human monocytic cells. USP18 knockout upregulates the protein level of STING and promotes STING activation-induced IFN production in response to HIV-1 infection and cytosolic DNA. These findings suggest that USP18 is a regulator of STING-triggered signaling pathways.

USP18 is a multifaceted protein that not only removes ISG15 from targeted proteins in a deconjugating activity-dependent manner but also limits type I IFN signaling by preventing the interaction of JAK1 and IFNR2 binding [228, 286]. It has been reported that USP18 interacts with the N-terminal transmembrane domain of STING (aa 1-160) after DNA virus infection, which recruits USP20 to deconjugate K48-linked ubiquitination from STING independent of its specific protease activity to enhance the stability of STING and the expression of type I IFN and proinflammatory cytokines in response to DNA virus [108]. In this study, our data revealed that STING protein levels were markedly reduced in the presence of USP18. Our results showed that neither proteasomal nor lysosome-

autophagy inhibitor treatment restored the protein level of STING, indicating that USP18 attenuates STING but not at the protein level. We further validated the regulatory role of USP18 on STING mRNA levels by qPCR and found that USP18 regulates *STING* mRNA stability. STING is an ISG [287]. Both IFN-I and IFN- γ induce STING expression at the mRNA level via a STAT1 binding site in the *STING* promoter [287]. A recent study showed that USP18 ectopic expression in THP-1 cells reduces the induction of several atypical ISGs by permitting IRF9/STAT2 binding to ISRE and IRE motifs in promoters [230]. It is currently unknown whether USP18 is a transcription factor that directly regulates the mRNA level of STING.

We next investigated how USP18 regulates STING mRNA stability and found that the enzymatically inactive mutant USP18-C64A but not wild-type USP18 restored the protein level of STING and STING-mediated induction of downstream genes and interferon. Moreover, USP18-C64A expression recovered the mRNA level of the *STING* gene, suggesting that USP18 catalytic activity is essential for STING-mediated antiviral immunity activation and mRNA stability. Studies have shown that the STING promoter is regulated by several transcription factors, such as c-MYC, CREB, and NF- κ B [116, 117]. Nrf2 can repress antiviral cytosolic sensing and the subsequent release of antiviral type I IFN by repressing the mRNA and protein levels of STING [120]. Additionally, p53 is activated in A549 cells exposed to actinomycin D and nutlin-3a (A+N), resulting in upregulating both mRNA and protein levels of STING, revealing that p53 may potentially regulate the transcriptional level of STING [119].

Interestingly, our previous studies found that ectopic expression of wild-type USP18 but not the enzymatic inactive mutant USP18-C64A in THP-1 cells induces the accumulation of misfolded p53. These results led us to explore whether USP18 modulates STING in a p53-dependent manner. p53 acts as a DNA-binding transcription factor that controls dozens of target genes with diverse biological functions [236]. However, mutations in *TP53* gene can disrupt p53 structure or DNA binding ability, thus leading to the inhibition of wild-type p53 transcriptional

function [254]. In general, the stability and activity of p53 are regulated by MDM2 and MDMX-mediated 26S proteasome degradation and ISGylation-mediated degradation through the 20S proteasome [247]. Indeed, ISGylation is important for the clearance of misfolded dominant negative p53 in myeloid cells [247, 250, 252]. Misfolded p53 accumulates in the ISG15 deficient THP-1 cells [252]. Furthermore, we observed that the diminished activation of STING-mediated signaling in response to stimulation with the STING agonist SR-717 is a consequence of ISG15 deletion. In addition, both the mRNA and protein stability of STING were decreased in ISG15-knockout THP-1 cells.

Further, we explored that the stability of STING in the presence of wild-type p53 and misfolded p53. Our data showed that misfolded CΔTp53 inhibited expression of STING at both mRNA and protein levels in comparison with wild-type p53 expressing THP-1 cells. This provides direct evidence that p53 regulates the expression of STING. Consistent with these observations, cytosolic DNA or STING agonist stimulation-induced type I IFN was impaired by misfolded CΔTp53 expression. Correlating with the decreased type I IFN production observed in the misfolded CΔTp53 expressing THP-1 cells, misfolded CΔTp53 was highly susceptible to HIV-1 infection. Our data provide evidence that the stability of STING is related to p53.

The *TP53* gene is the most frequent alteration in human cancers, which not only abolishes tumor suppressor capacities but also exhibits various gain-of-function activities that contribute to tumor development and progression [236]. Recently, more evidence has shown that p53 regulates cytosolic sensing of DNA and antiviral defense and antitumor immunity [268, 269]. Mutant p53 has been shown to suppress downstream signaling from the cGAS-STING pathway by binding to TBK1, thereby preventing the phosphorylation of its substrates and facilitating immune evasion [269]. In contrast, wild-type p53 promotes the degradation of the DNA exonuclease TREX1, leading to the accumulation of cytosolic DNA that activates the cGAS-STING-mediated type I IFN response and systemic inflammation [268]. USP18 ectopic expression or ISG15 knockout cause the

accumulation of misfolded p53 in cells [252], however, it is unclear whether misfolded p53 could require TREX1 degradation and promote the activation of the cytosolic DNA sensing pathway. In our study, this raises the possibility that p53 mutants interfere with STING expression and the STING-triggered pathway, suggesting limitations in the therapeutic approach of STING agonists for tumors with mutant p53.

In conclusion, our data reveal a novel mechanism by which USP18 regulates the STING-induced innate immune response through attenuated STING mRNA levels in a p53-dependent manner. This finding also provides strong evidence for the role of p53 in regulating innate immunity.

Furthermore, we identified a novel STING posttranslational modification mediated by ISG15 and this modification promotes stability, oligomerization and activation of STING after viral infection and DNA challenge, thus increasing the expression of downstream type I IFN and inflammatory cytokines. In this study, we indicate that lysine residues K224, K236, K289, K338, K347, and K370 on STING can be ISGylated upon viral infection or cytosolic DNA stimulation and that knockout of ISG15 impaired STING protein levels, suggesting a protective role of ISG15 conjugation on STING in the immune defense against viral infection. Mutations of ISGylation sites on STING-K6R and STING-K289R reduced STING-mediated interferon production by decreasing the oligomerization of STING. Collectively, our findings suggest that the ISGylation of STING is important for STING stability and oligomerization to initiate downstream signaling.

USP18 can specifically remove the ubiquitin-like protein ISG15 from ISGylated proteins by its protease activity [146]. The enzymatically inactive mutant USP18-C64A but not USP18 stabilizes STING suggesting that STING is modified by ISG15. Mass spectrometry-based proteomics studies have identified hundreds of host proteins that are ISGylated, and only a few proteins have been investigated [154]. ISGylation of IRF3 prevents the interaction between IRF3 and PIN1, preventing proteasomal degradation of IRF3 and enhancing the intracellular IFN

response [171]. ISGylation of STAT1 inhibited its polyubiquitylation and subsequent degradation of SATA1 [288]. Recently, ISGylation of MDA5 and cGAS was described to be essential for the viral infection-induced innate immune response [72, 169]. Whether and how STING undergoes ISGylation to regulate antiviral immunity and autoimmunity are completely unknown. In this study, we demonstrate that STING can be covalently linked to ISG15 upon HIV-1 infection, cytosolic DNA or interferon stimulation. Notably, STING activation-induced interferon production against viral infection is eliminated by depletion of ISG15, suggesting the role of ISGylation of STING in innate immunity. We found that only a small fraction of the total STING is modified by ISG15, thus it is still a challenge to understand how ISGylation affects the overall function of STING. One possibility is that the ISGylation of only a small fraction of the protein could promote the assembly of protein oligomerization, as has been observed with cGAS [72]. In addition, ISGylation on a protein alters its cellular localization and function, as was seen with the ISGylation of filamin B [289].

STING harbors six ISG-attachment sites that map to residues K224, K236, K289, K338, K347, and K370. By analyzing a larger panel of STING variants, where these amino acids were mutated individually or in various combinations, we determined that ISGylation on each site undergoes ISGylation. Notably, we discovered that the ISGylation site mutant K289R of STING abolishes STING-triggered antiviral immunity. Our data show that both transiently expressed STING-K6R in HEK293A and reconstituted STING-K6R THP-1 cells abrogated their dimerization, and oligomerization and failed to induce IFN production and downstream gene expression in response to cytosolic DNA stimulation. Interestingly, transiently expressed STING-K5R-R289K and reconstituted STING-K5R-R289K in THP-1 cells restored its dimerization and oligomerization, thus resulting in STING-induced type I IFN production upon HIV-1 infection or HS-DNA transfection. In collaboration with Renate König at the Paul-Ehrlich Institute (Langen, Germany), we further generated an endogenous mutation of STING at K289 in human iPSCs utilizing a CRISPR/Cas9-based knock-in method and found

that STING-K289R impaired cytosolic DNA stimulation or STING agonist SR-717-induced transcription of the *ISG54* gene compared with healthy cells (data not shown here). These findings suggest that ISGylation at K289 of STING is vital for STING-mediated innate immune signaling activation upon viral infection and DNA challenge.

STING signaling is dynamically regulated by polyubiquitination and relies on different types of polyubiquitin and modified STING at one or multiple lysine residues [290]. TRIM32 was reported to target STING for K63-linked polyubiquitination at residues K20, K150, K224, and K236 and to facilitate the recruitment of TBK1 to STING as a means of positive regulation [100]. The E3 ubiquitin ligase AMFR regulates the DNA-triggered STING-dependent signaling, which catalyzes K27-linked polyubiquitination of STING at K137, K150, K224, and K236, and polyubiquitin on STING facilitates TBK1 recruitment and activation [99]. RNF115 catalyzes K63-linked polyubiquitination of STING at K20, K224 and K289 promoting the oligomerization of STING and the recruitment of TBK1 [291]. In addition, TRIM38 was reported to mediate the SUMOylation of human STING at K338 during the early stages of viral infection and this SUMOylation promoted oligomerization of STING and triggered IRF3 recruitment and activation. From our results, we speculate that both SUMOylation and ISGylation of STING may play a synergistic role in regulating DNA-triggered STING-dependent signaling. Here, we found that STING can be modified by ISG15 at K224, K236, K338, K347, and K370. Some of these sites overlap with ubiquitin or SUMO modification. It will be a task for the future to describe the dynamics of diverse modifications at a single lysine and their impact on STING stability and function.

Here we demonstrated that ISGylation of STING promotes its dimerization, oligomerization, and activation. Loss of ISGylation of STING on combinations of K224, K236, K289, K338, K347, and K370 prevented their dimerization and oligomerization. In its inactive state, the STING molecule resides in the ER plasma membrane, and the ligand-binding domain of STING functions as a dimer, with a V-shaped ligand binding pocket for one cyclic dinucleotide ligand [38, 43].

Interestingly, the ligand-binding domain of STING contains these six lysine residues, suggesting that ISGylation may regulate the dimerization of STING. STING dimerization is essential for the formation of oligomers [38, 52]. Upon binding with cGAMP, STING forms a closed dimer and undergoes a 180° clockwise rotation of its ligand-binding domains and the formation of STING oligomers [38]. STING variants with mutations in the tetramer interface not only disrupt the oligomerization of STING in response to cGAMP stimulation but also abolish the phosphorylation of TBK1 and STING, suggesting that cGAMP induces STING activation by promoting oligomerization [38, 43, 45, 52]. In our findings, the loss of STING ISGylation at K289 blocked its oligomerization but not its dimerization, thereby inhibiting its activation and the recruitment of IRF3 in cells.

The natural mutation V155M in human STING can cause severe SAVI disease [91-94]. Patients with SAVI, constitutively activate STING, leading to increasing release of inflammatory cytokines and interferons [91, 92]. Mechanistically, STING-V155M localized to perinuclear compartments, not the ER, inducing a 180° rotation of the ligand-binding domain along a connector helix loop of STING in a cGAMP-independent manner [91, 92]. Our results showed that transient STING-V155M expression in HEK293A cells upregulated the activation of STING, IRF3 and ISG15 expression. In contrast, STING-V155M with the K289 or K6R mutation relieves its oligomers, resulting in STING activating IRF3 and inducing type I IFN response, suggesting that loss of ISGylation inhibits STING oligomerization and activation. Thus, suppression of ISGylation could inhibit a gain-of-function phenotype in SAVI–STING. Understanding how ISGylation of STING at K289 regulates STING oligomerization and activation depends on a more detailed structural and functional analysis of full-length STING.

ISGylation is a multistep process that requires E1, E2, and E3 enzymes [132]. Unlike ubiquitination, only three E3 ligases, EFP, HHARI and HERC5 were identified for ISGylation [140-145]. In our ISGylation assay system, both HEK293A and THP-1 cells express endogenous E3 ligases, such as EFP and HERC5 [252]. The E3 ligase HHARI selectively interacts with cGAS but not with other proteins

including RIG-I, MAVS, STING [72]. It will be a task for the future to describe the E3 ligase for STING ISGylation. ISGylation inhibits the replication of many viruses at multiple stages of viral replication [177, 292]. Mice lacking the E1 enzyme UBE1L exhibit hypersensitivity to viral infections [180, 293]. ISG15 deletion mice exhibit enhanced susceptibility to virus infection, which can be rescued by expressing wild-type ISG15, but not a mutant form of ISG15 that cannot form conjugates [159, 292]. Similar to ubiquitination, the removal of substrate ISGylation is catalyzed by USP18 [199, 206]. The papain-like protease of SARS-CoV-2 has been previously demonstrated to function as a putative deISGylase, which cleaves ISG15 chain conjugations from the target protein [177]. ISG15-dependent activation of IRF3 and MDA5 is antagonized through direct de-ISGylation mediated by the papain-like protease of SARS-CoV-2, facilitating immune evasion and viral spread [169, 218]. During SARS-CoV-2 infection, activation of the cGAS-STING pathway is mediated by SARS-CoV-2 S protein-induced cell fusion, causing a DNA damage response [294]. Upon SARS-CoV-2 infection, it is unclear whether cGAS and STING can be modified by ISG15 and contribute to antiviral defense. In addition, it is worth exploring whether the papain-like protease of SARS-CoV-2 functions to eliminate cellular immune responses by deISGylation at the level of cGAS and STING.

Although we have provided evidence supporting a role of ISGylation for STING in regulating innate immune responses through its ability to sense cytosolic DNA and pathogen infection, the examination of the *in vivo* relevance of these modifications and the associated mechanisms will require future studies. In summary, we proposed a novel regulatory mechanism of the cellular ISGylation system in the STING-mediated innate immune response. These findings open a new perspective to uncover the enigmatic aspects of STING-mediated viral restriction.

5 Reference list

1. Akira, S., S. Uematsu, and O. Takeuchi, *Pathogen recognition and innate immunity*. Cell, 2006. **124**(4): p. 783-801.
2. Tan, X., et al., *Detection of Microbial Infections Through Innate Immune Sensing of Nucleic Acids*. Annu Rev Microbiol, 2018. **72**: p. 447-478.
3. Wu, J. and Z.J. Chen, *Innate immune sensing and signaling of cytosolic nucleic acids*. Annu Rev Immunol, 2014. **32**: p. 461-88.
4. Marshall, J.S., et al., *An introduction to immunology and immunopathology*. Allergy Asthma Clin Immunol, 2018. **14**(Suppl 2): p. 49.
5. Turvey, S.E. and D.H. Broide, *Innate immunity*. J Allergy Clin Immunol, 2010. **125**(2 Suppl 2): p. S24-32.
6. Bonilla, F.A. and H.C. Oettgen, *Adaptive immunity*. J Allergy Clin Immunol, 2010. **125**(2 Suppl 2): p. S33-40.
7. Fearon, D.T. and R.M. Locksley, *The instructive role of innate immunity in the acquired immune response*. Science, 1996. **272**(5258): p. 50-3.
8. Akira, S., K. Takeda, and T. Kaisho, *Toll-like receptors: critical proteins linking innate and acquired immunity*. Nat Immunol, 2001. **2**(8): p. 675-80.
9. Medzhitov, R. and C. Janeway, Jr., *Innate immunity*. N Engl J Med, 2000. **343**(5): p. 338-44.
10. Medzhitov, R. and C.A. Janeway, Jr., *Innate immunity: impact on the adaptive immune response*. Curr Opin Immunol, 1997. **9**(1): p. 4-9.
11. Varki, A., *Since there are PAMPs and DAMPs, there must be SAMPs? Glycan "self-associated molecular patterns" dampen innate immunity, but pathogens can mimic them*. Glycobiology, 2011. **21**(9): p. 1121-4.
12. Mogensen, T.H., *Pathogen recognition and inflammatory signaling in innate immune defenses*. Clin Microbiol Rev, 2009. **22**(2): p. 240-73, Table of Contents.
13. Imler, J.L. and L. Zheng, *Biology of Toll receptors: lessons from insects and mammals*. J Leukoc Biol, 2004. **75**(1): p. 18-26.

14. Medzhitov, R., *Toll-like receptors and innate immunity*. Nat Rev Immunol, 2001. **1**(2): p. 135-45.
15. Dambuza, I.M. and G.D. Brown, *C-type lectins in immunity: recent developments*. Curr Opin Immunol, 2015. **32**: p. 21-7.
16. Takeuchi, O. and S. Akira, *Pattern recognition receptors and inflammation*. Cell, 2010. **140**(6): p. 805-20.
17. Wang, L., M. Wen, and X. Cao, *Nuclear hnRNPA2B1 initiates and amplifies the innate immune response to DNA viruses*. Science, 2019. **365**(6454).
18. Bartok, E. and G. Hartmann, *Immune Sensing Mechanisms that Discriminate Self from Altered Self and Foreign Nucleic Acids*. Immunity, 2020. **53**(1): p. 54-77.
19. Sato, M., et al., *Distinct and essential roles of transcription factors IRF-3 and IRF-7 in response to viruses for IFN-alpha/beta gene induction*. Immunity, 2000. **13**(4): p. 539-48.
20. Fitzgerald, K.A., et al., *LPS-TLR4 signaling to IRF-3/7 and NF-kappaB involves the toll adapters TRAM and TRIF*. J Exp Med, 2003. **198**(7): p. 1043-55.
21. Sharma, S., et al., *Triggering the interferon antiviral response through an IKK-related pathway*. Science, 2003. **300**(5622): p. 1148-51.
22. Darnell, J.E., Jr., I.M. Kerr, and G.R. Stark, *Jak-STAT pathways and transcriptional activation in response to IFNs and other extracellular signaling proteins*. Science, 1994. **264**(5164): p. 1415-21.
23. Biron, C.A., *Interferons alpha and beta as immune regulators--a new look*. Immunity, 2001. **14**(6): p. 661-4.
24. Johnson, S.F. and A. Telesnitsky, *Retroviral RNA dimerization and packaging: the what, how, when, where, and why*. PLoS Pathog, 2010. **6**(10): p. e1001007.
25. Schnoll, J.G., et al., J Neuroimmune Pharmacol, 2021. **16**(1): p. 113-129.
26. Yin, X., et al., *Sensor Sensibility-HIV-1 and the Innate Immune Response*. Cells, 2020. **9**(1).

27. Gringhuis, S.I., et al., *HIV-1 blocks the signaling adaptor MAVS to evade antiviral host defense after sensing of abortive HIV-1 RNA by the host helicase DDX3*. *Nat Immunol*, 2017. **18**(2): p. 225-235.
28. Ringear, M., et al., *FTSJ3 is an RNA 2'-O-methyltransferase recruited by HIV to avoid innate immune sensing*. *Nature*, 2019. **565**(7740): p. 500-504.
29. Wang, M.Q., et al., *RIG-I detects HIV-1 infection and mediates type I interferon response in human macrophages from patients with HIV-1-associated neurocognitive disorders*. *Genet Mol Res*, 2015. **14**(4): p. 13799-811.
30. Bode, C., et al., *Human plasmacytoid dendritic cells elicit a Type I Interferon response by sensing DNA via the cGAS-STING signaling pathway*. *Eur J Immunol*, 2016. **46**(7): p. 1615-21.
31. Gao, D., et al., *Cyclic GMP-AMP synthase is an innate immune sensor of HIV and other retroviruses*. *Science*, 2013. **341**(6148): p. 903-6.
32. Jakobsen, M.R., et al., *IFI16 senses DNA forms of the lentiviral replication cycle and controls HIV-1 replication*. *Proc Natl Acad Sci U S A*, 2013. **110**(48): p. E4571-80.
33. Lahaye, X., et al., *The capsids of HIV-1 and HIV-2 determine immune detection of the viral cDNA by the innate sensor cGAS in dendritic cells*. *Immunity*, 2013. **39**(6): p. 1132-42.
34. Lahaye, X., et al., *NONO Detects the Nuclear HIV Capsid to Promote cGAS-Mediated Innate Immune Activation*. *Cell*, 2018. **175**(2): p. 488-501 e22.
35. Yoh, S.M., et al., *Recognition of HIV-1 capsid by PQBP1 licenses an innate immune sensing of nascent HIV-1 DNA*. *Mol Cell*, 2022. **82**(15): p. 2871-2884 e6.
36. Yoh, S.M., et al., *PQBP1 Is a Proximal Sensor of the cGAS-Dependent Innate Response to HIV-1*. *Cell*, 2015. **161**(6): p. 1293-1305.

37. Zheng, J., et al., *Comprehensive elaboration of the cGAS-STING signaling axis in cancer development and immunotherapy*. Mol Cancer, 2020. **19**(1): p. 133.
38. Zhang, X., X.C. Bai, and Z.J. Chen, *Structures and Mechanisms in the cGAS-STING Innate Immunity Pathway*. Immunity, 2020. **53**(1): p. 43-53.
39. Zhang, X., et al., *The cytosolic DNA sensor cGAS forms an oligomeric complex with DNA and undergoes switch-like conformational changes in the activation loop*. Cell Rep, 2014. **6**(3): p. 421-30.
40. Gao, P., et al., *Cyclic [G(2',5')pA(3',5')p] is the metazoan second messenger produced by DNA-activated cyclic GMP-AMP synthase*. Cell, 2013. **153**(5): p. 1094-107.
41. Cai, X., Y.H. Chiu, and Z.J. Chen, *The cGAS-cGAMP-STING pathway of cytosolic DNA sensing and signaling*. Mol Cell, 2014. **54**(2): p. 289-96.
42. Huang, Y.H., et al., *The structural basis for the sensing and binding of cyclic di-GMP by STING*. Nat Struct Mol Biol, 2012. **19**(7): p. 728-30.
43. Shang, G., et al., *Cryo-EM structures of STING reveal its mechanism of activation by cyclic GMP-AMP*. Nature, 2019. **567**(7748): p. 389-393.
44. Zhang, C., et al., *Structural basis of STING binding with and phosphorylation by TBK1*. Nature, 2019. **567**(7748): p. 394-398.
45. Zhao, B., et al., *A conserved PLPLRT/SD motif of STING mediates the recruitment and activation of TBK1*. Nature, 2019. **569**(7758): p. 718-722.
46. Ouyang, S., et al., *Structural analysis of the STING adaptor protein reveals a hydrophobic dimer interface and mode of cyclic di-GMP binding*. Immunity, 2012. **36**(6): p. 1073-86.
47. Shang, G., et al., *Crystal structures of STING protein reveal basis for recognition of cyclic di-GMP*. Nat Struct Mol Biol, 2012. **19**(7): p. 725-7.
48. Taguchi, T., et al., *STING Operation at the ER/Golgi Interface*. Front Immunol, 2021. **12**: p. 646304.
49. Decout, A., et al., *The cGAS-STING pathway as a therapeutic target in inflammatory diseases*. Nat Rev Immunol, 2021. **21**(9): p. 548-569.

50. Barlowe, C. and A. Helenius, *Cargo Capture and Bulk Flow in the Early Secretory Pathway*. *Annu Rev Cell Dev Biol*, 2016. **32**: p. 197-222.
51. Gui, X., et al., *Autophagy induction via STING trafficking is a primordial function of the cGAS pathway*. *Nature*, 2019. **567**(7747): p. 262-266.
52. Ergun, S.L., et al., *STING Polymer Structure Reveals Mechanisms for Activation, Hyperactivation, and Inhibition*. *Cell*, 2019. **178**(2): p. 290-301 e10.
53. Tanaka, Y. and Z.J. Chen, *STING specifies IRF3 phosphorylation by TBK1 in the cytosolic DNA signaling pathway*. *Sci Signal*, 2012. **5**(214): p. ra20.
54. Balka, K.R., et al., *TBK1 and IKKepsilon Act Redundantly to Mediate STING-Induced NF-kappaB Responses in Myeloid Cells*. *Cell Rep*, 2020. **31**(1): p. 107492.
55. Yum, S., et al., *TBK1 recruitment to STING activates both IRF3 and NF-kappaB that mediate immune defense against tumors and viral infections*. *Proc Natl Acad Sci U S A*, 2021. **118**(14).
56. Smale, S.T., *Selective transcription in response to an inflammatory stimulus*. *Cell*, 2010. **140**(6): p. 833-44.
57. Gasser, S. and D.H. Raulet, *The DNA damage response arouses the immune system*. *Cancer Res*, 2006. **66**(8): p. 3959-62.
58. Luecke, S., et al., *cGAS is activated by DNA in a length-dependent manner*. *EMBO Rep*, 2017. **18**(10): p. 1707-1715.
59. Kawane, K., K. Motani, and S. Nagata, *DNA degradation and its defects*. *Cold Spring Harb Perspect Biol*, 2014. **6**(6).
60. Yang, Y.G., T. Lindahl, and D.E. Barnes, *Trex1 exonuclease degrades ssDNA to prevent chronic checkpoint activation and autoimmune disease*. *Cell*, 2007. **131**(5): p. 873-86.
61. Ma, R., et al., *The cGAS-STING pathway: The role of self-DNA sensing in inflammatory lung disease*. *FASEB J*, 2020. **34**(10): p. 13156-13170.
62. Yang, Y., Y. Huang, and Z. Zeng, *Advances in cGAS-STING Signaling Pathway and Diseases*. *Front Cell Dev Biol*, 2022. **10**: p. 800393.

63. Grieves, J.L., et al., *Exonuclease TREX1 degrades double-stranded DNA to prevent spontaneous lupus-like inflammatory disease*. Proc Natl Acad Sci U S A, 2015. **112**(16): p. 5117-22.
64. Lee, M.S. and R. Craigie, *A previously unidentified host protein protects retroviral DNA from autointegration*. Proc Natl Acad Sci U S A, 1998. **95**(4): p. 1528-33.
65. Ma, H., et al., *Barrier-to-Autointegration Factor 1 Protects against a Basal cGAS-STING Response*. mBio, 2020. **11**(2).
66. Wang, L., et al., *Spermine enhances antiviral and anticancer responses by stabilizing DNA binding with the DNA sensor cGAS*. Immunity, 2023.
67. Kujirai, T., et al., *Structural basis for the inhibition of cGAS by nucleosomes*. Science, 2020. **370**(6515): p. 455-458.
68. Zhao, B., et al., *The molecular basis of tight nuclear tethering and inactivation of cGAS*. Nature, 2020. **587**(7835): p. 673-677.
69. Ma, F., et al., *Positive feedback regulation of type I IFN production by the IFN-inducible DNA sensor cGAS*. J Immunol, 2015. **194**(4): p. 1545-54.
70. Chen, Q., L. Sun, and Z.J. Chen, *Regulation and function of the cGAS-STING pathway of cytosolic DNA sensing*. Nat Immunol, 2016. **17**(10): p. 1142-9.
71. Xia, T., et al., *Deregulation of STING Signaling in Colorectal Carcinoma Constrains DNA Damage Responses and Correlates With Tumorigenesis*. Cell Rep, 2016. **14**(2): p. 282-97.
72. Xiong, T.C., et al., *The E3 ubiquitin ligase ARIH1 promotes antiviral immunity and autoimmunity by inducing mono-ISGylation and oligomerization of cGAS*. Nat Commun, 2022. **13**(1): p. 5973.
73. Hong, Z., et al., *cGAS-STING pathway: post-translational modifications and functions in sterile inflammatory diseases*. FEBS J, 2022. **289**(20): p. 6187-6208.
74. Liu, H., et al., *Nuclear cGAS suppresses DNA repair and promotes tumorigenesis*. Nature, 2018. **563**(7729): p. 131-136.

75. Seo, G.J., et al., *Akt Kinase-Mediated Checkpoint of cGAS DNA Sensing Pathway*. Cell Rep, 2015. **13**(2): p. 440-9.
76. Sun, X., et al., *DNA-PK deficiency potentiates cGAS-mediated antiviral innate immunity*. Nat Commun, 2020. **11**(1): p. 6182.
77. Dai, J., et al., *Acetylation Blocks cGAS Activity and Inhibits Self-DNA-Induced Autoimmunity*. Cell, 2019. **176**(6): p. 1447-1460 e14.
78. Song, Z.M., et al., *KAT5 acetylates cGAS to promote innate immune response to DNA virus*. Proc Natl Acad Sci U S A, 2020. **117**(35): p. 21568-21575.
79. Xia, P., et al., *Glutamylation of the DNA sensor cGAS regulates its binding and synthase activity in antiviral immunity*. Nat Immunol, 2016. **17**(4): p. 369-78.
80. Seo, G.J., et al., *TRIM56-mediated monoubiquitination of cGAS for cytosolic DNA sensing*. Nat Commun, 2018. **9**(1): p. 613.
81. Wang, Q., et al., *The E3 ubiquitin ligase RNF185 facilitates the cGAS-mediated innate immune response*. PLoS Pathog, 2017. **13**(3): p. e1006264.
82. Hu, M.M., et al., *Sumoylation Promotes the Stability of the DNA Sensor cGAS and the Adaptor STING to Regulate the Kinetics of Response to DNA Virus*. Immunity, 2016. **45**(3): p. 555-569.
83. Ablasser, A., et al., *cGAS produces a 2'-5'-linked cyclic dinucleotide second messenger that activates STING*. Nature, 2013. **498**(7454): p. 380-4.
84. Kato, K., et al., *Structural insights into cGAMP degradation by Ecto-nucleotide pyrophosphatase phosphodiesterase 1*. Nat Commun, 2018. **9**(1): p. 4424.
85. Li, L., et al., *Hydrolysis of 2'3'-cGAMP by ENPP1 and design of nonhydrolyzable analogs*. Nat Chem Biol, 2014. **10**(12): p. 1043-8.
86. Ablasser, A., et al., *Cell intrinsic immunity spreads to bystander cells via the intercellular transfer of cGAMP*. Nature, 2013. **503**(7477): p. 530-4.

87. Bridgeman, A., et al., *Viruses transfer the antiviral second messenger cGAMP between cells*. Science, 2015. **349**(6253): p. 1228-32.
88. Gentili, M., et al., *Transmission of innate immune signaling by packaging of cGAMP in viral particles*. Science, 2015. **349**(6253): p. 1232-6.
89. Ruiz-Moreno, J.S., et al., *The common HAQ STING variant impairs cGAS-dependent antibacterial responses and is associated with susceptibility to Legionnaires' disease in humans*. PLoS Pathog, 2018. **14**(1): p. e1006829.
90. Chin, E.N., et al., *Antitumor activity of a systemic STING-activating non-nucleotide cGAMP mimetic*. Science, 2020. **369**(6506): p. 993-999.
91. Lin, B., et al., *Case Report: Novel SAVI-Causing Variants in STING1 Expand the Clinical Disease Spectrum and Suggest a Refined Model of STING Activation*. Front Immunol, 2021. **12**: p. 636225.
92. Wang, Y., F. Wang, and X. Zhang, *STING-associated vasculopathy with onset in infancy: a familial case series report and literature review*. Ann Transl Med, 2021. **9**(2): p. 176.
93. Fremond, M.L., et al., *Overview of STING-Associated Vasculopathy with Onset in Infancy (SAVI) Among 21 Patients*. J Allergy Clin Immunol Pract, 2021. **9**(2): p. 803-818 e11.
94. David, C. and M.L. Fremond, *Lung Inflammation in STING-Associated Vasculopathy with Onset in Infancy (SAVI)*. Cells, 2022. **11**(3).
95. Konno, H., K. Konno, and G.N. Barber, *Cyclic dinucleotides trigger ULK1 (ATG1) phosphorylation of STING to prevent sustained innate immune signaling*. Cell, 2013. **155**(3): p. 688-98.
96. Mukai, K., et al., *Activation of STING requires palmitoylation at the Golgi*. Nat Commun, 2016. **7**: p. 11932.
97. Tu, Y., et al., *MITA oligomerization upon viral infection is dependent on its N-glycosylation mediated by DDOST*. PLoS Pathog, 2022. **18**(11): p. e1010989.

98. Tsuchida, T., et al., *The ubiquitin ligase TRIM56 regulates innate immune responses to intracellular double-stranded DNA*. *Immunity*, 2010. **33**(5): p. 765-76.
99. Wang, Q., et al., *The E3 ubiquitin ligase AMFR and INSIG1 bridge the activation of TBK1 kinase by modifying the adaptor STING*. *Immunity*, 2014. **41**(6): p. 919-33.
100. Zhang, J., et al., *TRIM32 protein modulates type I interferon induction and cellular antiviral response by targeting MITA/STING protein for K63-linked ubiquitination*. *J Biol Chem*, 2012. **287**(34): p. 28646-55.
101. Sun, H., et al., *USP13 negatively regulates antiviral responses by deubiquitinating STING*. *Nat Commun*, 2017. **8**: p. 15534.
102. Ni, G., H. Konno, and G.N. Barber, *Ubiquitination of STING at lysine 224 controls IRF3 activation*. *Sci Immunol*, 2017. **2**(11).
103. Zhong, B., et al., *The ubiquitin ligase RNF5 regulates antiviral responses by mediating degradation of the adaptor protein MITA*. *Immunity*, 2009. **30**(3): p. 397-407.
104. Tian, M., et al., *MYSM1 Represses Innate Immunity and Autoimmunity through Suppressing the cGAS-STING Pathway*. *Cell Rep*, 2020. **33**(3): p. 108297.
105. Xing, J., et al., *TRIM29 promotes DNA virus infections by inhibiting innate immune response*. *Nat Commun*, 2017. **8**(1): p. 945.
106. Wang, Y., et al., *TRIM30alpha Is a Negative-Feedback Regulator of the Intracellular DNA and DNA Virus-Triggered Response by Targeting STING*. *PLoS Pathog*, 2015. **11**(6): p. e1005012.
107. Luo, W.W., et al., *iRhom2 is essential for innate immunity to DNA viruses by mediating trafficking and stability of the adaptor STING*. *Nat Immunol*, 2016. **17**(9): p. 1057-66.
108. Zhang, M., et al., *USP18 recruits USP20 to promote innate antiviral response through deubiquitinating STING/MITA*. *Cell Res*, 2016. **26**(12): p. 1302-1319.

109. Zhang, H.Y., et al., *USP44 positively regulates innate immune response to DNA viruses through deubiquitinating MITA*. PLoS Pathog, 2020. **16**(1): p. e1008178.
110. Ye, L., et al., *USP49 negatively regulates cellular antiviral responses via deconjugating K63-linked ubiquitination of MITA*. PLoS Pathog, 2019. **15**(4): p. e1007680.
111. Ogawa, E., et al., *The binding of TBK1 to STING requires exocytic membrane traffic from the ER*. Biochem Biophys Res Commun, 2018. **503**(1): p. 138-145.
112. Ran, Y., et al., *Correction: YIPF5 Is Essential for Innate Immunity to DNA Virus and Facilitates COPII-Dependent STING Trafficking*. J Immunol, 2022. **208**(5): p. 1310.
113. Sun, M.S., et al., *TMED2 Potentiates Cellular IFN Responses to DNA Viruses by Reinforcing MITA Dimerization and Facilitating Its Trafficking*. Cell Rep, 2018. **25**(11): p. 3086-3098 e3.
114. Motani, K., et al., *The Golgi-resident protein ACBD3 concentrates STING at ER-Golgi contact sites to drive export from the ER*. Cell Rep, 2022. **41**(12): p. 111868.
115. Dobbs, N., et al., *STING Activation by Translocation from the ER Is Associated with Infection and Autoinflammatory Disease*. Cell Host Microbe, 2015. **18**(2): p. 157-68.
116. Chen, L.Y., et al., *NF-kappaB regulates the expression of STING via alternative promoter usage*. Life Sci, 2022. **314**: p. 121336.
117. Wang, Y.Y., et al., *Mechanisms of transcriptional activation of the stimulator of interferon genes by transcription factors CREB and c-Myc*. Oncotarget, 2016. **7**(51): p. 85049-85057.
118. Xu, Y.Y., et al., *Involvement of GATA1 and Sp3 in the activation of the murine STING gene promoter in NIH3T3 cells*. Sci Rep, 2017. **7**(1): p. 2090.

119. Krzesniak, M., et al., *Synergistic activation of p53 by actinomycin D and nutlin-3a is associated with the upregulation of crucial regulators and effectors of innate immunity*. Cell Signal, 2020. **69**: p. 109552.
120. Olagnier, D., et al., *Nrf2 negatively regulates STING indicating a link between antiviral sensing and metabolic reprogramming*. Nat Commun, 2018. **9**(1): p. 3506.
121. Desai, S.D., et al., *Elevated expression of ISG15 in tumor cells interferes with the ubiquitin/26S proteasome pathway*. Cancer Res, 2006. **66**(2): p. 921-8.
122. Reich, N., et al., *Interferon-induced transcription of a gene encoding a 15-kDa protein depends on an upstream enhancer element*. Proc Natl Acad Sci U S A, 1987. **84**(18): p. 6394-8.
123. Malakhova, O., et al., *Lipopolysaccharide activates the expression of ISG15-specific protease UBP43 via interferon regulatory factor 3*. J Biol Chem, 2002. **277**(17): p. 14703-11.
124. Pitha-Rowe, I., B.A. Hassel, and E. Dmitrovsky, *Involvement of UBE1L in ISG15 conjugation during retinoid-induced differentiation of acute promyelocytic leukemia*. J Biol Chem, 2004. **279**(18): p. 18178-87.
125. Memet, S., et al., *Direct induction of interferon-gamma- and interferon-alpha/beta-inducible genes by double-stranded RNA*. J Interferon Res, 1991. **11**(3): p. 131-41.
126. Radoshevich, L., et al., *ISG15 counteracts Listeria monocytogenes infection*. Elife, 2015. **4**.
127. Jeon, Y.J., et al., *Chemosensitivity is controlled by p63 modification with ubiquitin-like protein ISG15*. J Clin Invest, 2012. **122**(7): p. 2622-36.
128. Park, J.M., et al., *Modification of PCNA by ISG15 plays a crucial role in termination of error-prone translesion DNA synthesis*. Mol Cell, 2014. **54**(4): p. 626-38.
129. Farrell, P.J., R.J. Broeze, and P. Lengyel, *Accumulation of an mRNA and protein in interferon-treated Ehrlich ascites tumour cells*. Nature, 1979. **279**(5713): p. 523-5.

130. Haas, A.L., et al., *Interferon induces a 15-kilodalton protein exhibiting marked homology to ubiquitin*. J Biol Chem, 1987. **262**(23): p. 11315-23.
131. Narasimhan, J., et al., *Crystal structure of the interferon-induced ubiquitin-like protein ISG15*. J Biol Chem, 2005. **280**(29): p. 27356-65.
132. Durfee, L.A. and J.M. Huibregtse, *The ISG15 conjugation system*. Methods Mol Biol, 2012. **832**: p. 141-9.
133. Cappadocia, L. and C.D. Lima, *Ubiquitin-like Protein Conjugation: Structures, Chemistry, and Mechanism*. Chem Rev, 2018. **118**(3): p. 889-918.
134. Hochstrasser, M., *Evolution and function of ubiquitin-like protein-conjugation systems*. Nat Cell Biol, 2000. **2**(8): p. E153-7.
135. Yuan, W. and R.M. Krug, *Influenza B virus NS1 protein inhibits conjugation of the interferon (IFN)-induced ubiquitin-like ISG15 protein*. EMBO J, 2001. **20**(3): p. 362-71.
136. Sandy, Z., I.C. da Costa, and C.K. Schmidt, *More than Meets the ISG15: Emerging Roles in the DNA Damage Response and Beyond*. Biomolecules, 2020. **10**(11).
137. Kim, K.I., et al., *Interferon-inducible ubiquitin E2, Ubc8, is a conjugating enzyme for protein ISGylation*. Mol Cell Biol, 2004. **24**(21): p. 9592-600.
138. Takeuchi, T., et al., *Link between the ubiquitin conjugation system and the ISG15 conjugation system: ISG15 conjugation to the Ubch6 ubiquitin E2 enzyme*. J Biochem, 2005. **138**(6): p. 711-9.
139. Zhao, C., et al., *The Ubch8 ubiquitin E2 enzyme is also the E2 enzyme for ISG15, an IFN-alpha/beta-induced ubiquitin-like protein*. Proc Natl Acad Sci U S A, 2004. **101**(20): p. 7578-82.
140. Wong, J.J., et al., *HERC5 is an IFN-induced HECT-type E3 protein ligase that mediates type I IFN-induced ISGylation of protein targets*. Proc Natl Acad Sci U S A, 2006. **103**(28): p. 10735-40.
141. Zou, W. and D.E. Zhang, *The interferon-inducible ubiquitin-protein isopeptide ligase (E3) EFP also functions as an ISG15 E3 ligase*. J Biol Chem, 2006. **281**(7): p. 3989-94.

142. Okumura, F., W. Zou, and D.E. Zhang, *ISG15 modification of the eIF4E cognate 4EHP enhances cap structure-binding activity of 4EHP*. Genes Dev, 2007. **21**(3): p. 255-60.
143. Versteeg, G.A., et al., *Species-specific antagonism of host ISGylation by the influenza B virus NS1 protein*. J Virol, 2010. **84**(10): p. 5423-30.
144. Ketscher, L., et al., *mHERC6 is the essential ISG15 E3 ligase in the murine system*. Biochem Biophys Res Commun, 2012. **417**(1): p. 135-40.
145. Oudshoorn, D., et al., *HERC6 is the main E3 ligase for global ISG15 conjugation in mouse cells*. PLoS One, 2012. **7**(1): p. e29870.
146. Basters, A., et al., *Molecular characterization of ubiquitin-specific protease 18 reveals substrate specificity for interferon-stimulated gene 15*. FEBS J, 2014. **281**(7): p. 1918-28.
147. Kim, K.I., et al., *Ube1L and protein ISGylation are not essential for alpha/beta interferon signaling*. Mol Cell Biol, 2006. **26**(2): p. 472-9.
148. Chin, L.S., J.P. Vavalle, and L. Li, *Staring, a novel E3 ubiquitin-protein ligase that targets syntaxin 1 for degradation*. J Biol Chem, 2002. **277**(38): p. 35071-9.
149. Zhang, Y., et al., *Parkin functions as an E2-dependent ubiquitin- protein ligase and promotes the degradation of the synaptic vesicle-associated protein, CDCrel-1*. Proc Natl Acad Sci U S A, 2000. **97**(24): p. 13354-9.
150. Dastur, A., et al., *Herc5, an interferon-induced HECT E3 enzyme, is required for conjugation of ISG15 in human cells*. J Biol Chem, 2006. **281**(7): p. 4334-8.
151. Woods, M.W., et al., *Human HERC5 restricts an early stage of HIV-1 assembly by a mechanism correlating with the ISGylation of Gag*. Retrovirology, 2011. **8**: p. 95.
152. Zou, W., J. Wang, and D.E. Zhang, *Negative regulation of ISG15 E3 ligase EFP through its autoISGylation*. Biochem Biophys Res Commun, 2007. **354**(1): p. 321-7.

153. Giannakopoulos, N.V., et al., *Proteomic identification of proteins conjugated to ISG15 in mouse and human cells*. *Biochem Biophys Res Commun*, 2005. **336**(2): p. 496-506.
154. They, F., D. Eggermont, and F. Impens, *Proteomics Mapping of the ISGylation Landscape in Innate Immunity*. *Front Immunol*, 2021. **12**: p. 720765.
155. Wang, J.M., et al., *ISG15 suppresses translation of ABCC2 via ISGylation of hnRNPA2B1 and enhances drug sensitivity in cisplatin resistant ovarian cancer cells*. *Biochim Biophys Acta Mol Cell Res*, 2020. **1867**(4): p. 118647.
156. Okumura, F., et al., *Activation of double-stranded RNA-activated protein kinase (PKR) by interferon-stimulated gene 15 (ISG15) modification down-regulates protein translation*. *J Biol Chem*, 2013. **288**(4): p. 2839-47.
157. Xu, D., et al., *Modification of BECN1 by ISG15 plays a crucial role in autophagy regulation by type I IFN/interferon*. *Autophagy*, 2015. **11**(4): p. 617-28.
158. Villarroya-Beltri, C., et al., *ISGylation controls exosome secretion by promoting lysosomal degradation of MVB proteins*. *Nat Commun*, 2016. **7**: p. 13588.
159. Lenschow, D.J., et al., *IFN-stimulated gene 15 functions as a critical antiviral molecule against influenza, herpes, and Sindbis viruses*. *Proc Natl Acad Sci U S A*, 2007. **104**(4): p. 1371-6.
160. Zhao, C., et al., *ISG15 conjugation system targets the viral NS1 protein in influenza A virus-infected cells*. *Proc Natl Acad Sci U S A*, 2010. **107**(5): p. 2253-8.
161. Jumat, M.R., et al., *Molecular and biochemical characterization of the NS1 protein of non-cultured influenza B virus strains circulating in Singapore*. *Microb Genom*, 2016. **2**(8): p. e000082.
162. Zhao, C., et al., *Influenza B virus non-structural protein 1 counteracts ISG15 antiviral activity by sequestering ISGylated viral proteins*. *Nat Commun*, 2016. **7**: p. 12754.

163. Sanyal, S., et al., *Type I interferon imposes a TSG101/ISG15 checkpoint at the Golgi for glycoprotein trafficking during influenza virus infection*. *Cell Host Microbe*, 2013. **14**(5): p. 510-21.
164. Kim, Y.J., et al., *Consecutive Inhibition of ISG15 Expression and ISGylation by Cytomegalovirus Regulators*. *PLoS Pathog*, 2016. **12**(8): p. e1005850.
165. Okumura, A., et al., *Innate antiviral response targets HIV-1 release by the induction of ubiquitin-like protein ISG15*. *Proc Natl Acad Sci U S A*, 2006. **103**(5): p. 1440-5.
166. Amorim, I.S., G. Lach, and C.G. Gkogkas, *The Role of the Eukaryotic Translation Initiation Factor 4E (eIF4E) in Neuropsychiatric Disorders*. *Front Genet*, 2018. **9**: p. 561.
167. Christie, M. and C. Igreja, *eIF4E-homologous protein (4EHP): a multifarious cap-binding protein*. *FEBS J*, 2023. **290**(2): p. 266-285.
168. Pincetic, A., et al., *The interferon-induced gene ISG15 blocks retrovirus release from cells late in the budding process*. *J Virol*, 2010. **84**(9): p. 4725-36.
169. Liu, G., et al., *ISG15-dependent activation of the sensor MDA5 is antagonized by the SARS-CoV-2 papain-like protease to evade host innate immunity*. *Nat Microbiol*, 2021. **6**(4): p. 467-478.
170. Kim, M.J., et al., *Negative feedback regulation of RIG-I-mediated antiviral signaling by interferon-induced ISG15 conjugation*. *J Virol*, 2008. **82**(3): p. 1474-83.
171. Shi, H.X., et al., *Positive regulation of interferon regulatory factor 3 activation by Herc5 via ISG15 modification*. *Mol Cell Biol*, 2010. **30**(10): p. 2424-36.
172. Malakhova, O.A., et al., *Protein ISGylation modulates the JAK-STAT signaling pathway*. *Genes Dev*, 2003. **17**(4): p. 455-60.
173. Malakhov, M.P., et al., *High-throughput immunoblotting. Ubiquitin-like protein ISG15 modifies key regulators of signal transduction*. *J Biol Chem*, 2003. **278**(19): p. 16608-13.

174. Kespohl, M., et al., *Protein modification with ISG15 blocks coxsackievirus pathology by antiviral and metabolic reprogramming*. Sci Adv, 2020. **6**(11): p. eaay1109.
175. Fan, J.B., et al., *Identification and characterization of a novel ISG15-ubiquitin mixed chain and its role in regulating protein homeostasis*. Sci Rep, 2015. **5**: p. 12704.
176. El-Asmi, F., et al., *Cross-talk between SUMOylation and ISGylation in response to interferon*. Cytokine, 2020. **129**: p. 155025.
177. Perng, Y.C. and D.J. Lenschow, *ISG15 in antiviral immunity and beyond*. Nat Rev Microbiol, 2018. **16**(7): p. 423-439.
178. D'Cunha, J., et al., *In vitro and in vivo secretion of human ISG15, an IFN-induced immunomodulatory cytokine*. J Immunol, 1996. **157**(9): p. 4100-8.
179. Knight, E., Jr. and B. Cordova, *IFN-induced 15-kDa protein is released from human lymphocytes and monocytes*. J Immunol, 1991. **146**(7): p. 2280-4.
180. Lai, C., et al., *Mice lacking the ISG15 E1 enzyme UbE1L demonstrate increased susceptibility to both mouse-adapted and non-mouse-adapted influenza B virus infection*. J Virol, 2009. **83**(2): p. 1147-51.
181. Werneke, S.W., et al., *ISG15 is critical in the control of Chikungunya virus infection independent of UbE1L mediated conjugation*. PLoS Pathog, 2011. **7**(10): p. e1002322.
182. Dos Santos, P.F. and D.S. Mansur, *Beyond ISGylation: Functions of Free Intracellular and Extracellular ISG15*. J Interferon Cytokine Res, 2017. **37**(6): p. 246-253.
183. Hare, N.J., et al., *Microparticles released from Mycobacterium tuberculosis-infected human macrophages contain increased levels of the type I interferon inducible proteins including ISG15*. Proteomics, 2015. **15**(17): p. 3020-9.
184. Sun, L., et al., *Exosomes contribute to the transmission of anti-HIV activity from TLR3-activated brain microvascular endothelial cells to macrophages*. Antiviral Res, 2016. **134**: p. 167-171.

185. Munnur, D., et al., *Altered ISGylation drives aberrant macrophage-dependent immune responses during SARS-CoV-2 infection*. Nat Immunol, 2021. **22**(11): p. 1416-1427.
186. Swaim, C.D., et al., *Extracellular ISG15 Signals Cytokine Secretion through the LFA-1 Integrin Receptor*. Mol Cell, 2017. **68**(3): p. 581-590 e5.
187. Recht, M., E.C. Borden, and E. Knight, Jr., *A human 15-kDa IFN-induced protein induces the secretion of IFN-gamma*. J Immunol, 1991. **147**(8): p. 2617-23.
188. D'Cunha, J., et al., *Immunoregulatory properties of ISG15, an interferon-induced cytokine*. Proc Natl Acad Sci U S A, 1996. **93**(1): p. 211-5.
189. Villarreal, D.O., et al., *Ubiquitin-like Molecule ISG15 Acts as an Immune Adjuvant to Enhance Antigen-specific CD8 T-cell Tumor Immunity*. Mol Ther, 2015. **23**(10): p. 1653-62.
190. Padovan, E., et al., *Interferon stimulated gene 15 constitutively produced by melanoma cells induces e-cadherin expression on human dendritic cells*. Cancer Res, 2002. **62**(12): p. 3453-8.
191. Owhashi, M., et al., *Identification of a ubiquitin family protein as a novel neutrophil chemotactic factor*. Biochem Biophys Res Commun, 2003. **309**(3): p. 533-9.
192. Baldanta, S., et al., *ISG15 governs mitochondrial function in macrophages following vaccinia virus infection*. PLoS Pathog, 2017. **13**(10): p. e1006651.
193. Du, Y., et al., *LRRC25 inhibits type I IFN signaling by targeting ISG15-associated RIG-I for autophagic degradation*. EMBO J, 2018. **37**(3): p. 351-366.
194. Xian, H., et al., *LRRC59 modulates type I interferon signaling by restraining the SQSTM1/p62-mediated autophagic degradation of pattern recognition receptor DDX58/RIG-I*. Autophagy, 2020. **16**(3): p. 408-418.
195. Nakashima, H., et al., *Interferon-stimulated gene 15 (ISG15) and ISG15-linked proteins can associate with members of the selective autophagic*

- process, histone deacetylase 6 (HDAC6) and SQSTM1/p62*. J Biol Chem, 2015. **290**(3): p. 1485-95.
196. Yasuda, J., et al., *Nedd4 regulates egress of Ebola virus-like particles from host cells*. J Virol, 2003. **77**(18): p. 9987-92.
197. Okumura, A., P.M. Pitha, and R.N. Harty, *ISG15 inhibits Ebola VP40 VLP budding in an L-domain-dependent manner by blocking Nedd4 ligase activity*. Proc Natl Acad Sci U S A, 2008. **105**(10): p. 3974-9.
198. Yeh, Y.H., et al., *A negative feedback of the HIF-1alpha pathway via interferon-stimulated gene 15 and ISGylation*. Clin Cancer Res, 2013. **19**(21): p. 5927-39.
199. Malakhova, O.A., et al., *UBP43 is a novel regulator of interferon signaling independent of its ISG15 isopeptidase activity*. EMBO J, 2006. **25**(11): p. 2358-67.
200. Tokarz, S., et al., *The ISG15 isopeptidase UB43 is regulated by proteolysis via the SCFSkp2 ubiquitin ligase*. J Biol Chem, 2004. **279**(45): p. 46424-30.
201. Zhang, X., et al., *Human intracellular ISG15 prevents interferon-alpha/beta over-amplification and auto-inflammation*. Nature, 2015. **517**(7532): p. 89-93.
202. Speer, S.D., et al., *ISG15 deficiency and increased viral resistance in humans but not mice*. Nat Commun, 2016. **7**: p. 11496.
203. Kang, D., et al., *Cloning and characterization of human ubiquitin-processing protease-43 from terminally differentiated human melanoma cells using a rapid subtraction hybridization protocol RaSH*. Gene, 2001. **267**(2): p. 233-42.
204. Liu, L.Q., et al., *A novel ubiquitin-specific protease, UB43, cloned from leukemia fusion protein AML1-ETO-expressing mice, functions in hematopoietic cell differentiation*. Mol Cell Biol, 1999. **19**(4): p. 3029-38.
205. Zhang, X., et al., *Molecular responses of macrophages to porcine reproductive and respiratory syndrome virus infection*. Virology, 1999. **262**(1): p. 152-62.

206. Basters, A., K.P. Knobeloch, and G. Fritz, *USP18 - a multifunctional component in the interferon response*. Biosci Rep, 2018. **38**(6).
207. Colonne, P.M., A. Sahni, and S.K. Sahni, *Rickettsia conorii infection stimulates the expression of ISG15 and ISG15 protease UBP43 in human microvascular endothelial cells*. Biochem Biophys Res Commun, 2011. **416**(1-2): p. 153-8.
208. Li, L., et al., *Suppression of USP18 Potentiates the Anti-HBV Activity of Interferon Alpha in HepG2.2.15 Cells via JAK/STAT Signaling*. PLoS One, 2016. **11**(5): p. e0156496.
209. Ye, H., et al., *USP18 Mediates Interferon Resistance of Dengue Virus Infection*. Front Microbiol, 2021. **12**: p. 682380.
210. Amerik, A.Y. and M. Hochstrasser, *Mechanism and function of deubiquitinating enzymes*. Biochim Biophys Acta, 2004. **1695**(1-3): p. 189-207.
211. Jimenez Fernandez, D., S. Hess, and K.P. Knobeloch, *Strategies to Target ISG15 and USP18 Toward Therapeutic Applications*. Front Chem, 2019. **7**: p. 923.
212. Ronau, J.A., J.F. Beckmann, and M. Hochstrasser, *Substrate specificity of the ubiquitin and Ubl proteases*. Cell Res, 2016. **26**(4): p. 441-56.
213. Ketscher, L., et al., *Selective inactivation of USP18 isopeptidase activity in vivo enhances ISG15 conjugation and viral resistance*. Proc Natl Acad Sci U S A, 2015. **112**(5): p. 1577-82.
214. Ritchie, K.J., et al., *Dysregulation of protein modification by ISG15 results in brain cell injury*. Genes Dev, 2002. **16**(17): p. 2207-12.
215. Frias-Staheli, N., et al., *Ovarian tumor domain-containing viral proteases evade ubiquitin- and ISG15-dependent innate immune responses*. Cell Host Microbe, 2007. **2**(6): p. 404-16.
216. Medina, G.N., et al., *Impairment of the DeISGylation Activity of Foot-and-Mouth Disease Virus Lpro Causes Attenuation In Vitro and In Vivo*. J Virol, 2020. **94**(13).

217. Mielech, A.M., et al., *MERS-CoV papain-like protease has deISGylating and deubiquitinating activities*. Virology, 2014. **450-451**: p. 64-70.
218. Shin, D., et al., *Papain-like protease regulates SARS-CoV-2 viral spread and innate immunity*. Nature, 2020. **587**(7835): p. 657-662.
219. Liu, X., et al., *USP18 inhibits NF-kappaB and NFAT activation during Th17 differentiation by deubiquitinating the TAK1-TAB1 complex*. J Exp Med, 2013. **210**(8): p. 1575-90.
220. Yang, Z., et al., *USP18 negatively regulates NF-kappaB signaling by targeting TAK1 and NEMO for deubiquitination through distinct mechanisms*. Sci Rep, 2015. **5**: p. 12738.
221. Cai, X., et al., *USP18 deubiquitinates and stabilizes Twist1 to promote epithelial-mesenchymal transition in glioblastoma cells*. Am J Cancer Res, 2020. **10**(4): p. 1156-1169.
222. Huang, F., et al., *USP18 directly regulates Snail1 protein through ubiquitination pathway in colorectal cancer*. Cancer Cell Int, 2020. **20**: p. 346.
223. Kang, J.A. and Y.J. Jeon, *Emerging Roles of USP18: From Biology to Pathophysiology*. Int J Mol Sci, 2020. **21**(18).
224. Liu, W., et al., *Deubiquitinase USP18 regulates reactive astrogliosis by stabilizing SOX9*. Glia, 2021. **69**(7): p. 1782-1798.
225. Song, C., et al., *USP18 promotes tumor metastasis in esophageal squamous cell carcinomas via deubiquitinating ZEB1*. Exp Cell Res, 2021. **409**(1): p. 112884.
226. Goldmann, T., et al., *USP18 lack in microglia causes destructive interferonopathy of the mouse brain*. EMBO J, 2015. **34**(12): p. 1612-29.
227. Meuwissen, M.E., et al., *Human USP18 deficiency underlies type 1 interferonopathy leading to severe pseudo-TORCH syndrome*. J Exp Med, 2016. **213**(7): p. 1163-74.
228. Arimoto, K.I., et al., *STAT2 is an essential adaptor in USP18-mediated suppression of type I interferon signaling*. Nat Struct Mol Biol, 2017. **24**(3): p. 279-289.

229. Hou, J., et al., *USP18 positively regulates innate antiviral immunity by promoting K63-linked polyubiquitination of MAVS*. Nat Commun, 2021. **12**(1): p. 2970.
230. Arimoto, K.I., et al., *Expansion of interferon inducible gene pool via USP18 inhibition promotes cancer cell pyroptosis*. Nat Commun, 2023. **14**(1): p. 251.
231. Baker, S.J., et al., *Chromosome 17 deletions and p53 gene mutations in colorectal carcinomas*. Science, 1989. **244**(4901): p. 217-21.
232. Hollstein, M., et al., *p53 mutations in human cancers*. Science, 1991. **253**(5015): p. 49-53.
233. Lane, D.P. and L.V. Crawford, *T antigen is bound to a host protein in SV40-transformed cells*. Nature, 1979. **278**(5701): p. 261-3.
234. Munoz-Fontela, C., et al., *Emerging roles of p53 and other tumour-suppressor genes in immune regulation*. Nat Rev Immunol, 2016. **16**(12): p. 741-750.
235. Bullock, A.N. and A.R. Fersht, *Rescuing the function of mutant p53*. Nat Rev Cancer, 2001. **1**(1): p. 68-76.
236. Oren, M., *Decision making by p53: life, death and cancer*. Cell Death Differ, 2003. **10**(4): p. 431-42.
237. Marei, H.E., et al., *p53 signaling in cancer progression and therapy*. Cancer Cell Int, 2021. **21**(1): p. 703.
238. Oren, M. and V. Rotter, *Mutant p53 gain-of-function in cancer*. Cold Spring Harb Perspect Biol, 2010. **2**(2): p. a001107.
239. Brosh, R. and V. Rotter, *When mutants gain new powers: news from the mutant p53 field*. Nat Rev Cancer, 2009. **9**(10): p. 701-13.
240. Shadfan, M., V. Lopez-Pajares, and Z.M. Yuan, *MDM2 and MDMX: Alone and together in regulation of p53*. Transl Cancer Res, 2012. **1**(2): p. 88-89.
241. Haupt, Y., et al., *Mdm2 promotes the rapid degradation of p53*. Nature, 1997. **387**(6630): p. 296-9.
242. Honda, R., H. Tanaka, and H. Yasuda, *Oncoprotein MDM2 is a ubiquitin ligase E3 for tumor suppressor p53*. FEBS Lett, 1997. **420**(1): p. 25-7.

243. Barak, Y., et al., *mdm2 expression is induced by wild type p53 activity*. EMBO J, 1993. **12**(2): p. 461-8.
244. Jones, S.N., et al., *Rescue of embryonic lethality in Mdm2-deficient mice by absence of p53*. Nature, 1995. **378**(6553): p. 206-8.
245. Montes de Oca Luna, R., D.S. Wagner, and G. Lozano, *Rescue of early embryonic lethality in mdm2-deficient mice by deletion of p53*. Nature, 1995. **378**(6553): p. 203-6.
246. Ringshausen, I., et al., *Mdm2 is critically and continuously required to suppress lethal p53 activity in vivo*. Cancer Cell, 2006. **10**(6): p. 501-14.
247. Menendez, D. and C.W. Anderson, *p53 vs. ISG15: stop, you're killing me*. Cell Cycle, 2014. **13**(14): p. 2160-1.
248. Shvarts, A., et al., *MDMX: a novel p53-binding protein with some functional properties of MDM2*. EMBO J, 1996. **15**(19): p. 5349-57.
249. Sabbatini, P. and F. McCormick, *MDMX inhibits the p300/CBP-mediated acetylation of p53*. DNA Cell Biol, 2002. **21**(7): p. 519-25.
250. Huang, Y.F., et al., *Isg15 controls p53 stability and functions*. Cell Cycle, 2014. **13**(14): p. 2200-10.
251. Huang, Y.F. and D.V. Bulavin, *Oncogene-mediated regulation of p53 ISGylation and functions*. Oncotarget, 2014. **5**(14): p. 5808-18.
252. Osei Kuffour, E., et al., *ISG15 Deficiency Enhances HIV-1 Infection by Accumulating Misfolded p53*. mBio, 2019. **10**(4).
253. Park, J.H., et al., *Positive feedback regulation of p53 transactivity by DNA damage-induced ISG15 modification*. Nat Commun, 2016. **7**: p. 12513.
254. Laptenko, O. and C. Prives, *Transcriptional regulation by p53: one protein, many possibilities*. Cell Death Differ, 2006. **13**(6): p. 951-61.
255. Kim, E. and W. Deppert, *The versatile interactions of p53 with DNA: when flexibility serves specificity*. Cell Death Differ, 2006. **13**(6): p. 885-9.
256. Gu, B. and W.G. Zhu, *Surf the post-translational modification network of p53 regulation*. Int J Biol Sci, 2012. **8**(5): p. 672-84.

257. Laptenko, O., et al., *The p53 C terminus controls site-specific DNA binding and promotes structural changes within the central DNA binding domain.* Mol Cell, 2015. **57**(6): p. 1034-1046.
258. el-Deiry, W.S., et al., *WAF1/CIP1 is induced in p53-mediated G1 arrest and apoptosis.* Cancer Res, 1994. **54**(5): p. 1169-74.
259. He, G., et al., *Induction of p21 by p53 following DNA damage inhibits both Cdk4 and Cdk2 activities.* Oncogene, 2005. **24**(18): p. 2929-43.
260. Osei Kuffour, E., et al., *USP18 (UBP43) Abrogates p21-Mediated Inhibition of HIV-1.* J Virol, 2018. **92**(20).
261. Textor, S., et al., *Human NK cells are alerted to induction of p53 in cancer cells by upregulation of the NKG2D ligands ULBP1 and ULBP2.* Cancer Res, 2011. **71**(18): p. 5998-6009.
262. Kadaja-Saarepuu, L., et al., *Tumor suppressor p53 down-regulates expression of human leukocyte marker CD43 in non-hematopoietic tumor cells.* Int J Oncol, 2012. **40**(2): p. 567-76.
263. Munoz-Fontela, C., et al., *p53 serves as a host antiviral factor that enhances innate and adaptive immune responses to influenza A virus.* J Immunol, 2011. **187**(12): p. 6428-36.
264. Yamanishi, Y., et al., *Regional analysis of p53 mutations in rheumatoid arthritis synovium.* Proc Natl Acad Sci U S A, 2002. **99**(15): p. 10025-30.
265. Margulies, L. and P.B. Sehgal, *Modulation of the human interleukin-6 promoter (IL-6) and transcription factor C/EBP beta (NF-IL6) activity by p53 species.* J Biol Chem, 1993. **268**(20): p. 15096-100.
266. Kawashima, H., et al., *Tumor suppressor p53 inhibits systemic autoimmune diseases by inducing regulatory T cells.* J Immunol, 2013. **191**(7): p. 3614-23.
267. Khoo, L.T. and L.Y. Chen, *Role of the cGAS-STING pathway in cancer development and oncotherapeutic approaches.* EMBO Rep, 2018. **19**(12).
268. Ghosh, M., et al., *p53 engages the cGAS/STING cytosolic DNA sensing pathway for tumor suppression.* Mol Cell, 2023. **83**(2): p. 266-280 e6.

269. Ghosh, M., et al., *Mutant p53 suppresses innate immune signaling to promote tumorigenesis*. *Cancer Cell*, 2021. **39**(4): p. 494-508 e5.
270. Mankan, A.K., et al., *Cytosolic RNA:DNA hybrids activate the cGAS-STING axis*. *EMBO J*, 2014. **33**(24): p. 2937-46.
271. Dull, T., et al., *A third-generation lentivirus vector with a conditional packaging system*. *J Virol*, 1998. **72**(11): p. 8463-71.
272. Bahr, A., et al., *Interferon but not MxB inhibits foamy retroviruses*. *Virology*, 2016. **488**: p. 51-60.
273. Sunseri, N., et al., *Human immunodeficiency virus type 1 modified to package Simian immunodeficiency virus Vpx efficiently infects macrophages and dendritic cells*. *J Virol*, 2011. **85**(13): p. 6263-74.
274. Livak, K.J. and T.D. Schmittgen, *Analysis of relative gene expression data using real-time quantitative PCR and the 2(-Delta Delta C(T)) Method*. *Methods*, 2001. **25**(4): p. 402-8.
275. Staib, C., I. Drexler, and G. Sutter, *Construction and isolation of recombinant MVA*. *Methods Mol Biol*, 2004. **269**: p. 77-100.
276. Hansen, K., et al., *Listeria monocytogenes induces IFNbeta expression through an IFI16-, cGAS- and STING-dependent pathway*. *EMBO J*, 2014. **33**(15): p. 1654-66.
277. Yang-Hartwich, Y., et al., *Detection of p53 protein aggregation in cancer cell lines and tumor samples*. *Methods Mol Biol*, 2015. **1219**: p. 75-86.
278. Zahid, A., et al., *Molecular and Structural Basis of DNA Sensors in Antiviral Innate Immunity*. *Front Immunol*, 2020. **11**: p. 613039.
279. Taylor, J.P., et al., *CRISPR/Cas9 knockout of USP18 enhances type I IFN responsiveness and restricts HIV-1 infection in macrophages*. *J Leukoc Biol*, 2018. **103**(6): p. 1225-40.
280. Li, M., et al., *Pharmacological activation of STING blocks SARS-CoV-2 infection*. *Sci Immunol*, 2021. **6**(59).
281. Dai, Y., et al., *Stimulator of Interferon Genes-Associated Vasculopathy With Onset in Infancy: A Systematic Review of Case Reports*. *Front Pediatr*, 2020. **8**: p. 577918.

282. Fremont, M.L. and Y.J. Crow, *STING-Mediated Lung Inflammation and Beyond*. J Clin Immunol, 2021. **41**(3): p. 501-514.
283. Gan, Y., et al., *The cGAS/STING Pathway: A Novel Target for Cancer Therapy*. Front Immunol, 2021. **12**: p. 795401.
284. Hopfner, K.P. and V. Hornung, *Molecular mechanisms and cellular functions of cGAS-STING signalling*. Nat Rev Mol Cell Biol, 2020. **21**(9): p. 501-521.
285. Kang, J., et al., *Post-Translational Modifications of STING: A Potential Therapeutic Target*. Front Immunol, 2022. **13**: p. 888147.
286. Malakhov, M.P., et al., *UBP43 (USP18) specifically removes ISG15 from conjugated proteins*. J Biol Chem, 2002. **277**(12): p. 9976-81.
287. Ma, F., et al., *Positive feedback regulation of type I interferon by the interferon-stimulated gene STING*. EMBO Rep, 2015. **16**(2): p. 202-12.
288. Ganesan, M., et al., *Acetaldehyde Disrupts Interferon Alpha Signaling in Hepatitis C Virus-Infected Liver Cells by Up-Regulating USP18*. Alcohol Clin Exp Res, 2016. **40**(11): p. 2329-2338.
289. Jeon, Y.J., et al., *ISG15 modification of filamin B negatively regulates the type I interferon-induced JNK signalling pathway*. EMBO Rep, 2009. **10**(4): p. 374-80.
290. Zhang, Z., et al., *Multifaceted functions of STING in human health and disease: from molecular mechanism to targeted strategy*. Signal Transduct Target Ther, 2022. **7**(1): p. 394.
291. Zhang, Z.D., et al., *RNF115 plays dual roles in innate antiviral responses by catalyzing distinct ubiquitination of MAVS and MITA*. Nat Commun, 2020. **11**(1): p. 5536.
292. Zhang, M., et al., *ISGylation in Innate Antiviral Immunity and Pathogen Defense Responses: A Review*. Front Cell Dev Biol, 2021. **9**: p. 788410.
293. Giannakopoulos, N.V., et al., *ISG15 Arg151 and the ISG15-conjugating enzyme UbE1L are important for innate immune control of Sindbis virus*. J Virol, 2009. **83**(4): p. 1602-10.

294. Liu, X., et al., *SARS-CoV-2 spike protein-induced cell fusion activates the cGAS-STING pathway and the interferon response*. *Sci Signal*, 2022. **15**(729): p. eabg8744.

Acknowledgements

To begin with, I would like to express my deepest gratitude to my supervisor Prof. Dr. Carsten Münk for his mentorship and generous support over the years. I am very grateful for the opportunity to work in his lab and to do my PhD work under his supervision. I deeply appreciate his enthusiasm and sincere involvement for the project, and his trust, encouragement, and patience that helped me during my whole PhD. Secondly, I would like to express my gratitude to my second supervisor Prof. Dr. Philipp Lang for his insightful contributions, valuable suggestions, and support for my research.

I'd like to express my thank to the following people who have helped me with this research: Dr. Renate König, Dr. Edmund Osei Kuffour, Dr. Nina Hein-Fuchs, Prof. Konstantin M. J. Sparrer, Dr. Boris Görg, Prof. Dr. med. Ingo Drexler, Prof. Dr. Holger Gohlke, Prof. Dr. Thomas Kurz, Dr. Xu, Haifeng C, Dr. Christoph Gertzen, Maximilian Hirschenberger, Oliver Michel, Ronny Tao. Thanks to all our collaborators who not only contributed to the success of this project through reagents and technical support, but also invested their valuable time and generous help.

A great thanks to all the members of Prof. Dr. Carsten Münk's lab for creating such a great working environment. Special thanks to Wioletta Hörschken for her excellent technical assistance and support. I would like to thank the Department of Gastroenterology, Hepatology and Infectious Diseases at Universitätsklinikum Düsseldorf for providing me with the resources and a great working environment to pursue studies and I am also thankful to all our department's staff for all the considerate help.

Furthermore, special thanks to China Scholarship Council and German Research Foundation which provided the financial support to complete my PhD research and live in Germany. To conclude, I cannot forget to thank my family and friends for all their understanding and unconditional support during my whole PhD.